TRABAJO ESPECIAL DE GRADO

MIX DESIGN AND PERFORMANCE-RELATED CHARACTERIZATION OF RICH BITUMEN BASE MIXTURES FOR PERPETUAL PAVEMENTS.

TUTOR ACADÉMICO: Prof. Ezio Santagata; Prof. Maria Korody.

Presentado ante la Ilustre
Universidad Central de Venezuela
Por el Br.:
Scuzzarello Velásquez, José Alejandro
Para optar al Título de
Ingeniero Civil

Caracas, 2010

Scuzzarello V. José A.

MIX DESIGN AND PERFORMANCE-RELATED CHARACTERIZATION OF RICH BITUMEN BASE MIXTURES FOR PERPETUAL PAVEMENTS.

Tutor Académico: Prof. Ezio Santagata; Maria Korody.

Trabajo Especial de Grado. Caracas, U.C.V. Facultad de Ingeniería.

Escuela de Ingeniería Civil. Año 2010, nº pág. 154.

Palabras Clave: (Perpetual Pavements; Rich Bitumen Base; SUPERPAVE)

Resumen

Se estudió y analizó el comportamiento de una mezcla SUPERPAVE, para un estrato de base, con tres diferentes contenidos de bitumen, siendo el contenido óptimo de bitumen el obtenido mediante la metodología SUPERPAVE y 2 contenidos de bitumen adicionales en los cuales se incrementa la porcentual de bitumen para obtener una mezcla de base enriquecida con bitumen (Rich Bitumen Base).

En la fase preliminar de experimentación en el laboratorio, cuatro mezclas para un estrato de base fueron proyectadas y analizadas de acuerdo con el protocolo SUPERPAVE. Para cada mezcla se definió la distribución granulométrica, el contenido de bitumen y se verificó que las mezclas obtenidas cumplieran con los requisitos impuestos por SUPERPAVE. De estas cuatro mezclas solo una fue considerada idónea y a ésta le fue incrementado el porcentual de bitumen en un 0,5% y 1% para el diseño de dos mezclas enriquecidas de bitumen.

Estas tres mezclas (una con el contenido óptimo de bitumen, otra con el contenido óptimo +0,5% y una con el contenido óptimo +1%) fueron analizadas desde el punto de vista volumétrico y mecánico. Analizando las prestaciones mecánicas estudiadas, se puede decir que fue desarrollada una campaña de caracterización mecánica completa, de hecho, fueron determinados las siguientes características: módulo de rigidez (a través de la prueba ITT), propensión al acúmulo de las deformaciones permanentes (a través de la prueba de creep estático), la resistencia a la fatiga (evaluada en la configuración de flexión sobre 4 puntos) y la resistencia a la propagación de las fisuras (mediante la prueba SCB).

Los resultados obtenidos durante la campaña experimental de cada prueba fueron analizados, determinando el valor medio, la desviación estándar y el coeficiente de variación. Además, donde fuese posible, fueron propuestas las regresiones lineares de los datos con la finalidad de individualizar más fácilmente las eventuales tendencias locales en la respuesta mecánica relevada.

Es posible resumir los principales resultados obtenidos con los siguientes gráficos:

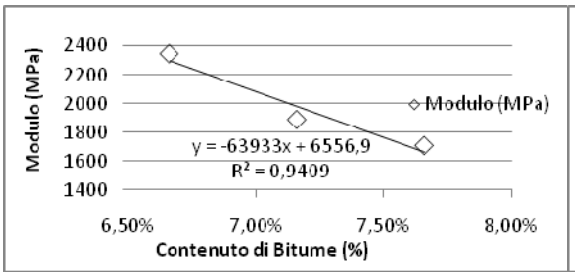

Figura 1: Módulo de rigidez

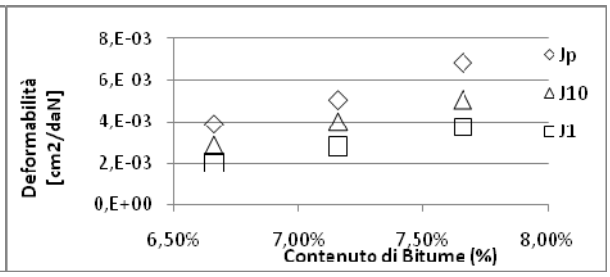

Figura 2: Deformabilidad (Creep)

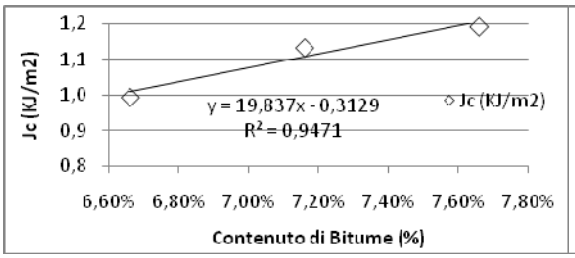

Figura 3: Resistencia a la propagación de las fisuras (SCB test)

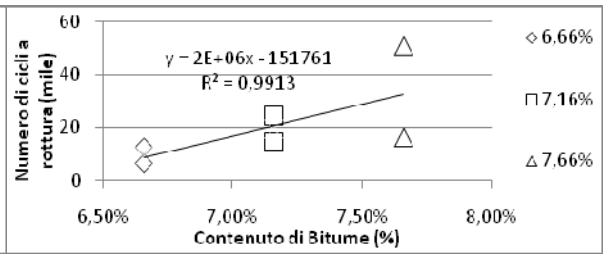

Figura 4: Prueba de fatiga (flexión sobre 4 puntos)

En estos gráficos se puede observar el andamiento de los diversos parámetros prestacionales en función del contenido porcentual de bitumen en la mezcla. Es de notar como al aumentar la porcentual de bitumen se obtienen tendencialmente valores inferiores del módulo de rigidez, mayor resistencia a la propagación de las fisuras, y mayor deformabilidad a creep, mientras que el material se muestra más resistente en lo que respecta al daño por fatiga.

Comparando los resultados obtenidos para cada prueba, se observó un comportamiento mejor para la mezcla de base enriquecida con un 1% de bitumen adicional. De hecho, la misma mostró tener una mayor resistencia a la propagación de las fisuras y ser más resistente a las solicitaciones cíclicas. Sin embargo, también fue observado que la mezcla enriquecida con 0,5% de bitumen presenta prestaciones mecánicas, expresas en términos de módulo de rigidez y deformabilidad, inferiores con respecto a la mezcla base, pero con una mayor resistencia a la fatiga y a la propagación de las fisuras.

Se concluyó que para un estrato de base para una pavimentación perpetua, con la finalidad de impedir la falla por fatiga, resulta apropiado el estrato de base proyectado de acuerdo con el protocolo SUPERPAVE y enriquecido con un 1% de bitumen adicional logrando la mayor resistencia a las solicitaciones cíclicas así como a la propagación de las fisuras.

Considerando la fuerte heterogeneidad del material y la consecuente repercusión sobre la dispersión de los resultados obtenidos, se recomienda desarrollar estudios adicionales con un mayor número de muestras y un mayor control de las características volumétricas. También sería interesante analizar el comportamiento de la resistencia a la propagación de las fisuras en el caso de mezclas enriquecidas con más del 1% de bitumen con respecto a la porcentual óptima determinada.

POLITECNICO DI TORINO
I Faculty of Engineering
Degree in Civil Engineering

Master of Science Thesis

Mix Design and Performance-related Characterization of Rich Bitumen Base Mixtures for Perpetual Pavements.

Supervisors:
Full Prof. Ezio Santagata

Eng. Gianluca Cossale

Prof. Maria Eugenia Korody

Candidate:
José Alejandro Scuzzarello Velásquez

March 2010

Acknowledgments

First I thank God for giving me everything I have ever need, for giving me the best mother anyone could have and for give her the strength to bring me all this way, Thanks mom I love you and I hope to made you proud. Thanks to my family, those who teach me, raise me and made me who I am today, you made a great work.

A special thank to Professor Santagata for giving me the opportunity of developing this thesis and Eng. Cossale for his corrections. Also I would like to thank everyone at the Ditic which have show me their support and also help me doing this thesis, Simone, Pier, Davide (both), Enea, Lucy, Mauro, Peppino, thanks to you all I really appreciate it.

Thanks to all my friends, those old and those new, in both ways I expect you will be there for a long time, thank you for your support during all the years at our lovely UCV, specially to Kari and Luisa; and for this 2,5 years at Turin, it is nice to know that family is also made by friendship, thank you Elyka, Tomas, Elka, Miguel, Pepe and Nathan.

Last but certainly not least, You, my dear Melissa, thank for being there even with a entire ocean in the middle, it is amazing that we made it, and I am so glad we did.

There are many others to whom I should be grateful, and I am... Thank you all!

Objectives

General objective:

To design a Rich Bitumen Base mixture following the SUPERPAVE protocol and make its performance-related characterization.

Specific objectives:

1. Design a bituminous mixture for a base layer following the SUPERPAVE protocol.
    a. Determine the granulometrical gradation
    b. Determine the bitumen percentage
    c. Control if the mixtures accomplished SUPERPAVE requirements.

2. Generate other two mixtures with the same granulometrical gradation but increasing the bitumen percentage in 0,5% and 1%.

3. Determine the deformability of the three mixtures using the static creep test.

4. Determine the crack propagation resistance of the three mixtures using the Semicircular bending test.

5. Determine the fatigue behavior of the three mixtures using the four points bending test.

6. Compare the results of the three mixtures in each test.

Contents

CHAPTER V

Introduction

Advancements in milling, recycling and HMA technology over the last few decades have created HMA pavements that perform better, longer and with lower life-cycle costs than was previously possible. Today's HMA pavements can be designed to last in perpetuity thanks to an idea that was born many years ago, perpetual pavements.

Perpetual pavement refers to a pavement that due to how it is designed it will last longer than 50 years without requiring major structural rehabilitation or reconstruction, and needing only periodic surface renewal. The basic concept is that pavements over a minimum strength are not likely to exhibit structural damage.

To have the pavement over this minimum it is used a thick three-layers-pavement over a strong foundation and each layer is tailored to resist specific stresses. These three layer from up down are: the wearing surface which is designed to resist surface-initiated distresses, an intermediate layer which is designed to carry most of the traffic load; and the *HMA base layer* which is designed specifically to resist fatigue cracking. Two approaches can be used to resist fatigue cracking in the base layer. First, the total pavement thickness can be made great enough such that the tensile strain at the bottom of the base layer is insignificant. Alternatively, the HMA base layer could be made using an extra-flexible HMA also called Rich bitumen base.

A Rich bitumen base is design starting from a mix design SUPERPAVE for a base layer with an optimum bitumen content and then adding more bitumen to the mixture, generally 0,5% more.

The main scope of this thesis was to design a rich bitumen base and characterize it according to its performance. In order to do this, four different granulometrical gradations were tested and the gradation which respect all the

requirements was taken as the base mixture; based on this mixtures 2 more mixtures were made adding an extra 0,5% and 1% of bitumen, obtaining two enriched bitumen bases. These three mixtures were tested and the results were compared to see if actually a Rich Bitumen base behave better than a normal base regarding the deformability, fatigue resistance and crack propagation resistance.

Chapter I

GENERAL APPROACH TO HOT MIXTURE ASPHALT AND PERPETUAL PAVEMENT.

Hot Mixture Asphalt (HMA) refers to bounded layers of a flexible or semi flexible pavement. It is constituted by aggregate (stone and filler) generally in a 92% to 96% of total mass and bitumen; being aggregate the load-bearing skeleton and bitumen the binding medium.

1.1 Bitumen

1.1.1 General conceptions

"Bitumen" is a dark brown to black, highly viscous, organic and heterogenic compose produced from petroleum distillation residue. It is constitute by a complex mixture of high molecular weight hydrocarbon. Besides carbon and hydrogen, which constitute more than 90% in weight, we can find metals like nickel and vanadium, and components like sulfur, oxygen and nitrogen.

Bitumen can be used as a tie material to allow the formation of bituminous mixtures, but it can also be used as a waterproof material. The behavior of this material is considered viscoelastic.

Bitumen distillation can occur naturally, resulting in asphalt lakes, or occur in a petroleum refinery.

.

Natural Bitumen

Derives from the evaporation and oxidation of the more volatile components of petroleum. These deposits can be found in various forms, the

most important one is a lake in Trinidad Island. In this case the bitumen is almost 50% mixed with water, sand and clay.

Industrial Bitumen

It derives from the fractional distillation of petroleum. This occurs in a two column distillation process. One column works at atmosphere pressure; in this case we obtain gasoline and other products of this nature. The residue of this process is distillated under pressure; from this second process the bitumen is obtained.

1.1.1.1 Bitumen chemical composition

Bitumen is an organic compose, complex and heterogenic. The principal components are carbon (C) and hydrogen (H), but it can also be found nitrogen, sulfur, oxygen, nickel, and others. The proportion of these components varies and is difficult to define. The different chains of C – H form variations of the electro-chemical equilibrium, they are long and complex chains that intertwine.

A simplification is made and different groups are used to define the characteristic which come in hand. The two principal groups are asphaltenes and maltenes.

Asphaltenes

They represent around 5% to 25% of the weight of the bitumen; they are complex hydrocarbons with the following components:

- Condensed aromatic hydrocarbons with sidechains up to $C_{30.}$
- Hetero-aromatic compounds with sulfur present in benzothiophene rings and nitrogen in pyrrole and pyridine rings
- Bi or polyfunctional molecules with nitrogen as amines, amides, and oxygen in groups such as: ketones, armides, phenols, and carboxylic acids.
- Nickel and vanadium complex with pyrrole nitrogen atoms in porphyrin ring structures.

Considering the atomic mass unit (A.M.U.) of the asphaltenes, there has been many studies with results that vary depending on the method apply for the calculation. This is because in almost every case, bitumen has to be mixed with a solvent and this can contribute to the modification of the morphologic structure or the dilution of the heaviest molecules. The range of the atomic weight is generally taken from 800 to 2500 A.M.U.

Maltenes

Maltenes constitute the fraction of asphalt which is soluble in n-alkane solvent such as pentane and heptanes. Their chemical characteristics are:

- Contain smaller molecular weight versions of asphaltenes called resins;
- Contain aromatic hydrocarbons with or without O, N and S;
- Contain straight chained or cyclic unsaturated hydrocarbons called oleifins;
- Contain cyclic saturated hydrocarbons known as naphthenes (saturates);
- Contain straight or branch chain saturated hydrocarbons (also saturates);
- Their molecules are also known as naphthene-aromatics.

The resins are the most polar components, with a molecular weight from 500 to 100 A.M.U. The oil components (saturates and aromatics) have the lowest molecular weight, under 500 A.M.U.

A theory commonly accepted states that asphaltenes are a colloidal system stabilized by the absorption of resins and is maintained as a solution by the aromatic components. According to the proportions of asphaltenes, resins and oils, they can combine in a less stable form.

It is very important that resins, which determined the stability of the system, present matching characteristic with oils and asphaltenes. In oils, the aromatic components determines the solvent capacity, which has to be powerful in confront with the asphaltenes.

Asphaltenes are the ones responsible for the consistency properties, resistance to mechanical solicitations and bond properties of the bitumen. Resins give elasticity and ductility. Oils give fluidity to the bitumen at high temperatures (Migliorini 2009).

1.1.1.2 Bitumen Physical Properties

Bitumen can be classified by its chemical composition and physical properties. The pavement industry typically relies on physical properties for performance characterization. An aggregate's physical properties are a direct result of its chemical composition. Typically, the most important physical properties are:

- *Durability*. Durability is a measure of how asphalt binder physical properties change with age (sometimes called age hardening). In general, as an asphalt binder ages, its viscosity increases and it becomes more stiff and brittle.

- *Rheology*. Rheology is the study of deformation and flow of matter. Deformation and flow of the asphalt binder in HMA is important in HMA pavement performance. HMA pavements that deform and flow too much may be susceptible to rutting and bleeding, while those that are too stiff may be susceptible to fatigue cracking.

- *Safety*. Asphalt cement like most other materials, volatilizes (gives off vapor) when heated. At extremely high temperatures (well above those experienced in the manufacture and construction of HMA) asphalt cement can release enough vapor to increase the volatile concentration immediately above the asphalt cement to a point where it will ignite (flash) when exposed to a spark or open flame. This is called the flash point. For safety reasons, the flash point of asphalt cement is tested and controlled.

- *Purity*. Asphalt cement, as used in HMA paving, should consist of almost pure bitumen. Impurities are not active cementing constituents and may be detrimental to asphalt performance.

1.1.2 Characterization test

Bitumen is classified with traditional tests; this type of test determines empirical characteristics. In time, a new type of test was developed, one that determines the intrinsic properties of the material: the rheological tests.

1.1.2.1 Traditional tests

Determination of needle penetration

This standard test specifies the method for the determination of bitumen consistency. It has to be performed with the bitumen at 25°C and an applied load of 100g, the loading time duration is 5 s. If the penetration is considered to be above 33 mm, the test temperature shall be reduced to 15°C but the operating parameters of the applied load and the loading time duration remain unchanged.

Softening point

Is the temperature at which a bitumen disc can no longer bear a metal ball of standard dimensions. If the temperature is considered to be lower than 80°C, the bitumen has to be conditioned at 5°C; if it is considered to be between 80°C and 150°C, it has to be conditioned at 25°C. The softening point is approximately the temperature in which a non modified asphalt has a viscosity of around 1200 Pa*s. This test is also known as ring and ball test.

Determination of the Fraass breaking point

This test measures the brittleness of the bitumen at low temperatures. A sample of the bitumen is applied to a metal plate at an even thickness; this plate is submitted to a constant cooling rate and flexed repeatedly until the binder

layer breaks. The temperature at which the first crack appears is reported as the Fraass breaking point.

Ductility

Measures the maximum lengthening of a bituminous sample at a specific temperature and speed. This test is use to determined the bonding and elasticity of the bitumen.

1.1.2.2 Rheological tests

This type of test is more accurate in the determination of the mechanical properties of the material. In traditional testing, the parameters determined were empirical, and the acceptance of the material was based on the experience. Rheological testing is based on experimental procedures which allow to establish with precision the bitumen behavior.

For the determination of the performance behavior, we have different instruments that are employed. These are:

Rotational viscometer

It's used to determine the workability of the bitumen at high temperatures (range of manufacturing and construction).

Dynamic shear rheometer

It is used to determine the viscoelastic behavior of the bitumen at medium to high temperatures. In particular it determines the complex modulus and phase angle.

Bending beam rheometer and Direct tension tester

They provide a measure of low temperature stiffness and relaxation properties of asphalt binders. These parameters give an indication of an asphalt binder's ability to resist low temperature cracking.

1.1.3 Grading Systems

Asphalt binders are typically categorized by one or more shorthand grading systems according to their physical characteristics. These systems range from simple to complex and represent an evolution in the ability to characterize asphalt binder. Today it is in general use the SUPERPAVE performance grading (PG) system, although brief mention of the older systems is still worthwhile.

1.1.3.1 Penetration grading.

Based on the depth a standard needle will penetrate an asphalt binder sample when placed under a 100 g load for 5 seconds. The test is simple and easy to perform but it does not measure any fundamental parameter and can only characterize asphalt binder at one temperature. Penetration grades are listed as a range of penetration units (one penetration unit = 0.1 mm).

1.1.3.2 Viscosity grading.

Measures penetration (as in penetration grading) but also measures an asphalt binder's viscosity at 60°C and 135°C. Testing can be done on virgin (AC) or aged (AR) asphalt binder. Grades are listed in poises (cm-g-s = dyne-second/cm^2) or poises divided by 10. Viscosity grading is a better grading system but it does not test low temperature asphalt binder rheology.

1.1.3.3 SUPERPAVE Performance Grading (PG) System

The SUPERPAVE PG system was developed as part of the SUPERPAVE research effort to more accurately and fully characterize asphalt binders for use in HMA pavements. The PG system is based on the idea that an HMA asphalt binder's properties should be related to the conditions under which it is used. For asphalt binders, this involves expected climatic conditions as well as aging considerations. Therefore, the PG system uses a common

battery of tests (as the older penetration and viscosity grading systems do) but specifies that a particular asphalt binder must pass these tests at specific temperatures that are dependent upon the specific climatic conditions in the area of intended use.

SUPERPAVE performance grading is reported using two numbers – the first being the average seven-day maximum pavement temperature (in °C) and the second being the minimum pavement design temperature likely to be experienced (in °C). Thus, a PG 58-22 is intended for use where the average seven-day maximum pavement temperature is 58°C and the expected minimum pavement temperature is -22°C. Notice that these numbers are pavement temperatures and not air temperatures.

1.1.4 Viscoelastic materials

1.1.4.1 General conceptions

In order to predict the engineering performance of any material, it is necessary to understand its stress-strain behavior. To determine how a given material will respond to an applied load, laboratory test must be performed and analyzed. To characterize the stress-strain behavior of materials in laboratory, the simplest test methods are uniaxial and shear test. Such test may be conducted under controlled stress or controlled strain conditions.

Elastic materials strain instantaneously when a stress is applied and return to its original form once the stress is remove; this behavior for the stress-strain test is largely independent of time and temperature. This kind of elastic response in solids occurs because of the atomic crystalline structure which is capable of developing high internal forces for small strains.

A viscous material will deform at a constant rate when the load is applied at time t_0 and will continue to deform at that rate until the load is removed; at this point there is no further deflection or recovery.

A viscoelastic material has both components of response. When loaded, there is an immediate deformation, corresponding to the elastic response, followed by a gradual time-dependent deformation. This deformation may further be divided into a purely viscous component and a delayed elastic component. Upon removing the load at time t_i, the viscous flow ceases and none of this deformation is recovered. The delayed elastic deformation is, however, recovered, but not immediately as with pure elastic deformation. Instead, once the load is removed, the delayed elastic deformation is slowly recovered, at a decreasing rate. Viscous materials resist shear flow and strain linearly with time when a stress is applied; this kind of fluids present weak bonding in their molecules; the internal forces depend on the relative movement, the internal force is proportional to the strain velocity.

Materials such as bitumen, are viscoelastic materials, and must be characterized with test methods and analytical techniques that account for the time of loading and the loading temperature.

One test used for characterizing the stress-strain response of a material is the creep test. In this test, a load of constant magnitude is applied to a material at time t_0 and removed at time t_i. The inherent differences between elastic, viscous and viscoelastic behavior are readily apparent in such a test (Figure 1.1).

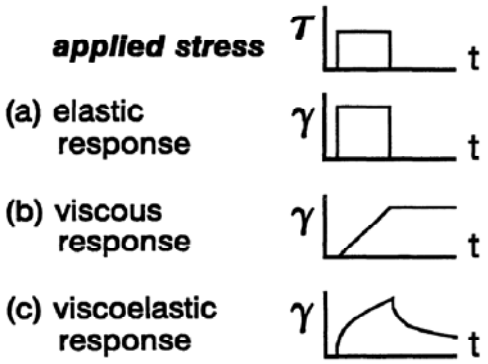

Figure 1.1: Idealized response of elastic, viscous and viscoelastic materials under constant stress loading

1.1.4.2 Complex modulus and phase angle

In dynamic mechanical analysis, a sinusoidal strain is applied to a specimen and the resulting stress is monitored as a function of frequency (ω). This can be represented by the following formulation:

$$\gamma = \gamma_0 * \sin(\omega * t)$$

The stress follows the sinusoidal behavior of the strain but with a phase displacement (δ):

$$\tau = \tau_0 * \sin(\omega * t + \delta)$$

The primary response in dynamic testing is the complex modulus, which is computed in strain-controlled testing using the following equation:

$$G^*(\omega) = \frac{|\tau(\omega)|}{|\gamma(\omega)|}$$

The phase angle (δ) indicates the lag in the stress response compared with the applied strain. For purely elastic materials, the phase angle will be zero, whereas for purely viscous materials, the phase angle will be 90°.

There are two other parameters that appear in dynamic testing: the storage modulus G'(ω); and the loss modulus G"(ω).

$$G'(\omega) = G^*(\omega) * \cos(\delta)$$
$$G"(\omega) = G^*(\omega) * \sin(\delta)$$

The storage modulus represents the in-phase component of the complex modulus. The loss modulus represents the out of phase component of the complex modulus. Both of these parameters reflect a portion of the delayed

elastic response, so they cannot be interpreted as elastic and viscous modulus (Figure 1.2).

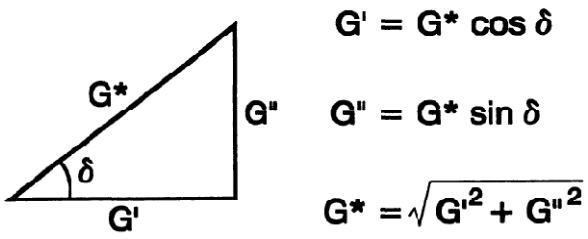

Figure 1.2: Relationship among Complex modulus, storage modulus, loss modulus and phase angle.

1.2 Aggregate

"Aggregate" is a collective term for sand, gravel and crushed stone mineral materials in their natural or processed state (NSSGA, 1991). Roads and highways constitute the largest single use of aggregate at 40 percent of the total (NSSGA, 2002). In HMA, aggregates are combined with an asphalt binding medium to form a compound material. By weight, aggregate generally accounts for between 92 and 96 percent of HMA and makes up about 30 percent of the cost of an HMA pavement structure. Aggregate is also used by itself or with a stabilizer for base and sub base courses.

Figure 1.3: Sand and Gravel Pit (WAPA)

Figure 1.4: Aggregate Stockpile (WAPA)

1.2.1 Aggregate Origins and Production

Aggregates can either be natural or manufactured. Natural aggregates are generally extracted from larger rock formations through an open excavation (quarry). Usually the rock is blasted or dug from the quarry walls then reduced in size using a series of screens and crushers. Some quarries are also capable of washing the finished aggregate. Manufactured rock typically consists of industrial byproducts such as slag (byproduct of the metallurgical processing – typically produced from processing steel, tin and copper) or specialty rock that is produced to have a particular physical characteristic not found in natural rock (such as the low density of lightweight aggregate). (WAPA)

Figure 1.5: Quarry Overview (WAPA)

1.2.2 Aggregate Physical Properties

Aggregates can be classified by their mineral, chemical and physical properties. The pavement industry typically relies on physical properties for performance characterization. An aggregate's physical properties are a direct result of its mineral and chemical properties.

1.2.2.1 Maximum Size

Maximum aggregate size can affect HMA and base/sub base courses in several ways. In HMA, instability may result from excessively small maximum sizes; and poor workability and/or segregation may result from excessively large maximum sizes (Roberts et al., 1996). ASTM C 125 defines the maximum aggregate size in one of two ways:

- *Maximum size*. The smallest sieve through which 100 percent of the aggregate sample particles pass. SUPERPAVE defines the maximum aggregate size as "one sieve larger than the nominal maximum size" (Roberts et al., 1996).

- *Nominal maximum size*. The largest sieve that retains some of the aggregate particles but generally not more than 10 percent by weight. SUPERPAVE defines nominal maximum aggregate size as "one sieve size larger than the first sieve to retain more than 10 percent of the material" (Roberts et al., 1996).

It is important to specify whether "maximum size" or "nominal maximum size" is being referenced.

1.2.2.2 Gradation

Aggregate is typically crushed to certain size or gradation specifications. Each crushed gradation is typically stored as a different aggregate stockpile. While some mixes can be met using a single aggregate stockpile (with the possible addition of some blending sand), SUPERPAVE mixes often require combinations of up to three or four different stockpiles to meet gradation requirements.

An aggregate's particle size distribution, or gradation, is one of its most influential characteristics. In HMA, gradation helps to determine almost every important property including stiffness, stability, durability, permeability, workability, fatigue resistance, frictional resistance and resistance to moisture damage (Roberts et al., 1996). Because of this, gradation is a primary concern in HMA mix design and thus most agencies specify allowable aggregate gradations.

1.2.2.2.1 Measurement

Gradation is usually measured by a sieve analysis. In a sieve analysis, a sample of dry aggregate of known weight is separated through a series of sieves with progressively smaller openings. Once separated, the weight of particles retained on each sieve is measured and compared to the total sample

weight. Particle size distribution is then expressed as a percent retained by weight on each sieve size. Results are usually expressed in tabular or graphical format. The typical graph uses the percentage of aggregate by weight passing a certain sieve size on the y-axis and the sieve size raised to the n^{th} power (n = 0.45 is typically used) as the x-axis units. The maximum density appears as a straight line from zero to the maximum aggregate size.

1.2.2.2.2 Typical Gradations

- *Dense or well-graded*. Refers to a gradation that is near maximum density. The most common HMA mix designs in the U.S. tend to use dense graded aggregate.

- *Gap graded*. Refers to a gradation that contains only a small percentage of aggregate particles in the mid-size range. The curve is flat in the mid-size range. These mixes can be prone to segregation during placement.

- *Open graded*. Refers to a gradation that contains only a small percentage of aggregate particles in the small range. This results in more air voids because there are not enough small particles to fill in the voids between the larger particles. The curve is flat and near-zero in the small-size range.

- *Uniformly graded*. Refers to a gradation that contains most of the particles in a very narrow size range. In essence, all the particles are the same size. The curve is steep and only occupies the narrow size range specified.

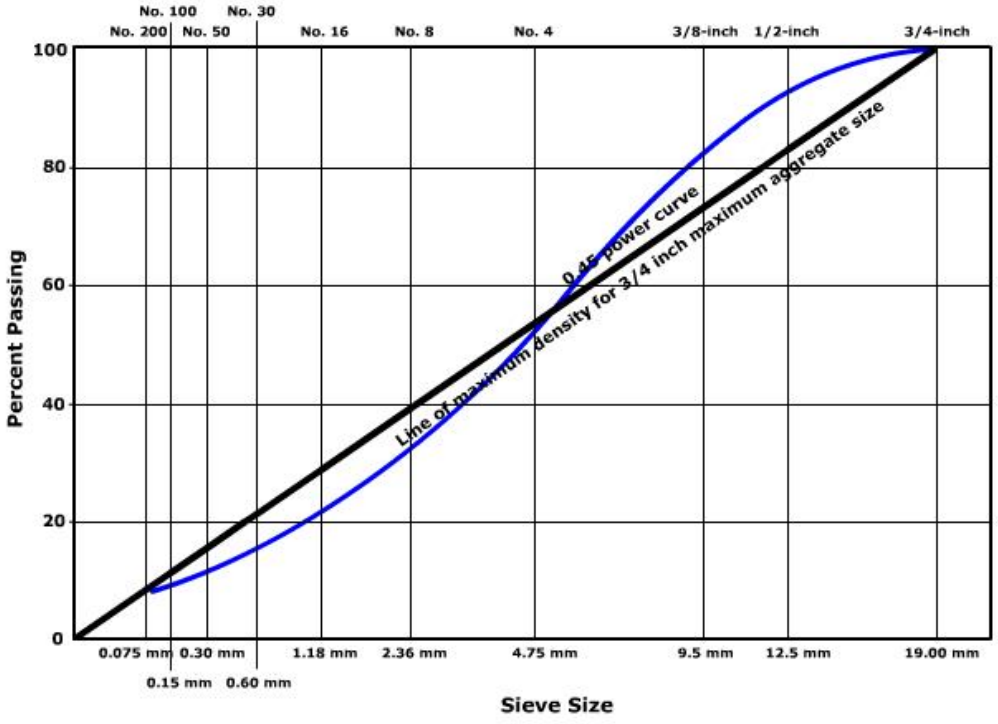

Figure 1.6: Dense Gradation (WAPA)

1.2.2.2.3 Other Gradation Terms

- *Fine aggregate (sometimes just referred to as "fines")*. Defined by AASHTO M 147 as natural or crushed sand passing the No. 10 sieve and mineral particles passing the No. 200 sieve.

- *Coarse aggregate*. Defined by AASHTO M 147 as hard, durable particles or fragments of stone, gravel or slag retained on the No. 10 sieve. Usually coarse aggregate has a toughness and abrasion resistance requirement.

- *Fine gradation*. A gradation that, when plotted on the 0.45 power gradation graph, falls mostly above the 0.45 power maximum density line. The term generally applies to dense graded aggregate.

- *Coarse gradation*. A gradation that, when plotted on the 0.45 power gradation graph, falls mostly below the 0.45 power maximum density line. The term generally applies to dense graded aggregate.

- *Mineral filler*. Defined by the Asphalt Institute as a finely divided mineral product at least 65 percent of which will pass through a No. 200 sieve. Pulverized limestone is the most commonly manufactured mineral filler, although other stone dust, silica, hydrated lime, Portland cement and certain natural deposits of finely divided mineral matter are also used (Asphalt Institute, 1962).

1.2.3 Other Properties

Other important aggregate physical properties are:

- *Toughness and abrasion resistance*. Aggregates should be hard and tough enough to resist crushing, degradation and disintegration from activities such as manufacturing, stockpiling, production, placing and compaction.

- *Durability and soundness*. Aggregates must be resistant to breakdown and disintegration from weathering (wetting/drying) or else they may break apart and cause premature pavement distress.

- *Particle shape and surface texture*. Particle shape and surface texture are important for proper compaction, load resistance and workability. Generally, cubic angular-shaped particles with a rough surface texture are best.

- *Specific gravity*. Aggregate specific gravity is useful in making weight-volume conversions and in calculating the void content in compacted HMA (Roberts et al., 1996).

- *Cleanliness and deleterious materials*. Aggregates must be relatively clean when used in HMA. Vegetation, soft particles, clay lumps, excess dust and vegetable matter may affect performance by quickly degrading, which causes a loss of structural support and/or prevents binder-aggregate bonding.

1.3 PAVEMENTS TYPES

Road surface or pavement, is the durable surface material laid down on an area intended to sustain traffic. There are two typical categories for pavements, flexible and rigid pavements. The most common paving methods are asphalt, for flexible pavements, and concrete for rigid pavements. (WAPA)

1.3.1 Flexible pavements.

The flexible pavements are those which are surfaced with bituminous (or asphalt) materials and which load respond is elastic or more precisely viscoelastic. These types of pavements are called "flexible" since the total pavement structure "bends" or "deflects" due to traffic loads. The structure is typically composed of several layers of material which can accommodate this "flexing". Each layer receives the loads from the above layer, spreads them out, and then passes on these loads to the next layer below.

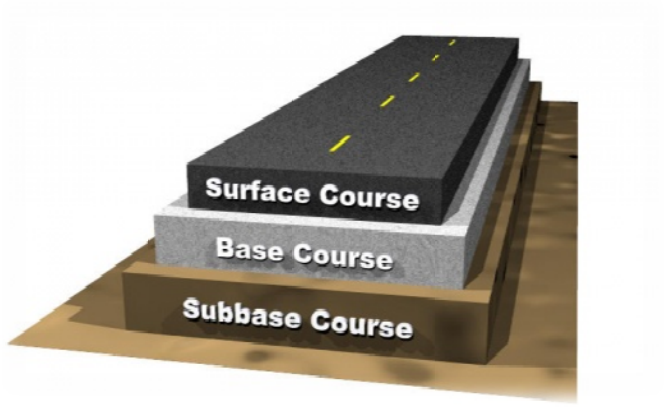

Figure 1.7: Basic flexible pavement structure. (WAPA)

Figure 1.8: Flexible Pavement Load distribution (WAPA)

A typical flexible pavement structure consists of the surface course and the underlying base and sub base courses. Each of these layers contributes to structural support and drainage.

Surface course

Is the layer in contact with traffic loads and generally has the highest quality materials. It provides characteristics such as friction, smoothness, noise control, rut and shoving resistance and drainage. It also serves to avoid the excessive entrance of surface water into the underlying base, sub base and subgrade. It can be divided into two layers:

- Wearing course: Is in direct contact with traffic. Distresses can be identify in this layer and rehabilitated before it propagates into the underlying course.

- Intermediate/Binder course: Provides the bulk of the hot-mix asphalt structure. Its purpose is to distribute loads.

Base course

Is immediately beneath the surface course, and provides additional load distribution and contributes to drainage and frost resistance. This layer is commonly constructed with durable aggregates that will not damage by moisture or frost action. If a hot mix is used in this layer, it usually contains larger maximum aggregate size than surface courses.

Subbase course

Is between the base course and the subgrade, and has the function of giving structural support. It can also minimize the intrusion of fines from the subgrade into the pavement structure, improve drainage, etc. It consists of lower quality materials that the base course but better than the subgrade soils. It is not always needed or used

1.3.2 Rigid pavements.

Those which are surfaced with cement concrete (PCC). These types of pavements are called "rigid" because they are substantially stiffer than flexible pavements due to PCC's high stiffness.

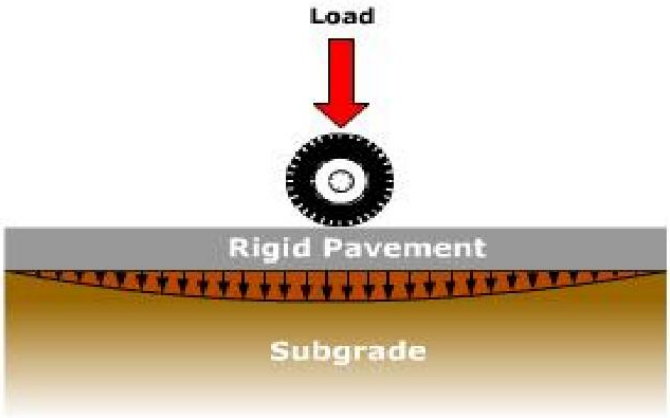

Figure 1.9: Rigid Pavement Load distribution (WAPA)

Each of these pavement types distributes load over the subgrade in a different fashion. Rigid pavement, because of PCC's high stiffness, tends to distribute the load over a relatively wide area of subgrade. The concrete slab itself supplies most of a rigid pavement's structural capacity. Flexible pavement uses more flexible surface course and distributes loads over a smaller area. It relies on a combination of layers for transmitting load to the subgrade.

In general, flexible and rigid pavements can be designed for long life (e.g., in excess of 30 years) with only minimal maintenance. Both types have been used for just about every classification of road. Certainly there are many

different reasons for choosing one type of pavement or the other, some practical, some economical, and some political.

1.4 HMA MIX TYPES

The most common type of flexible pavement surfacing is hot mix asphalt (HMA). Hot mix asphalt is known by many different names such as hot mix, asphalt concrete (AC or ACP), asphalt, blacktop or bitumen. HMA is distinguished by its design and production methods and includes traditional dense-graded mixes as well as stone matrix asphalt (SMA) and various open-graded HMAs. Reclaimed asphalt pavement (RAP) is generally considered a material within HMA, while forms of in-place recycling are considered separately.

1.4.1 Dense-Graded Mixes

A dense-graded mix is a well-graded HMA intended for general use. When properly designed and constructed, a dense-graded mix is relatively impermeable. Dense-graded mixes are generally referred to by their nominal maximum aggregate size. They can further be classified as either fine-graded or coarse-graded. Fine-graded mixes have more fine and sand sized particles than coarse-graded mixes.

1.4.2 Stone Matrix Asphalt (SMA)

Stone matrix asphalt (SMA), sometimes called stone mastic asphalt, is a gap-graded HMA originally developed in Europe to maximize rutting resistance and durability. The mix goal is to create stone-on-stone contact. Since aggregates do not deform as much as asphalt binder under load, this stone-on-stone contact greatly reduces rutting. SMA is generally more expensive than a typical dense-graded HMA because it requires more durable aggregates, higher asphalt content, modified asphalt binder and fibers. In the right situations it

should be cost-effective because of its increased rut resistance and improved durability.

Mineral fillers and additives are used to minimize asphalt binder drain-down during construction, increase the amount of asphalt binder used in the mix and to improve mix durability.

1.4.3 Open-Graded Mixes

Unlike dense-graded mixes and SMA, an open-graded HMA mixture is designed to be water permeable. Open-graded mixes use only crushed stone (or gravel) and a small percentage of manufactured sands. The two most typical open-graded mixes are:

1. *Open-graded friction course (OGFC)*. Typically 15 percent air voids and no maximum air voids specified.
2. *Asphalt treated permeable bases (ATPB)*. Less stringent specifications than OGFC since it is used only under dense-graded HMA, SMA or PCC for drainage.

OGFC is more expensive per ton than dense-graded HMA, but the unit weight of the mix when in-place is lower, which partially offsets the higher per-ton cost. The open gradation creates pores in the mix, which are essential to the mix's proper function. Anything that tends to clog these pores, such as low-speed traffic, excessive dirt on the roadway or deicing sand, can degrade performance.

OGFC is susceptible to studded tires. Tire studs will tend to dislodge aggregate from the mix causing a sort of raveling phenomenon in the wheelpaths causing ruts. ATPB can be used as a base course for both flexible and rigid pavements.

1.5 Perpetual Pavements

Advancements in milling, recycling and HMA technology over the last few decades have created HMA pavements that perform better, longer and with lower life-cycle costs than was previously possible. Today's HMA pavements can be designed to last in perpetuity.

A Perpetual Pavement is defined as an asphalt pavement designed and built to last longer than 50 years without requiring major structural rehabilitation or reconstruction, and needing only periodic surface renewal in response to distresses confined to the top of the pavement. The concept of Perpetual Pavements, or long-lasting HMA pavements, is not new. Full-depth and deep-strength HMA pavement structures have been constructed since the 1960s, and those that were well-designed and well-built have been very successful in providing long service lives under heavy traffic (APA, 2002).

The basic concept is that HMA pavements over a minimum strength are not likely to exhibit structural damage even when subjected to very high traffic flows over long periods of time. Rather, deterioration seens to initiate in the pavement surface as either top-down cracking or rutting. If surface-initiated cracking and rutting can be detected and remedied before they impact the structural integrity of the pavement, the pavement design life could be greatly increased.

Researchers have used this idea as well as pavement materials research to develop a basic perpetual pavement structural concept. This concept uses a thick HMA pavement over a strong foundation design with three layers, each one tailored to resist specific stresses (TRB, 2001), from bottom up:

1. *HMA base layer*.

   This is the bottom layer designed specifically to resist fatigue cracking. Two approaches can be used to resist fatigue cracking in the base layer. First, the total pavement thickness can be made great enough such that the

tensile strain at the bottom of the base layer is insignificant. Alternatively, the HMA base layer could be made using an extra-flexible HMA. This can be most easily accomplished by increasing the asphalt content. Combinations of these two approaches can also work.

2. *Intermediate layer*.

This is the middle layer designed specifically to carry most of the traffic load. Therefore it must be stable (able to resist rutting) as well as durable. Stability can best be provided by using stone-on-stone contact in the coarse aggregate and using a binder with the appropriate high-temperature grading.

3. *Wearing surface*.

This is the top layer designed specifically to resist surface-initiated distresses such as top-down cracking and rutting. Other specific distresses of concern would depend upon local experience.

with the purpose of the pavement structure above works properly, it must be built on a solid foundation. Nunn (1998) notes that rutting on roads built on subgrade with a CBR greater than 5 percent originates almost solely in the HMA layers, which suggests that a subgrade with a CBR greater than 5 percent (resilient modulus greater than about 7,000 psi) should be considered adequate. As always, proper construction techniques are essential to a perpetual pavement's performance.

Chapter II

STUDY OF FATIGUE BEHAVIOR IN BITUMINOUS MIXTURES.

As defined by ASTM, fatigue (N_f) is the number of stress cycles of a specified character that a specimen sustains before failure of a specified nature occurs.

Fatigue cracking results from cyclic stresses that are below the ultimate tensile stress, or even the yield stress of the material. The name “fatigue” is based on the concept that a material becomes “tired” and fails at a stress level below the nominal strength of the material.

The fatigue life of a component can be expressed as the number of loading cycles required to initiate a fatigue crack and to propagate the crack to critical size. Therefore, it can be said that fatigue failure occurs in three stages: crack initiation; slow, stable crack growth; and rapid fracture.

In the first stage, dislocations accumulate near surface stress concentrations and form structures called persistent slip bands (PSB) after a large number of loading cycles. PSBs are areas that rise above (extrusion) or fall below (intrusion) the surface of the component due to movement of material along slip planes. This leaves tiny steps in the surface that serve as stress risers where tiny cracks can initiate. These tiny cracks (called microcracks) nucleate along planes of high shear stress which is often 45^o to the loading direction.

In the second stage of fatigue, some of the tiny microcracks join together and begin to propagate through the material in a direction that is perpendicular to the maximum tensile stress. Eventually, the growth of one or a few crack of the larger cracks will dominate over the rest of the cracks. With continued cyclic loading, the growth of the dominate crack or cracks will continue until the

remaining uncracked section of the component can no longer support the load. At this point, the fracture toughness is exceeded and the remaining cross-section of the material experiences rapid fracture. This rapid overload fracture is the third stage of fatigue failure.

2.1 Distresses on flexible pavements

Flexible pavements suffer distresses, which have different causes, and lead to different types of failure. The most characteristic are:

2.1.1 Fatigue (alligator) cracking

Interconnected cracks caused by fatigue failure under repeated traffic loading. The cracks can develop from the bottom or from the top of the surface layer depending if it's thin or tick. After repeated loading, the longitudinal cracks connect forming many sided and sharp-angled pieces.

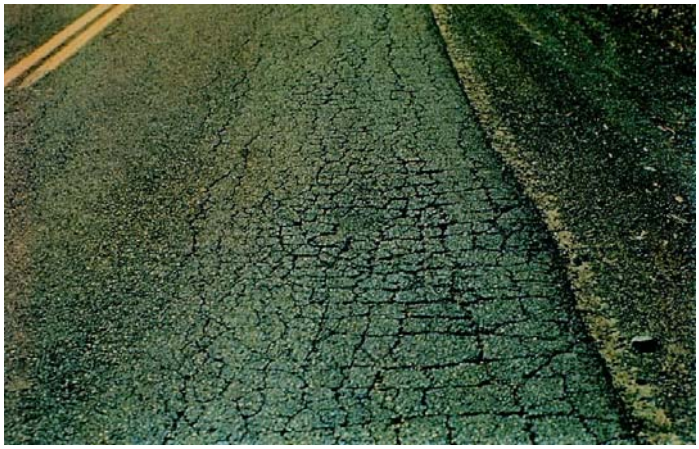

Figure 2.1: Alligator cracking

The causes can be many, but principally inadequate structural support given by a decrease in pavement load supporting characteristics, by the increase in loading or by and inadequate structural design.

2.1.2 Block cracking

Interconnected cracks that divide the pavement up into rectangular pieces. The temperature cycling at which the asphalt undergoes is the main cause of this distress.

2.1.3 Depression

Localized pavement surface areas with slightly lower elevations than the surrounding pavement, these depressions are very noticeable after a rain when they fill with water. The causes can be resumed to a frost heave or subgrade settlement resulting from inadequate compaction during construction.

2.1.4 Longitudinal cracking

Cracks parallel to the pavement's centerline or laydown direction. Usually a type of fatigue cracking, that once it happens, allows moisture infiltration, roughness, indicates possible onset of alligator cracking and structural failure.

2.1.5 Transverse cracking

Cracks that are predominately perpendicular to pavement centerline and are not located over Portland cement concrete joints. Thermal cracking is typically in this category.
There are many other distresses that a flexible pavement can suffer, such as bleeding, corrugation, shoving, raveling, potholes and rutting.

2.2 Study of fatigue

Engineering materials have been observed to fail as a result of the repeated application of stresses that are of considerably less than their single cycle or static load fracture stress. The repeated stresses that are insufficient in magnitude to produce failure in one cycle nonetheless induce damage in the

material with every cycle. This damage accumulates and ultimately leads to failure. Such failure in a material is known as fatigue failure. Traditionally, engineers have designed against fatigue by using S-N diagrams in which the magnitude of the alternating stresses (S) is plotted versus the logarithm of the number (N) of cycles to failure.

An engineering structure may be designed to resist fatigue by limiting the magnitude of the stress applied to the structure to values less than those described by the S-N curve. In case of some materials, the S-N diagram identifies a stress amplitude threshold below which fatigue failure would not occur even after an infinite number of load applications. Thus, using this information, design stresses can be limited to a value below the failure threshold.

Although a simple concept, the S-N diagram approach has two drawbacks:

- Large numbers of time-consuming tests are required to prepare the S-N diagrams.

- The concept does not address the mechanics of the fatigue process.

Recognizing this need, Paris (1962) used concepts of fracture mechanics to demonstrate that the rate of change of crack length with the number of applied stress cycles was proportional to the difference in stress intensity factors, ΔK_I, computed at applied stress levels. Paris and Erdogan (1963) later proposed the following equation:

$$\frac{dA}{dN} = A(\Delta K_I)^m$$

In this equation, dA and dN represent the rate of change of crack growth with the number of applied cycles. The parameters A and m are material constants.

This concept was extracted from the fracture studies, and it had to be adapted to the viscoelastic materials. With other types of materials, the area around the crack tip is small enough, and its effect on the total elastic deformation can be neglected. A viscoelastic material goes through a time-dependent flow, which are irreversible deformations which dissipated energy.

2.1.1 Energy dissipation model

Under the repeated loading that is used in fatigue testing, energy is designated with each loading cycle. In materials such as asphalt cement and asphalt concrete, the energy dissipation results from viscoelastic and plastic flow mechanisms. In the energy dissipation criterion for fatigue developed here, it is hypothesized that failure under cyclic loading occurs when the energy absorbed in each cycle in excess of a certain non-damaging amount accumulates to a critical value. The total dissipated energy obtained by summing the areas of hysteresis loops under cyclic loading is assumed to be a measure of fatigue damage. In order to develop the energy dissipation model for fatigue, it is necessary to determine the energy dissipated per cycle, which can be mathematically represented by the following equation:

$$\Delta W = \sigma_t * d \in_t$$

In this equation, ΔW represents the energy dissipated per cycle, the other parameters represent the stress and strain.

2.1.2 SUPERPAVE protocol

The study of fatigue is directly related to the rheological parameter G*sinδ, which represents the loss portion of the complex modulus and is related to the total energy dissipated per cycle. This parameter is obtained in the linear viscoelastic range, which represents a simplification of the phenomena.

The concepts of viscous flow and energy dissipation were explored in an effort to derive binder parameters that more effectively relate binder to mixture

performance. Suggested specification parameters and test protocols were developed for three concepts:

- Permanent deformation, the viscous component of the binder creep stiffness, *GV*, measured by a repeated creep test in the dynamic shear rheometer (DSR).

- Fatigue cracking, the number of cycles to crack propagation, N_p, measured by a repeated cyclic loading test in the DSR.

- Low-temperature cracking, a direct measurement of the binder's glass-transition temperature combined with failure stress and strain for a region-specific design cooling rate measured with the bending beam rheometer and the direct tension device.

Chapter III

SUPERPAVE MIX DESIGN.

3.1 Strategic Highway Research Program (SHRP)

In 1987 the U.S. Congress established a 5-year, $150 million applied research program aimed at improving the performance, durability, safety, and efficiency of the Nation's highway system. Called the Strategic Highway Research Program (SHRP), this program was officially authorized by the Surface Transportation and Uniform Relocation Act of 1987 and consisted of research concentrated in four key areas (FHWA, 1998):

1 *Asphalt*. This area consists of research to develop a completely new approach to HMA mix design.

2 *Concrete and structures*. This area consists of research in the areas of mix design and assessing, protecting and rehabilitating concrete pavements and structures.

3 *Highway operations*. This area consists of pavement preservation, work zone safety and snow and ice control research.

3 *Pavement performance*. This area consists of the Long Term Pavement Performance Program (LTPP), a 20-year study of over 2,000 test sections of in-service U.S. and Canadian pavements to improve guidelines for building and maintaining pavements.

The SHRP asphalt research program had three primary objectives (NECEPT, 2001):

- Investigate why some pavements perform well, while others do not.
- Develop tests and specifications for materials that will out-perform and outlast the pavements being constructed today.

- Work with highway agencies and industry to have the new specifications put to use.

SHRP research activities were completed in 1992 and SHRP was closed down in 1993. To date, SHRP has produced more than 100 new devices, tests and specifications and, perhaps more importantly, has spawned a full-scale on-going implementation drive by such organizations as the FHWA, AASHTO and TRB. The final result of SHARP is "SUPERPAVE".

“SUPERPAVE”, which stands for SUperior PERforming Asphalt PAVEments, is an overarching term for the results of the asphalt research portion of the 1987 - 1993 Strategic Highway Research Program (SHRP). SUPERPAVE, in its final form consists of three basic components:

1. *An asphalt binder specification*. This is the PG asphalt binder specification.

2. *A design and analysis system based on the volumetric properties of the asphalt mix*. This is the SUPERPAVE mix design method.

3. *Mix analysis tests and performance prediction models*. This area is not yet complete. Test development and evaluation is on-going as of 2002.

Each one of these components required new specifications and performance standards as well as new testing methods and devices.

3.1.1 Used materials

3.1.1.1 Bitumen

For this thesis, following the mix design SUPERPAVE, first was chosen a bitumen. The chosen bitumen was a plain 50-70 penetration Grade bitumen.

A 50/70 Bitumen is a thermoplastic material which softens as it is heated and hardens as it is cooled. This unique temperature/viscosity relationship is important when determining its performance parameters and application temperatures. For classifying a bitumen as a 50-70 Bitumen it should accomplished some requirements:

Binder properties	Requirements		Test Method
	Min	Max	
Penetration @ 25 °C/100g/5s, dmm	50	70	ASTM D5
Softening Point, °C	46	56	ASTM D36
Dynamic viscosity @ 60 °C, Pa·s	140	250	ASTM D4402
Dynamic viscosity @ 135 °C, Pa·s	0,22	0,45	ASTM D4402
Spot test, % Xylene	-	30	AASHTO 102

Table 3.1: Binder required properties

Used bitumen, for this mix design, accomplished previous requirements, having:

Binder properties	Test result
Penetration @ 25 °C/100g/5s, dmm	63
Softening Point, °C	48,3
Dynamic viscosity @ 60 °C, Pa·s	186
Dynamic viscosity @ 135 °C, Pa·s	0,33

Table 3.2: Binder properties

Considering bitumen characteristics there are some recommendations of use that can be applied without further studies, these are:

Asphalt mixing temperature	150 – 160 °C	
Asphalt compaction temperature	135 – 145 °C	
Maximum storage temperature	< 24 hours	>One day
	160 °C	140 °C

Table 3.3: Mixing and compaction temperatures

Was chosen an asphalt mixing temperature of 160°C and a compaction temperature of 140°C.

Considering that this bitumen was going to be employed in laboratory experimental trails it was not classified with the SUPERPAVE Performance Grade, retaining to be enough a penetration grade classification.

3.1.1.2 Aggregate

Following bitumen selection, it has to be choose the load-bearing skeleton, it means, the aggregate gradation.

It was decided to prepare an aggregate gradation starting from 4 different granulometrical classes plus filler. The 4 granulometrical classes were taken from the CoGeFa cave in Torrazza, Piemonte, provincia di Torino; it was a crushed stone aggregate classified according to Cogefa in:

CoGeFa's granulometrical Classes (100% passing sieve – 100% Retained sieve)			
30-15	15-8	8-3	0-5

Table 3.4: CoGeFa's granulometrical Classes

According to preliminary calculation it was necessary to take:

	Granulometrical Classes			
	30-15	15-8	8-3	0-5
Mass Required (Kg)	70	20	50	110

Table 3.5: Mass required for each granulometrical class.

All this material was washed to eliminate all fine (<75μm), doing so, it could be controlled the proportion of fines in the final mixture. The material was washed with water, making it go through two sieves of 2 mm and 75μm.

Figure 3.1: Sieves used to wash the aggregates

After washed the material, it was desiccated in an oven at 110”C for at least 12 hours; Having the dried aggregate, a specific mass, of every granulometrical class was sieve in an electric sieve shaker with Timer SS 207/2 (Figure 3.2) for 20 minutes, using the sieve serie of 25; 19; 12,5; 4,75; 2,36; 1,18; 0,6; 0,3; 0,15; 0,075 mm.

Figure 3.2: Electric Sieve with Timer

Weighting the retained material in every sieve and calculating the proportion respect the total weigh it was built the granulometrical curve for every granulometrical class obtaining:

D	(15-30) %p	(8-15) %p	(3-8) %p	(0-5) %p	%p
25	100,0%	100,0%	100,0%	100,0%	100,0%
19	64,1%	100,0%	100,0%	100,0%	100,0%
12,5	0,8%	69,5%	100,0%	100,0%	100,0%
9,5	0,1%	11,2%	100,0%	100,0%	100,0%
4,75	0,1%	0,2%	33,9%	100,0%	100,0%
2,36	0,1%	0,1%	1,1%	75,6%	100,0%
1,18	0,1%	0,1%	0,5%	51,4%	100,0%
0,6	0,1%	0,1%	0,3%	34,2%	100,0%
0,3	0,1%	0,1%	0,3%	22,3%	100,0%
0,15	0,1%	0,1%	0,2%	11,3%	100,0%
0,075	0,0%	0%	0%	0%	100,0%

Table 3.6: Granulometrical gradation for each granulometrical class.

3.1.2 Aggregate gradation selection

For obtaining an aggregate gradation, knowing the different proportions contained in every granulometrical class, these were combined considering SUPERPAVE and CIRS restriction.

The SUPERPAVE mix design system guides selection of an acceptable aggregate gradation for a dense graded paving mix by means of control points and a restricted zone.

The control points and restricted zone are graphed on the Federal Highway Administration grading chart on which the percentage of aggregate passing a sieve size is plotted against the sieve opening size raised to the 0.45 power. The ASTM sieves specified for the SUPERPAVE system are presented in table 3.6 (SHARP A-407).

These control points, maximum density line and restricted zone proposed by SUPERPAVE are according to aggregate nominal maximum size. In specific, it was chosen a 19 mm aggregate nominal maximum size, and the corresponding control points, maximum density line and restricted zone for this nominal maximum size are presented in the following tables:

Control Points [19.0]			
Sieve [mm]	**D^0,45**	**Minimum**	**Maximum**
0,075	0,312	2	8
2,36	1,472	23	49
12,5	3,116		90
19	3,762	90	100
25	4,257	100	100

Table 3.7: SUPERPAVE gradation control points for 19mm Nominal Maximum Size.

Sieve Size Within Restricted Zone	D^0,45	Minimum and Maximum Boundaries of Sieve Size (minimum/maximum percent passing)	
		19 [mm]	
4,75	2,01610025	-	-
2,36	1,47166988	34,6	34,6
1,18	1,07732541	22,3	28,3
0,6	0,79463568	16,7	20,7
0,3	0,58170737	13,7	13,7

Table 3.8: SUPERPAVE gradation restricted zone for 19mm Nominal Maximum Size.

Maximum density line, Dmax 25 (mm)	
di (mm)	**(di/Dmax)^0,45**
25	100,00
15	79,46
10	66,21
5	48,47
2	32,09
0,4	15,55
0,18	10,86
0,075	7,32

Table 3.9: SUPERPAVE gradation maximum density line for 25mm maximum size.

By the other way, the CIRS normative proposed, according with maximum grain size, 2 granulometrical gradations, one a maximum gradation curve and the other a minimum gradation curve; between these two curves it should be the used granulometrical gradation. For make it easy it was proposed a middle gradation, so using the minimum quadratics method could be designed

a gradation that was for sure between the maximum and the minimum CIRS gradations. CIRS gradations are showed below.

CIRS Specifications Dmax 25mm				
Serie UNI		**% Passing**		
	D (mm)	**Min**	**Max**	**middle**
Sieve	25	100%	100%	100,0%
Sieve	19	79%	91%	85,0%
Sieve	15	65%	85%	75,0%
Sieve	10	55%	75%	65,0%
Sieve	5	35%	55%	45,0%
Sieve	2	25%	38%	31,5%
Sieve	1,18	17%	29%	23,0%
Sieve	0,4	10%	20%	15,0%
Sieve	0,18	5%	15%	10,0%
Sieve	0,075	4%	8%	6,0%

Table 3.10: CIRS gradations for 25mm maximum size.

Using the specific surface method, can be calculated how much bitumen should be used to cover every aggregate, being this quantity the bitumen percent first attempt. This method applies the next formula:

$$\%B = K * \Sigma^{1/5}$$

Where K is a constant that depends on which layer is being design. In specific it has been chosen K= 3,8; and Σ came from the next formula:

$$\Sigma = 0{,}17G + 0{,}33g + 2{,}3A + 12Q + 135f$$

where:

$$G = 1 - CP_{10}$$
$$g = CP_{10} - CP_5$$
$$A = CP_5 - CP_{03}$$
$$Q = CP_{04} - CP_{075}$$
$$f = CP_{075}$$

Where:

CP_{10}: 10 mm sieve passing

CP_5: 5 mm sieve passing.

CP_{03}: 0,03 mm sieve passing.

CP_{075}: 0,075 mm sieve passing.

Notably, this formula is an iterative cycle because it is needed the gradation curve for calculating the bitumen percentage and vice versa. It can be solve using linear programming with the following condition:

$$0{,}6 < \frac{filler\ mass}{bitumen\ mass} < 1{,}2$$

So, using a calculus sheet program it was design 4 different granulometrical gradations, each of them respecting the previous conditions, obtaining:

D (mm)	Mix 1	Mix 2	Mix 3	Mix 4
25	100,0%	100,0%	100,0%	100,0%
19	91,0%	100,0%	91,0%	90,0%
12,5	71,8%	85,5%	75,2%	71,0%
9,5	65,2%	57,8%	75,0%	68,0%
4,75	47,1%	52,5%	48,5%	55,1%
2,36	30,5%	40,6%	28,6%	39,0%
1,18	22,0%	28,8%	21,6%	29,0%
0,6	16,1%	20,4%	16,7%	21,9%
0,3	12,0%	14,6%	13,4%	17,1%
0,15	8,3%	9,2%	10,3%	12,6%
0,075	4,3%	3,6%	7,0%	7,8%

Table 3.11: Granulometrical gradations for Mix 1, Mix 2, Mix 3 and Mix 4.

For each of the previous gradations the results obtained from the specific surface method are showed in the next table:

Mix 1 %Bitumen first attempt		Mix 2 %Bitumen first attempt		Mix 3 %Bitumen first attempt		Mix 4, %Bitumen first attempt	
K	3,80	**K**	3,80	**K**	3,80	**K**	3,80
G	28,19%	**G**	14,49%	**G**	24,82%	**G**	29,03%
q	6,60%	**q**	27,71%	**q**	0,18%	**q**	2,97%
A	34,72%	**A**	17,17%	**A**	46,40%	**A**	28,97%
Q	26,18%	**Q**	37,02%	**Q**	21,60%	**Q**	31,19%
F	4,30%	**F**	3,60%	**F**	7,00%	**F**	7,84%
Σ	9,81	**Σ**	9,81	**Σ**	13,14	**Σ**	15,05
%B	6,00%	**%B**	6,00%	**%B**	6,36%	**%B**	6,54%
F/B	0,72	**F/B**	0,6	**F/B**	1,1	**F/B**	1,2

Table 3.12: Specific surface Method.

Drawing every curve it can be checked that every of them respect SUPERPAVE and CIRS restrictions. Doing this the following curves have been obtained:

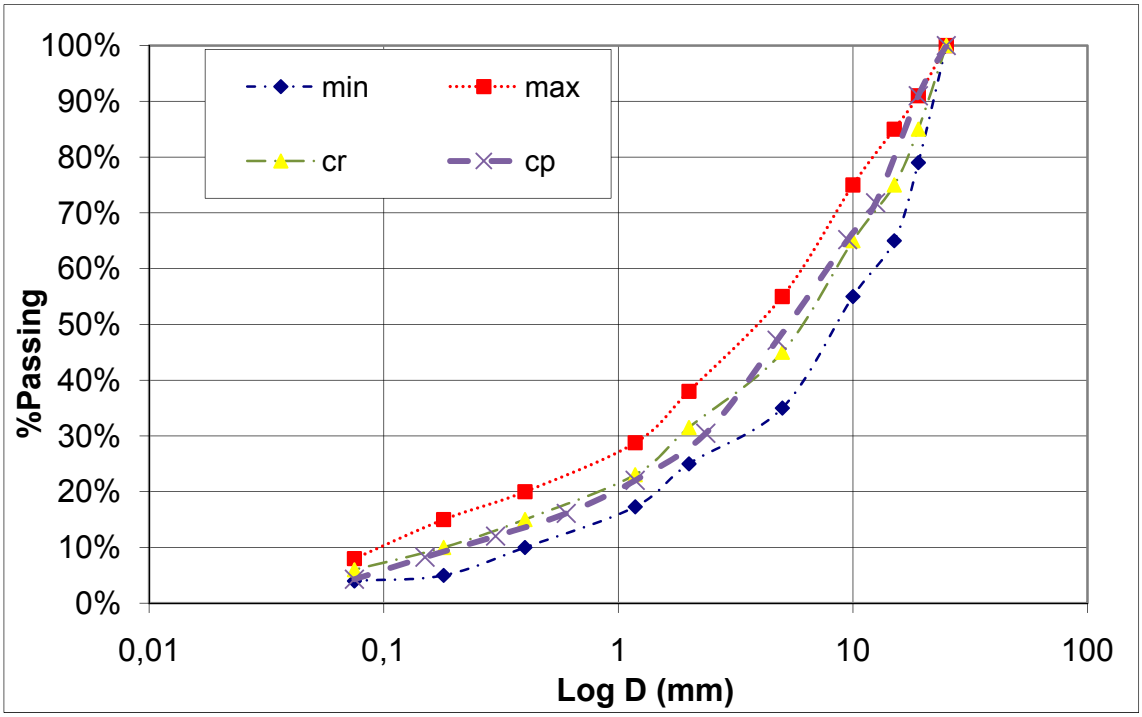

Diagram 3.1: Granulometrical curve of Mix 1 referred to CIRS curves.

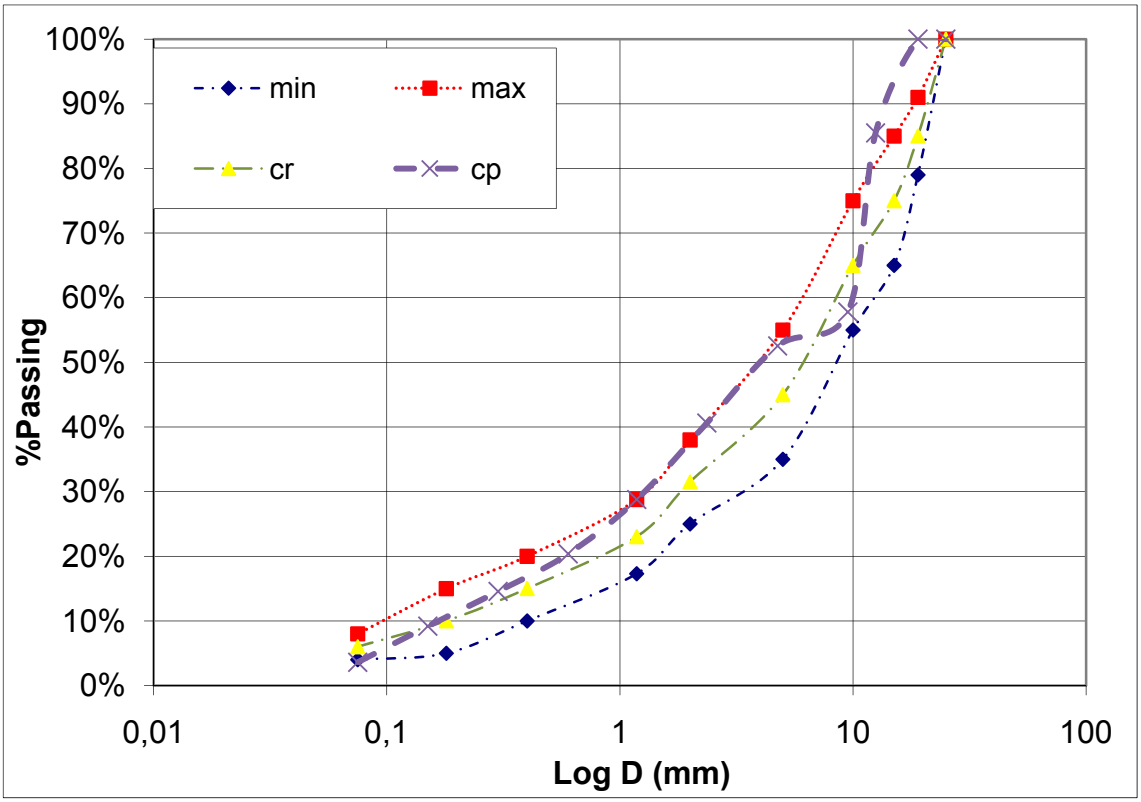

Diagram 3.2: Granulometrical curve of Mix 2 referred to CIRS curves.

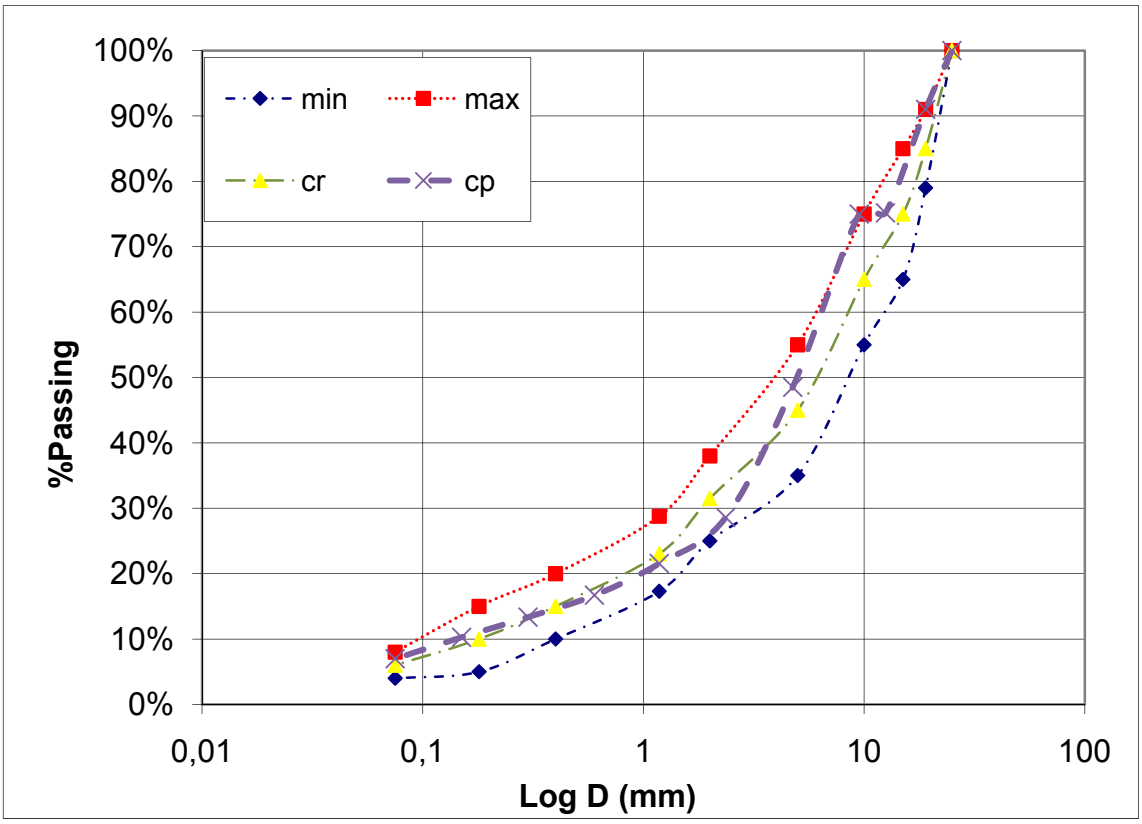

Diagram 3.3: Granulometrical curve of Mix 3 referred to CIRS curves.

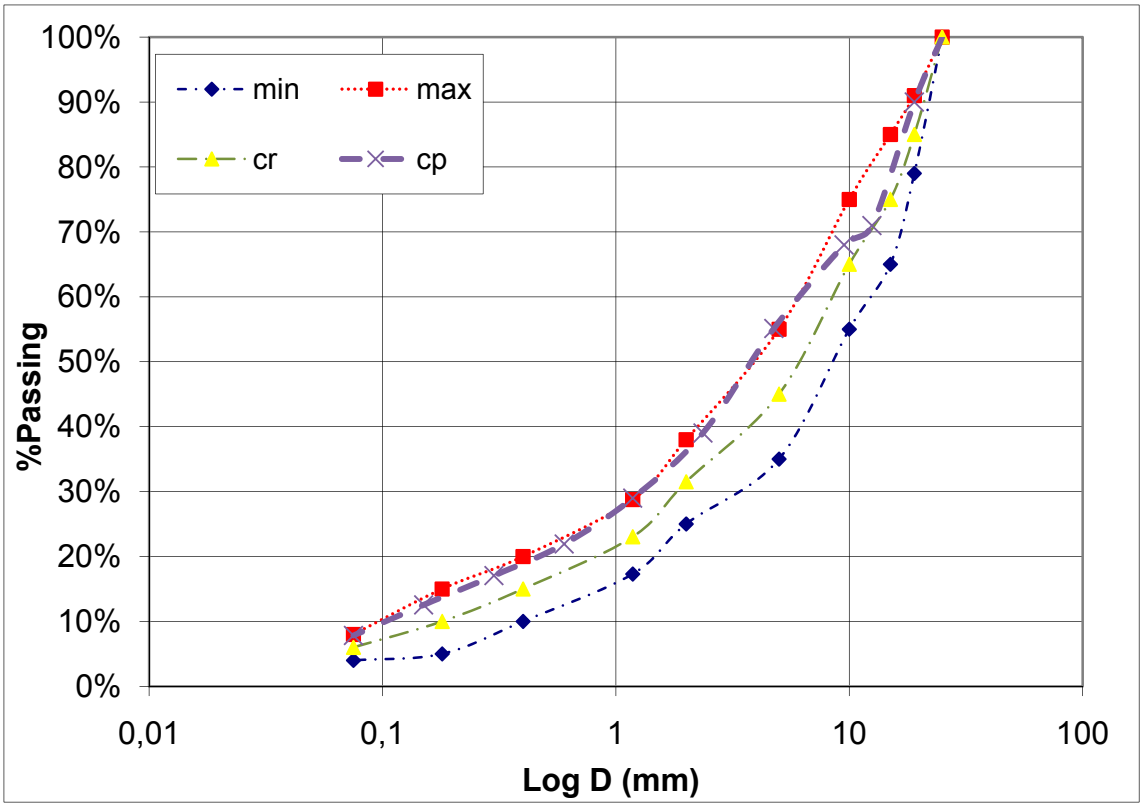

Diagram 3.4: Granulometrical curve of Mix 4 referred to CIRS curves.

Drawing the same curves considering SUPERPAVE requirements it has been obtained the following figures:

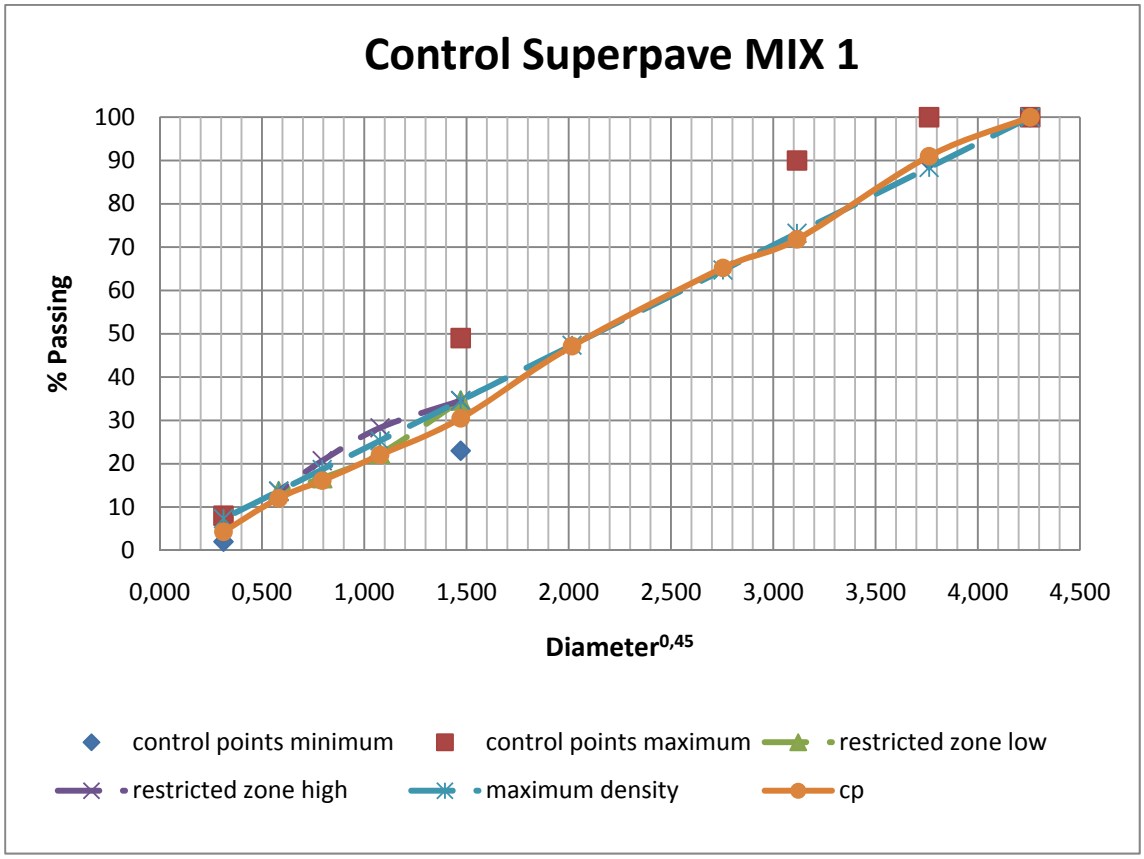

Diagram 3.5: Granulometrical curve of Mix 1 referred to SUPERPAVE restrictions.

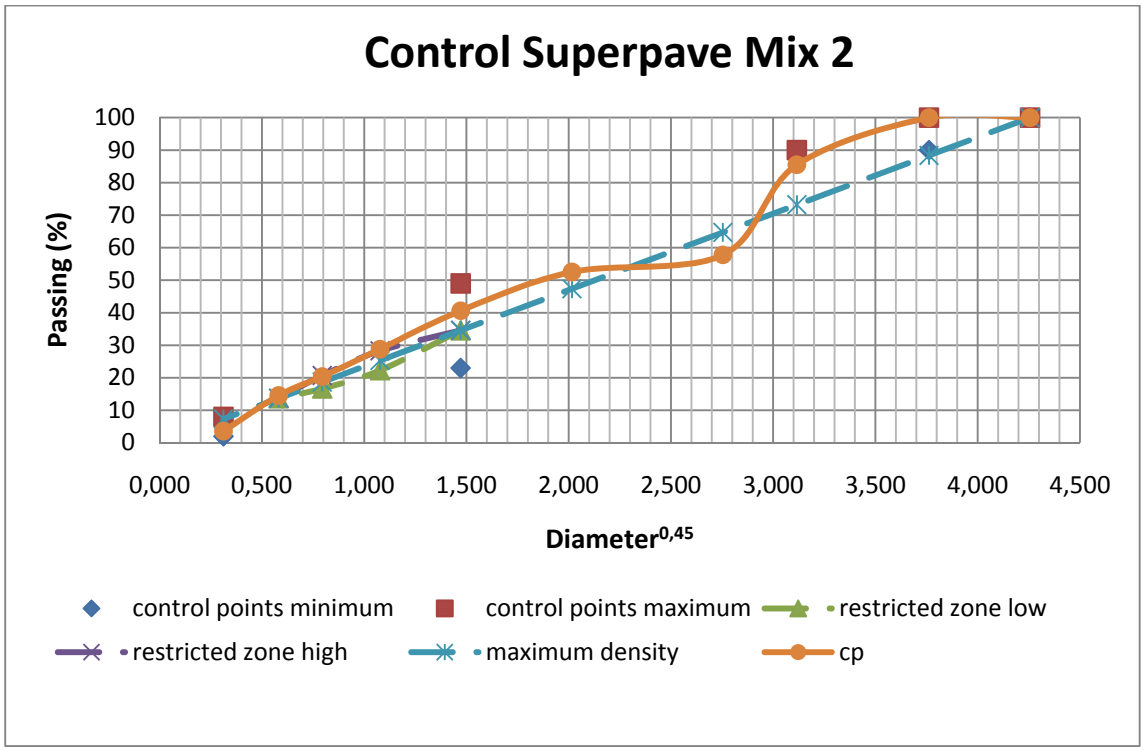

Diagram 3.6: Granulometrical curve of Mix 2 referred to SUPERPAVE restrictions.

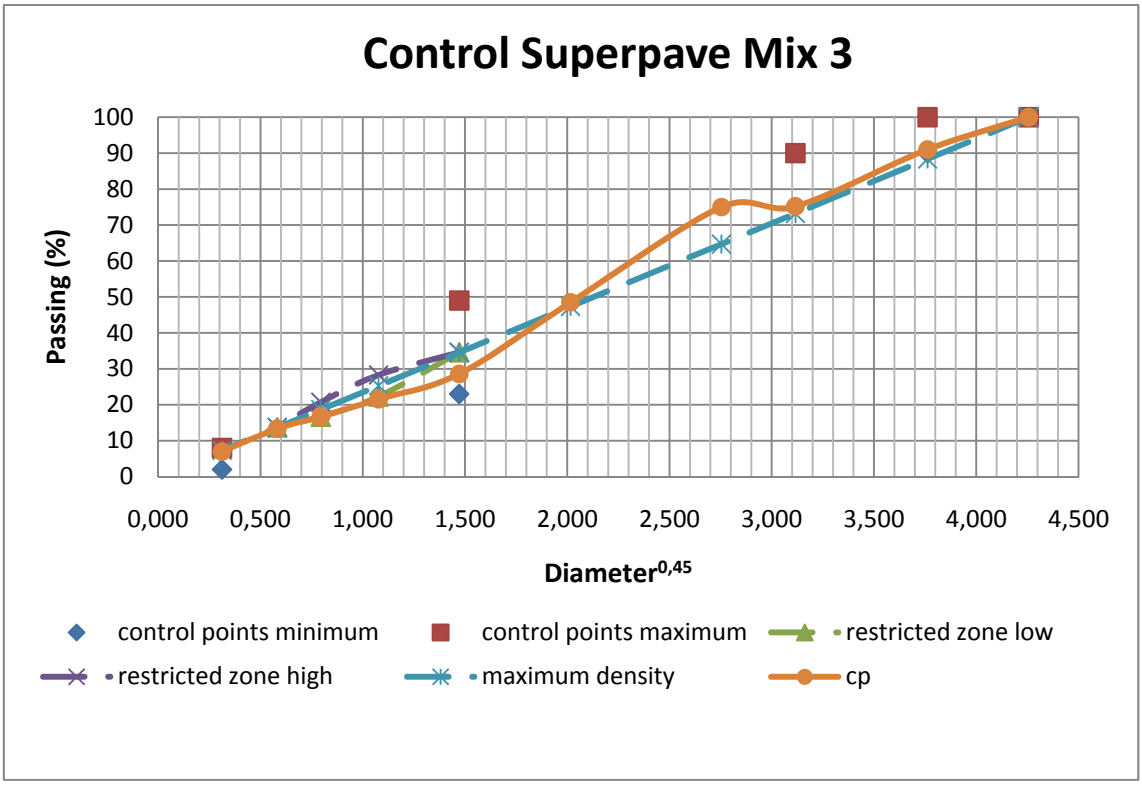

Diagram 3.7: Granulometrical curve of Mix 3 referred to SUPERPAVE restrictions.

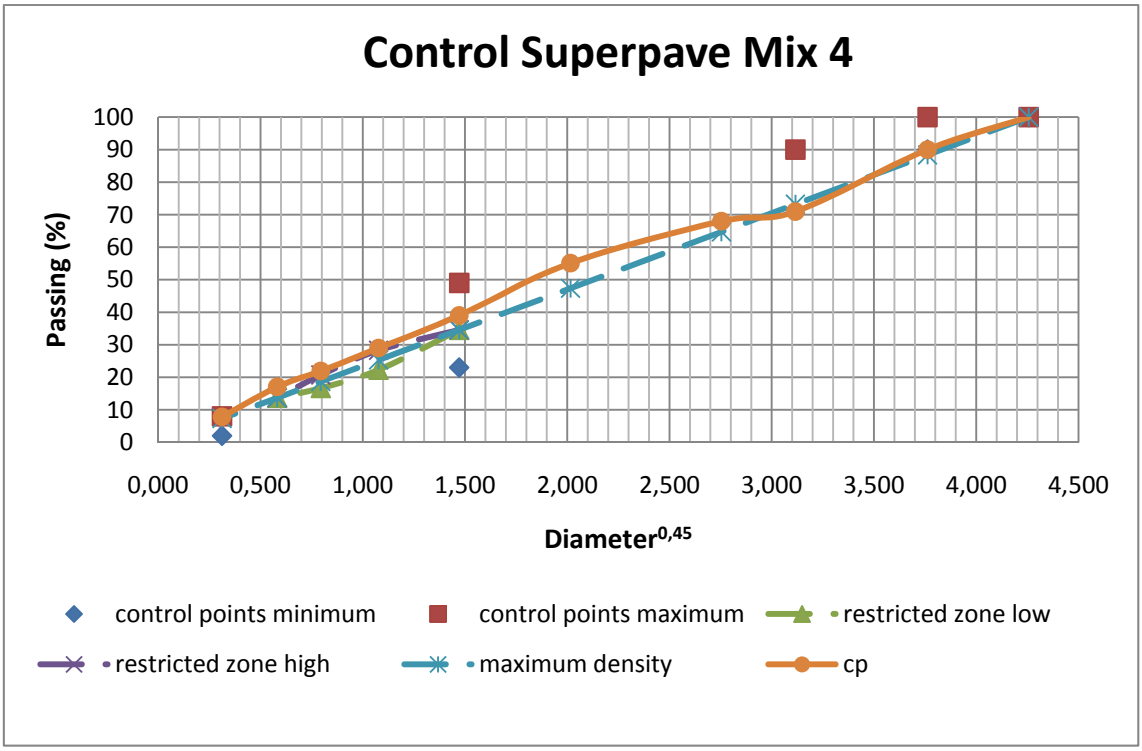

Diagram 3.8: Granulometrical curve of Mix 4 referred to SUPERPAVE restrictions.

It has been seen that generally all mixes respect either CIRS or SUPERPAVE requirements. After having the granulometrical gradations, samples of each mix have to be compacted with the gyratory compactor (refers to chapter IV for specific information about the gyratory compactor and the specimens preparation), to see if they accomplish the SUPERPAVE compaction requirements, these requirements are: Voids in Mineral Aggregate, Voids filled with asphalt and Voids percentage at a certain gyrations number (Nd) in the gyratory compactor.

3.1.3 Mixture selection

The compaction requirements were chosen considering a medium traffic level of ≤3x10^6 ESALS and a design 7-day Maximum Air Temperature (°C) of ≤39. With these considerations the compaction requirements are shown in the following tables.

Void in Mineral Aggregate Criteria		
Nominal Maximun Size		**Minimum VMA %**
9,5	mm	15
12,5	mm	14
19	**mm**	**13**
25	mm	12
37,5	mm	11
50	mm	10

Table 3.13: Voids in mineral aggregate Criteria.

Voids filled With Asphalt Criteria	
Traffic Level-ESALs	Design VFA %
<3*10^5	70-80
<3*10^6	**65-78**
<1*10^8	65-75
>1*10^8	65-75

Table 3.14: Voids filled with asphalt criteria.

TRAFFIC ESALS	DESIGN 7-day Maximum Air Temperature (°C)		
	<39		
	Ni	Nd	Nm
<3*10^5	7	68	104
<1*10^6	7	76	117
<3*10^6	**7**	**86**	**134**
<1*10^7	8	96	152
<3*10^7	8	109	174
<1*10^8	9	126	204
>1*10^8	9	143	235

Table 3.15: Gyrations number respect to traffic volume.

After having chosen the compaction requirements, the gyrations number at which samples should be compacted to obtain a 4% of voids is known, so it could be done the compaction with the gyratory compactor.

Two samples of each mix were compacted at Nf=134 and were evaluated their volumetric properties using the hydrostatic weight method and the pycnometer method; obtaining that Mixes 1, 2 and 3 at 134 gyrations did not accomplished a 4%±1% of Voids content, due to that they were discarded; instead Mix 4 Voids content was in range. To obtain a 4% voids content it

should be calculated a bitumen quantitative to add to the Mix to achieve the 4% voids content. This quantity could be calculated as:

$$\%B_{ad.} = -0{,}4 * (4 - (100 - \%C_{Nd}))\%$$

Obtaining that the bitumen quantity to add is:

$$\%B_{ad.} = 0{,}12\%$$

Considering that initial bitumen content ($\%B_i$) in Mix 4 was 6,54% respect aggregate, the resulting bitumen content was:

$$\%B_c = \%B_i + \%B_{ad.} \rightarrow \%B_c = 6{,}66\%$$

SUPERPAVE indicates that a Mix should be tested varying the bitumen content in -0,5%; +0,5% and +1%. Doing this is obtained 3 sub-mixes for Mix 4, being the bitumen contents as follow:

MIX 4			
%Bc-0,5%	%Bc	%Bc+0,5%	%Bc+1%
6,16%	6,66%	7,16%	7,66%

Table 3.16: Four different bitumen percentages for Mix 4.

These four mixes were compacted in the gyratory compactor at Nf=134 and were evaluated their volumetric properties using the hydrostatic weight method and the pycnometer method; obtaining that Mix %Bc-0,5% at 134 gyrations did not accomplished a 4% of Voids content, due to that it was discarded; instead all other mixes achieve a 4% voids content or lower.

After knowing which mixes accomplished a 4% voids content it has to be checked if they respect SUPERPAVE limits for voids in mineral aggregate (VMA) and voids filled with asphalt (VFA). The first step is to calculate the

bitumen content respect the whole mix not only respect the aggregate weight.in order to do this, it should be normalized every value respect the total mix, knowing that aggregates percentage are:

% aggregate		
(15-30) %p	β_1	0,28
(8-15) %p	β_2	0,05
(3-8) %p	β_3	0,19
(0-5) %p	β_4	0,41
Filler %p	β_5	0,08
	$\Sigma\beta$	1

Table 3.17: aggregate percentage in Mix 4.

It can be referred to the total mix adding the bitumen quantity and dividing by this sum. Doing this it was obtained:

		%Bc-0,5%	%Bc	%Bc+0,5%	%Bc+1%	
	%B	6,16%	6,66%	7,16%	7,66%	
	Σβ+%B	106,16%	106,66%	107,16%	107,66%	MV (g/cm3)
(15-30) %p	β_1 normalized	26,20%	26,08%	25,96%	25,84%	2,691
(8-15) %p	β_2 normalized	4,47%	4,45%	4,43%	4,41%	2,799
(3-8) %p	β_3 normalized	17,59%	17,51%	17,43%	17,35%	2,812
(0-5) %p	β_4 normalized	38,54%	38,36%	38,18%	38,01%	2,814
Filler %p	β_5 normalized	7,39%	7,35%	7,32%	7,29%	3,050
	Σβ normalized (%A)	94,20%	93,75%	93,32%	92,88%	
	%B normalized	5,80%	6,25%	6,68%	7,12%	

Table 3.18: Normalization of aggregate and bitumen percentage in Mix 4 referred to the total mixture.

Knowing the volumetric mass of each aggregate and how much of it is contained in the mix it could be calculated the γ_{max} of the aggregate mix as:

$$\gamma_{MAX} = \frac{\sum_{i=1}^{4} \beta_i * MV_i)}{\sum_{i=1}^{4} \beta_i}$$

From this formula it was obtained:

	%Bc-0,5%	%Bc	%Bc+0,5%	%Bc+1%
γmax	2,80	2,80	2,80	2,80

Table 3.19: Maximum aggregate density in mix 4.

From the compaction test with the gyratory compactor is known the voids content for Nd, and knowing the volumetric parameters VMA and VFA could be calculated as:

$$VMA = 1 - \frac{MV}{\gamma_{MAX}} * \%A$$

$$VFA = \frac{VMA - \%V_{Nd}}{VMA}$$

Obtaining:

	%Bc-0,5%	%Bc	%Bc+0,5%	%Bc+1%
MV	2,432	2,453	2,439	2,444
%V	5,26%	4,12%	3,71%	2,63%
VMA	18,11%	17,80%	18,63%	18,85%
VFA	70,96%	76,87%	80,11%	86,05%

Table 3.20: Mass density (MV), voids percentage, Voids in mineral aggregate and Voids filled with asphalt in mix 4.

Analyzing the data it is seen that the only mix that accomplished the compaction requirements is the mix with a bitumen quantitative of 6,66% respect the aggregate mass.

Because in this thesis was wanted to study a Rich Bitumen Base, the mixtures with a bitumen content of 7,16% and 7,66% were retained for the following studies, considering the mix with a bitumen content of 6,66% as the base mixtures and the others two as the enriched bitumen mixtures.

Chapter IV

EXPERIMENTAL TESTS

The work developed was intended to characterize a rich bottom base layer and its resistance to fatigue, crack propagation and its deformability. All tests were developed in the Laboratorio di Strade at the Politecnico di Torino. It was chosen a plain asphalt for all the different mixes prepared in the laboratory, this was the TOTAL 50/70.

This bitumen, for an easier handling, were poured from 5kg containers into 50g aluminum containers, and then stored in a place with no sudden or drastic temperature changes.

Figure 4.1: Different containers used for the bitumen

The bitumen TOTAL 50/70 was tested in the laboratory to determine:

- Its softening point, following the “UNI EN 1427:2007. Determination of the softening point with the ring and ball method” (Table 4.1). The equipment used for this test was a MATEST S.r.l. Automatic Ring & Ball B070N (Figure 4.2), found in the Laboratorio di Materiali Stradali.

TOTAL 50/70			
Softening Point (°C):	48,5	48,3	**mean**
			48,4

Table 4.1: Results from Softening Point test on TOTAL 50/70.

Figure 4.2: Automatic Ring & Ball

With this bitumen all the mixtures described in chapter III were prepared; from all those mixtures only 3 mixtures were retained as adequate for this thesis, these 3 mixtures were tested as follow.

4.1 Compaction of cylindrical samples with the Gyratory Compactor

The samples have been compacted after mixing and short-aging; they have 150 mm diameter, in height and weight they are variable according to test's requirements. The next table shows height, weight and cylindrical specimens number tested in each test:

test	Number of specimens	Approximate mean Height (mm)	Approximate mean weight (kg)
Mix design and TMD	12	52	2,15
SCB test	6	65	2.76
Modulus and Creep	11	60	2.57

Table 4.2: quantity and approximate mean dimensions of cylindrical specimens.

These specimens were compacted with the gyratory shear compactor supplied by the DITIC.

4.1.1 The gyratory shear compactor

The gyratory shear compactor, which was used for the compaction of cylindrical specimens, was produced by the U.S. manufacturer “Pine Instrument”. The dimensions of the machine are approximately 1220 mm wide, 730 mm deep and 1800 mm high with a total weight of 500 kg. The machine consists of these elements:

- A cell where the hollow punch containing the specimen is placed for compaction.
- A display for setting the compaction parameters and, when necessary, for calibration or verification of the machine.
- An internal computer for controlling all compaction stages and for storing data and heights during every gyration.
- Special program (which allows to determine the compaction curves).

- A hydraulic jack associated with three bond elements for the extrusion of compacted specimens.
- A work plan in steel.
- A compartment where the hollow punches are kept.
- A red emergency button that can lock the machine in case of need.

Inside the chamber of compaction the main elements are listed below and then indicated in the figure (Figure 4.4):

1) The ends of the press.
2) The rotating mechanical system: main arm fixed and united to the base.
3) The mechanical rotating system: movable main arm can tilt the hollow punch angle established.
4) The hollow punch.
5) Disc that allows the connection of the hollow punch to the tilt system using 2 rolls for each of the 3 arms.
6) The basis with a truncated cone shape.

Figure 4.3: gyratory shear compactor of the DITIC laboratory

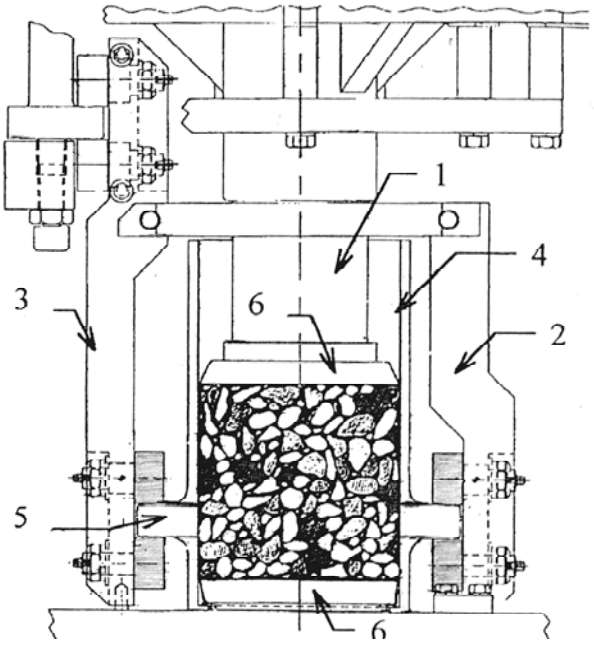

Figure 4.4: compaction chamber

The press is the only machine that doesn't compact the sample by gravity, but it acts through a mixed solicitation, shear and perpendicular to the sample axis. This method comes from the need to simulate, as precisely as possible, the on-field compaction; this operation is often performed on site with

rollers, or machines equipped with large cylinder (wheeled or not) that shrink the stretched thoroughly mix and reducing the gaps rolling on the pavement and applying a large normal force shrink the stretched thoroughly mix and reducing the gaps. The rotation of the hollow punch is made along an axis tilted at an angle to the vertical barycentric axis of the target. This asymmetrical rotation leads to a skewed and unbalanced movement, which generates a compact compression accompanied by a reshuffling of the mix due to shear forces similar to those generated by the rollers on the ground.

The simulative ability of the gyratory shear compactor (by compaction) enables high fidelity compared to other mechanisms of compaction even though it might seen very different from the compaction with the rollers. Regarding the more operational steps we can say that the control of all stages of compaction is performed by the internal computer: the operator simply enters the parameters of compaction and starts the procedure. The rotation of the hollow punch begins only when the desired set pressure and angle of inclination are reached. During compaction, the cell is closed by a glass door that stops the machine in case it came inadvertently open. For safety the machine is equipped with an emergency button that stops it when needed and a light inside the cell compaction to make visible the hollow punch during compaction.

During the operation, the internal computer checks that the correct pressure is applied to compaction and that the rotation takes place at an appropriate speed to detect the heights at every turn. It is possible to package samples with the 2 following methods:

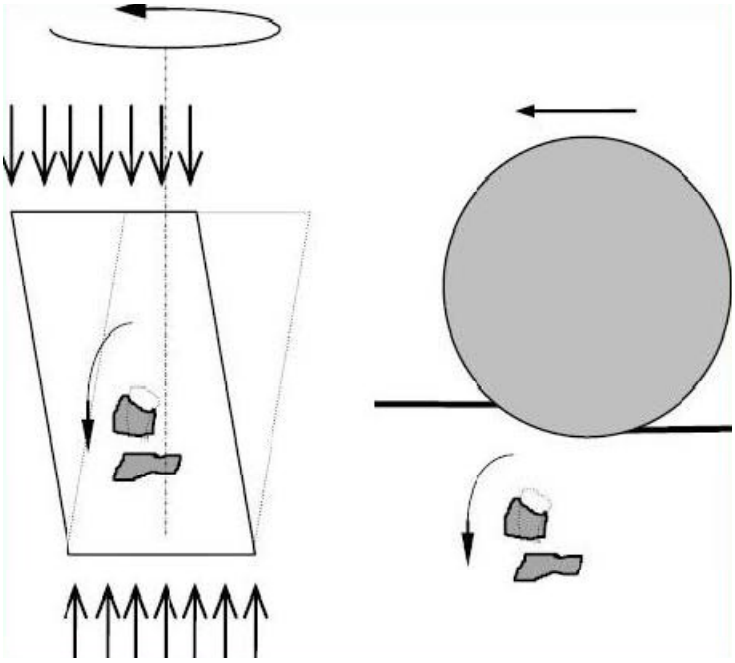

Figure 4.5: compactor operation scheme

- Compaction using the number of revolutions: in this situation the number of revolutions of compaction is set by the operator. Consequently, with the compaction pressure applied, the specimen reaches a variable height at the end of compaction;

- Compaction using the height of the sample: in this case the height of the sample at the end of compaction is imposed by the user instead. Consequently, with the compaction pressure applied, the number of laps will bring the specimen to reach the height set. With this method of compaction the user must also enter the maximum number of laps that the machine must perform: this value is necessary to prevent the machine continues to perform rotations trying to reach heights that the sample cannot reach.

It is possible the compaction of specimens with a diameter of 100mm or 150mm; in both cases, the manufacturer provides the suitable equipment (upper and lower plate, hollow punch and load head). The parameters for the compaction can be digitally selected and set to the machine using a control panel with display (Figure 4.7). The following parameters can be set:

- rotation angle: 0.5 ° - 2 ° (+/- 0.02 °);
- rotation speed: 30 (+/- 0.5) rotations per minute;
- vertical pressure: 200-1000 psi (+/- 18 kPa to 600 kPa)
- Speed: 0-999 rpm.

The system is equipped with a PC, which collects on the spreadsheet the gyrations number and height that the sample reaches at every lap. With this data you can achieve compaction curves representing in a fairly comprehensive way the height variation in function of the compaction progress.

4.1.2 Preparation of cylindrical specimens

The aging process of the material was performed as described in SRHP-A-379 protocol, after aging were heated at compaction temperature (160°C) with the hollow punch (figure 4.6), the funnel and the closing plates (with a truncated cone shape).

Figure 4.6: hollow punch and closing plates

Before starting with the production of the sample, the gyratory shear compactor has to be digitally set using the front control panel (Figure 4.7). Pushing the button “SELECT” it is possible to scroll through the menu, with the button “ENTER” the feature can be selected and it can be changed trough the arrows on the side. The parameters to change once again depends on the test in which will be used the sample; for the Mix design process the compaction

was made setting the gyrations number at 134 gyrations, once the mix was determined compaction was made setting the specimen height according to what was needed for each test.

Figure 4.7: control panel

In order to catch all the output given by the gyratory shear compactor; the computer has to be turned on and so the program used by the gyratory shear compactor called “Pine PRJ” (an application of “Excel”). When the temperature of the mixture and of the gyratory compactor tools reaches 160°C, the process of compaction can start.

The hollow punch, their closing plates and the funnel are removed from the oven and placed on a level close enough to the compactor. After entering the bottom plate of the hollow punch is necessary to insert a filter of blotting paper (with the same size of the hollow punch) so that the conglomerate will not stick to the plate. Then the funnel is inserted into the hollow punch and the conglomerate, just extracted from the oven is poured inside; once completed this operation another filter of blotting paper is placed inside the hollow punch to separate the conglomerate from the closing plate.

The hollow punch is inserted into the compaction compartment and it is rotated clockwise until the contrast in the bottom is in contact with the cell. After closing the compartment, the compaction can be started pressing the key “START” on the control panel. When the compactor has completed the 134 laps, the door of the compartment is opened and the hollow punch is blocked on the steel plain of the compactor with the three bonds elements (figure 4.8) near the hydraulic jack for the extrusion.

Figure 4.8: The steel plain of the compactor with the three bonds elements.

The specimen is allowed to cool for about twenty minutes; to speed up the operation compressed air can be used. Through the hydraulic pump the inner plate is traced along the hollow punch and slowly the specimen is extruded. Even during the extrusion compressed air is insufflate on the sample to help it cooling.

When the extrusion is finished, the sample is put on a paper over a shelf and allowed to cool for one night. Turning the knob near the hydraulic jack, the plate returns to its original position and the hollow punch can be placed in the oven

with the other compaction tools. After 15-20 minutes the hollow punch reaches the compaction temperature and another sample can be produced.

4.2 TMD

As described in chapter II, the bitumen was mixed with aggregate following the SUPERPAVE procedure; this procedure required the volumetric characterization of the bituminous mix, and one of the volumetric characteristic is the Theoretical Maximum Density, TMD.

The theoretical maximum specific gravity (often referred to as theoretical maximum density and thus abbreviated TMD) is the HMA density excluding air voids. The Theoretical Maximum Density (TMD) represents the volumetric mass of a mixture that has the maximum grade of thickening (a void percentage equal to zero). It is call theoretical because it is impossible in real life to be obtained.

This volumetric mass depends upon the relation between the mass of a specimen and the volume at the same temperature. It is an intrinsic property of the material that depends on the type and quantity of the bitumen and the aggregate.

This test is determined by the European regulation UNI-EN 12697-5, where the methodology for the calculation is established for a bituminous mixture that is ready to be used on the field but that hasn't been compacted. The TMD is calculated using the following equation:

$$TMD = \frac{MM}{(MM + MPW) - (MPMW + H)} * \frac{dw}{0{,}997}$$

Where:

MM = MPM – MP is the air mass of the untie material.

MPM is the mass of the pycnometer with the material.

MP is the mass of the pycnometer.
MPW is the mass of the pycnometer full of water.
MPMW is the mass of the pycnometer with the material and full of water.
H is the correction factor that takes into consideration the expansion of the bitumen with the change of temperature.
dw is the water density at the test temperature.

The TMD test was conducted using three different and calibrated pycnometers. For this test the material needs to be in loose condition, for untied the material the samples were heated approximate at 100°C and hand-forced to untie it, then about 700g of material were put into each pycnometer and filled with distillated water until about 2/3 of the pycnometer volume. After this is done, the pycnometers need to be attached to a void pump at about 27mbar for 20 minutes, to remove any entrapped air. It is important to move the pycnometers from time to time to make easier the air freeing.

Figure 4.9: Different steps of the TMD process

Registering the mass of the empty pycnometers, pycnometer plus material and full of water with the meniscus allows to determine the different values of TMD. The results obtained (Table 4.3) are a critical HMA characteristic; it is used to calculate percent air voids in compacted HMA, provide target values for HMA compaction, to determine others mixture volumetric characteristics as VMA and VFA and also to determine the quantity

of material that is needed to make the bituminous samples for each other test with a desired void percentage.

%bitumen	TMD
6,16%	2,567
6,66%	2,558
7,16%	2,533
7,66%	2,510

Table 4.3: Results of the TMD test for each bitumen percentage in Mix 4.

4.3 Hydrostatic weight

The hydrostatic weight is used to measure the materials density. It could be made on samples which voids content is low. It consist on three steeps. First the dry weight is measured, second the samples is immerged on water for at least 15 minutes or until the weight is constant and it is weighted immerged in water, after the measure is made the sample is taken out of water and as fast as possible is dried only superficially and weighted once more, this last measure is called saturated weight. For the calculation of the density is used the following formula:

$$D = \frac{dry\ weight}{(satured - immerged)}$$

For the measures depending on the sample there were used two different scales, which are shown in figure 4.10.

Figure 4.10: Scales used for hydrostatic weight.

4.4 Nottingham Asphalt Tester (NAT)

The NAT allows the measuring and assessing of the mechanical properties of asphaltic materials. It was developed at the University of Nottingham by its Research Group. It can perform a variety of test, in our case it was used for the indirect tensile test (stiffness modulus), static creep test and four-point bending fatigue test.

4.5 Stiffness Modulus

The stiffness modulus is the absolute value of the complex modulus $|E^*|$ or the value of the secant modulus, which is the relationship between stress and strain at the loading time, *t*, for a material subjected to controlled strain rate loading [EN 12697-26]:

$$E(t) = \frac{\sigma(t)}{\varepsilon(t)}$$

The complex modulus is the relationship between stress and strain for a linear viscoelastic material submitted to a sinusoidal wave form at time, *t*, where

applying a stress σx sin(ω x *t*) results in a strain ε x sin(ωx(t-Φ)) that has a phase angle, Φ, with respect to the stress

$$E^* = |E^*| \times (\cos(\Phi) + i \times \sin(\Phi))$$

The complex modulus is characterized by a pair of two components. This pair can be expressed in two ways: the real component E_1 and the imaginary components E_2:

$$E_1 = |E^*| \times \cos(\Phi)$$
$$E_2 = |E^*| \times \sin(\Phi)$$

The absolute value of the complex modulus $|E^*|$ and the phase angle, Φ:

$$|E^*| = \sqrt{(E_1^2 + E_2^2)}$$

$$\Phi = arctan\left(\frac{E_2}{E_1}\right)$$

The EN 12697-26 norm describes the different methods to perform the test like bending tests, direct and indirect tensile tests. The tests are performed on compacted bituminous material under a sinusoidal loading or other controlled loading, using different types of specimens and supports. The principle is that suitable shaped samples are deformed in their linear range, under repeated load or controlled strain rate loads. The amplitudes of the stress and strain are measured, together with the phase difference between stress and strain.

The test methods that can be adopted to calculate stiffness are:

- bending tests;
- indirect tensile test;
- Direct uniaxial tests.

In every kind of test the amplitude and the frequency of the loading signal shall be controlled by a feedback control, which may be based either on the force or on the displacement; furthermore, the amplitude of the load shall be such that no damage can be generated during the time needed to perform the measurements.

The temperature of the climatic chamber, in the vicinity of the specimen, shall be equal to the specified temperature to ±0,5°C other than for the direct tension test.

The measurements that shall be obtained during the test are the applied force, *F*, the displacement, *z*, and their phase angle Φ. The two components of the complex modulus shall be calculated in Pascal (Pa) using the following equations:

$$E_1 = \gamma \times \left(\frac{F}{z} \times \cos(\Phi) + \frac{\mu}{10^3} \times \omega^2\right)$$

$$E_2 = \gamma \times \left(\frac{F}{z} \times \sin(\Phi)\right)$$

The mechanical material characteristics shall be derived from the measurements using the specific factors given in table 2 of the norm (Figure 4.11) where:

- γ is a form factor as a function of specimen size and form
- μ is the mass factor which is a function of the mass of the specimen, *M*, in grams (g) and the mass of the movable parts, *m*, in grams (g) that influence the resultant force by their inertial effects.

The stiffness modulus (the absolute value of the complex modulus $|E^*|$) and the phase angle Φ, an equivalent representation of the complex modulus, shall be derived using the equations. For the indirect tensile test, the stiffness modulus is produced directly by the test equipment.

The Nottingham Asphalt Tester (NAT) calculates a stiffness applying indirect tension to cylindrical specimen (IT-CY).

Type of loading		Form factor, γ L^{-1}	Mass factor, μ
IT-CY	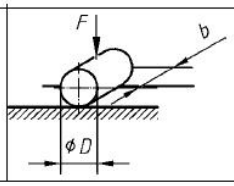	$\frac{1}{b} \times (\nu + 0{,}27)$	–

Figure 4.11: specific factors for indirect tension test for the measurement of stiffness modulus

The method is applicable to cylindrical specimens of various diameters and thickness, manufactured in the laboratory. The equipment used to perform this test is composed by:

- a steel load frame (Figure 4.12);
- Two stainless steel loading strips conforming to the table C.1 of the norm.
- A loading system. A suitable load actuator is incorporated by means of which a load can be applied along the vertical diameter of the specimen via the loading platens. The load actuator is capable of applying repeated load pulses with rest period. The load produced by the NAT has a haversine waveform or close to it. The loading time shall be controlled during the test. The rise-time, measured from when the load pulse commences and which is the time taken for the applied load to increase from zero to maximum value, is approximately (124 ± 4) ms. the applied load is measured using a load cell with an accuracy of 2 %. The pulse repetition period (Figure 4.13) is normally (3,0 ± 0,1) s. The recommended load area factor is 0,60. The recommended rise-time is (124 ± 4) ms but other rise-times may be used. The load pulse applied is selected to achieve a transient peak horizontal deformation. Experience indicates suitable values of peak horizontal deformation are (7 ± 2) μm

for a 150 mm nominal diameter specimen and (5 ± 2) µm for a 100 mm nominal diameter specimen;

- A deformation measurement system, capable of monitoring the transient horizontal diametral deformation of the specimen during the application of a load pulse. The accuracy of measurement shall be better than 1 µm over the range ±50 µm. The recorded peak horizontal deformation shall be the amplitude of the change in the horizontal diameter of the specimen. Two Linear Variable Differential Transformers (LVDTS) are mounted opposite one another in a rigid frame clamped to the specimen (Figure 4.14). During the test, the frame shall only be supported by the clamps and it shall not be in contact with any other part of the equipment;
- recording equipment, comprising a digital interface unit connected to a microcomputer;
- Constant temperature enclosure, consisting of a cabinet or a suitable room with forced air circulation, in which the specimen can be conditioned and in which the test can be performed.

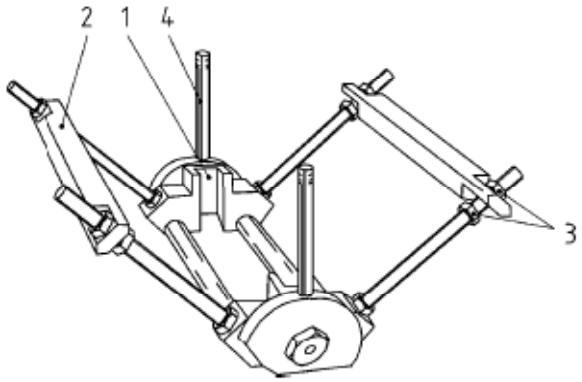

Key

1 Locating channel for loading frame
2 LVDT frame alignment frame
3 Alignment bar adjusting nuts
4 Alignment bar release lever

Figure 4.12: steel load frame

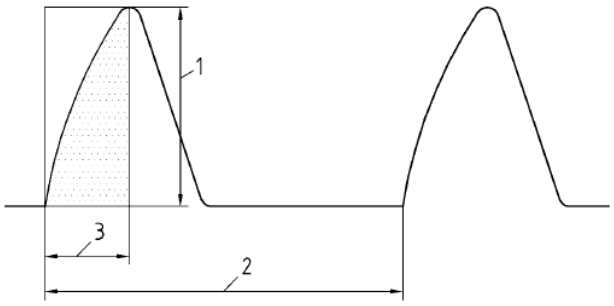

Key
1 Peak load
2 Pulse repetition period
3 Rise-time

Figure 4.13: pulse repetition period

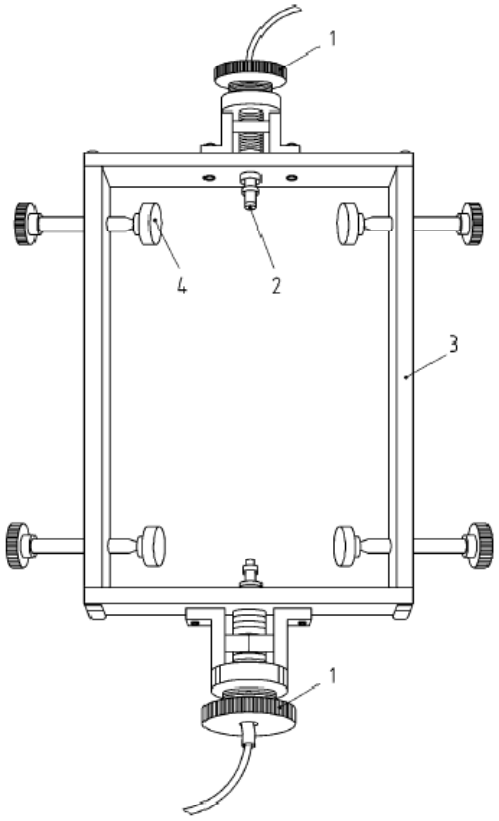

Key
1 LVDT adjuster
2 LVDT
3 LVDT mounting frame
4 Securing clamps

Figure 4.14: rigid frame and LVDT positioning

The thickness of each specimen shall be measured in accordance with EN 12627-29. Using a suitable marker, a diameter shall be drawn on one flat face of the specimen. A second diameter shall be drawn at (90 ± 10)° to the first. Both diameters shall be labeled appropriately. The storage temperatures

and time shall be recorded. Specimens shall be stored on a flat face on a horizontal surface and shall not be stacked.

The specimen shall be placed in a controlled temperature environment and monitored until it has attained the test temperature. The temperature of the specimen is determined using an electronic thermometer pointed on the surface of the specimen. The specimens were conditioned at the test temperature for one night in the refrigerator where the NAT is laid, so they had the same temperature both internally and externally. The temperature of the climatic chamber shall be within ± 0.5°C of the target temperature. The recommended test temperature for routine testing is 20°C, at higher test temperature, some mixtures may exhibit excessive deformation leading to collapse.

Before the use of the loading platens, they must be wiped clean using a solvent. After bringing the specimen to the specified temperature, the specimen shall be set up for the test with one of the marked diameters vertical. The setting up procedure, including the adjustment of the transducers and measurement system, shall be in accordance with the manufacturer's instructions. It is important that, in the case of LVDT, the mounting frame is clamped evenly and securely to the specimen. Care should be taken to ensure that no over-tightening of the securing clamps occurs.

The stiffness modulus is calculated after further 5 load pulses using the following formula:

$$S_m = \frac{F \times (\upsilon + 0{,}27)}{(z \times h)}$$

Where:

- S_m is the measured stiffness modulus, expressed in MegaPascal (MPa);
- F is the peak value of the applied vertical load, expressed in Newton (N);
- z is the amplitude of the horizontal deformation obtained during the load cycle, expressed in millimeters (mm);

- *h* is the mean thickness of the specimen, expressed in millimeters (mm);
- υ is the Poisson's ratio (0,35).

The measured stiffness modulus is adjusted by the software to a load area factor of 0.60 using the following formula:

$$S_m^{'} = S_m \times (1 - 0{,}322 \times (\log(S_m) - 1{,}82) \times (0{,}60 - k))$$

Where:

- $S_m^{'}$ is the stiffness modulus, expressed in MegaPascal (MPa), adjusted to a load area factor of 0,60;
- *k* is the measured load area factor.

4.5.1 Procedure

This test procedure is applied on all the 11 cylindrical specimen of the 3 bituminous mixtures in dry conditions.

The samples are stored for one night at the temperature of 20°C in a thermostatic cell. Before the storage, samples are measured in accordance with EN 12627-29.

Before starting the test, the transducers are mounted at the end of a steel support frame, fitted with screw clamps that allow the attachment of the entire frame at the diameter of a cylindrical sample. A system of rods to V, however, allows to place the frame horizontally. This system, at its base, has an asymmetrical crown which allows him to move away from the frame during testing. The displacement transducers LVDTs (linear variable differential transducers) are used to measure displacements up to 250 μm whose calibration be conducted annually. At this point, the sample is inserted into the frame and it is fixed with four screws and the transducers are adjusted. The cylindrical specimen is positioned along a diameter inside a frame bearing the additional bar system to V. The transducers are fixed to the sample by a support and the frame is positioned below the load structure by interposing a

centering ball between the piston of the load cell and the top element of the frame. This gives the test configuration, with the entire system inside the climatic chamber for accurate temperature control of the test.

The test is performed with the help of a software called “ITSM” that allows to select the time of peak load applied (between 60 and 120 ms) and the horizontal deflection. The control of such magnitudes is due to the acquisition and management system that operates a series of loop calibration during pulses of conditioning before the actual test. The load pulses are applied in order to enable the equipment to adjust the load magnitude and duration to give the specified horizontal diametral deformation and time.

Data to be entered on the computer connected to the machine are (Figure 4.15):

- diameter of the sample;
- Poisson ratio (0.35 at 20 ° C);
- test temperature [° C];
- peak time [120 ms];
- horizontal deformation (5 μm);
- Sample thickness [mm].

The proper choice of test conditions (speed of application of loads and temperature) is small enough to be applied to the linear theory of elasticity. The material is assumed to be homogeneous and isotropic. The elastic modulus of the amplitude function is therefore dependent on the geometry of the sample, the horizontal deformation resulting from the rate of Poisson. After entering the data, the position of the heads of the transducers to the specimen must be checked. The red flag means that the transducer is in contact with the sample, although there is a white flag. After this passage the conditioning of the specimen starts and it is performed by imposing load of 50 pulses at a pressure of 7 bar. The goal is to allow the sample to settle in order to have during the test, for each diameter, values of similar modules.

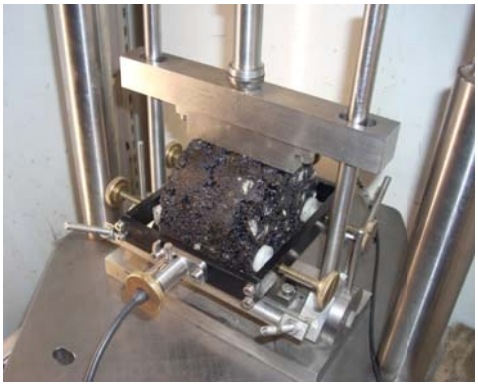

Figure 4.15: positioning of the specimen in the load frame before test

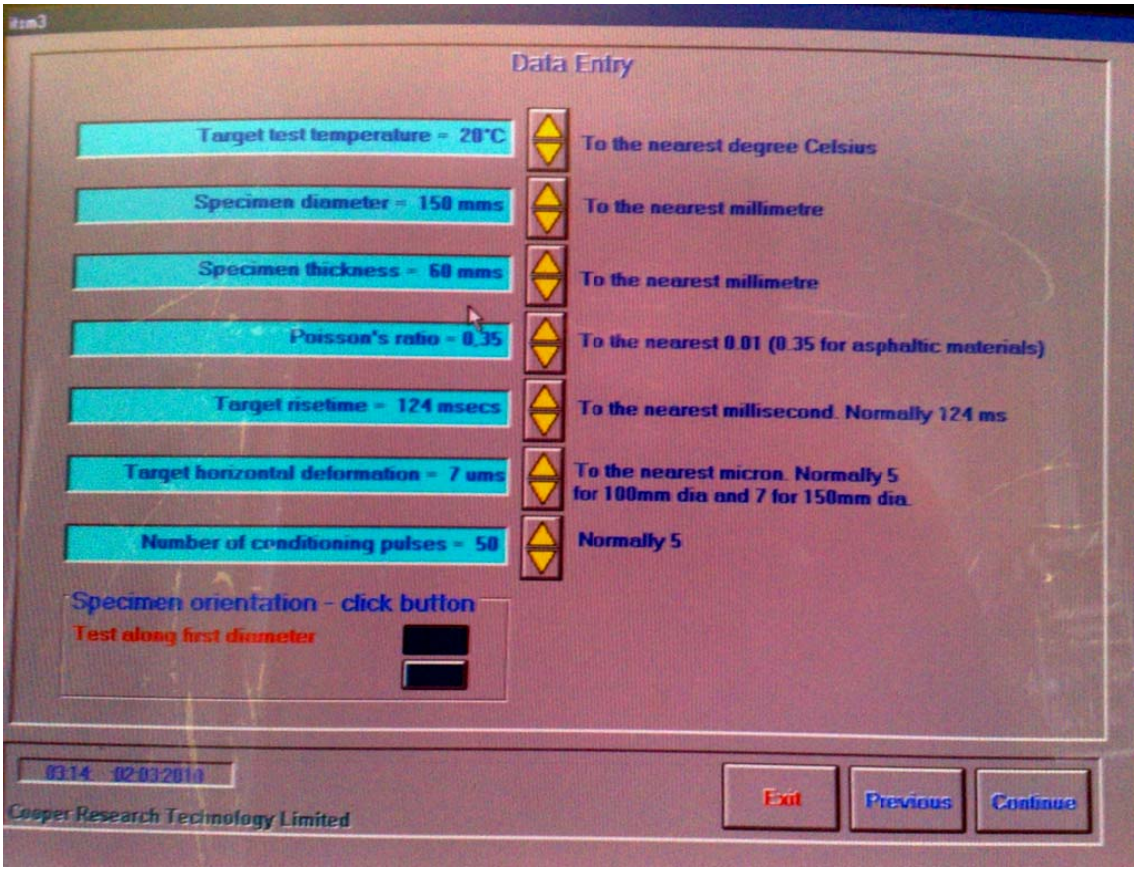

Figure 4.16: setting menu of the N.A.T. software

Once this first stage, the position of the heads of the transducers to the specimen must be checked again, in the case had gone off-center scale.

The second part of the test starts and 5 load pulses are applied; the monitor displays the data for the testing, which are:

- Vertical force (KN).
- Horizontal stress (KPa).
- Rise time (ms).
- Horizontal deformation (microns).
- Pulse shape factor (%).
- Stiffness modulus measured and adjusted (MPa).

After this operation the specimen shall be removed from the test equipment, rotated through (90 ± 10)° about its horizontal axis and replaced according to the test procedure described above. In this new position one more value of stiffness modulus is calculated. In this study was measured a third value of the stiffness modulus in a third diameter, according to the norm this procedure is necessary only if the first two measure differs in more than a 10%, even when in this study generally the first two measures differed less than 10% for every sample three measure were made. On completion of the test, no further test on specimen to this standard shall be carried out within 24 h.

The results obtained from the indirect tensile test for determining the stiffness modulus for mix 4 at each bitumen percentage are show below.

Mix 6,66%			
Statistic parameters	**stiffness Modulus (Mpa)**		**VARIATION**
	measured	**adjusted**	
MEAN	2259	2345	6,39%
STANDAR DEVIATION	148	150	
Mix 7,16%			
Statistic parameters	**stiffness Modulus (Mpa)**		**VARIATION**
	measured	**adjusted**	
MEAN	1816	1887	13,04%
STANDAR DEVIATION	235	246	
Mix 7,66%			
Statistic parameters	**stiffness Modulus (Mpa)**		**VARIATION**
	measured	**adjusted**	
MEAN	1643	1706	17,92%
STANDAR DEVIATION	294	306	

Table 4.4: Stiffness Modulus

4.6 Static Creep Test

The static creep test is characterized by a constant load acceleration. In particular, the static creep test is used to evaluate the characteristics of the material rather than uniaxial, triaxial stress, depending on whether or not the specimen is confined.

In creep testing, a cylindrical asphalt specimen is placed between two parallel steel-plates, of which only the lower one is fixed; on the top plate, which can translate vertically, a constant load is applied and the resulting deformation is analyzed as a function of time. Usually the results are relative and measure the height variation of the top plate position, this specification is made due to one uncertain with this test is that as the measure is not made on the specimen, it may be that part of the height variation measured is due to the plate seat in the top centimeters of the cylinder but the sample at its base is not disturbed.

For the asphalt is already known that for very short load times is predominant the elastic response while for longer time or higher temperatures, the response is predominantly viscous.

Through this test is measured the supposed deformation pattern of the specimen height over time under a constant load. Deformation is increased over time until the release of the load, after which the material tends to recover part of the deformation, due to the viscous component; this recovery will never be total.

This uniaxial test is a useful tool for assessing the effects on resistance to permanent deformation of the various mixture parameters (voids percentage, aging time, and test temperature). Usually it is tend to be used a test temperature of 40 ° C, because the high temperatures accentuate the viscous phenomenon.

The test was conducted on cylindrical asphalt samples 60 mm height and with a 150 mm diameter, in simple compression configuration, first an initial 6 minutes preloading period with a compressive stress of 10 KPa, after that the test start with a loading phase lasting 3600 seconds, during which it imposes a compressive stress of 100 kPa and a subsequent discharge of the same duration.

The significant parameters obtained are essentially the final deformation (εf) and deformability, equal to the inverse of the stiffness modulus S (t) and Diagrams ε vs t (figure 4.17). In the creep test It is also obtained the gradient of the deformation curve, in semi-logarithmic scale, expressing the greater or lesser tendency to accumulate the material deformation under constant load, the slope of the discharge curve in semi-logarithmic scale that expresses the ability to recover the deformation, the immediate elastic recovery percentage that has at the end of the loading phase and is equal to the difference of the deformation obtained after reversible discharge in relation to the deformation just prior to t = 3600 s.

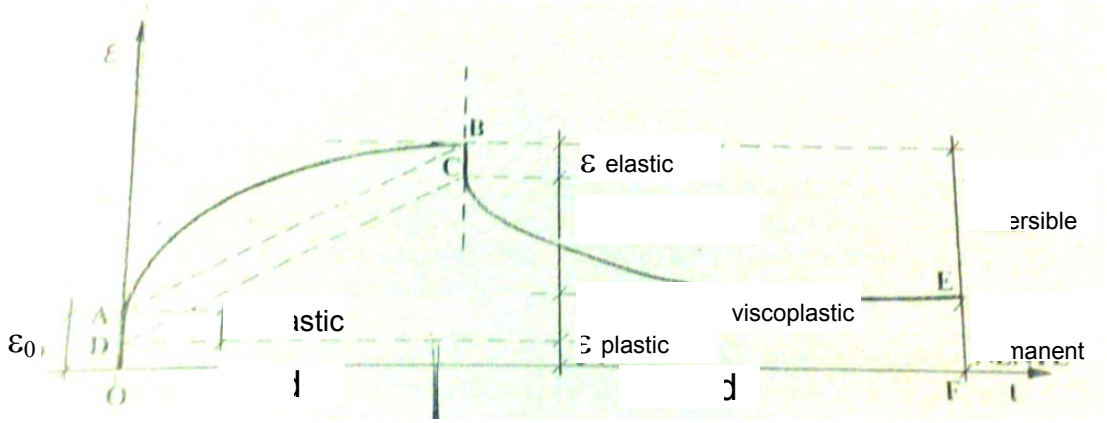

Figure 4.17:Typical Diagram Strain versus time for a Creep test

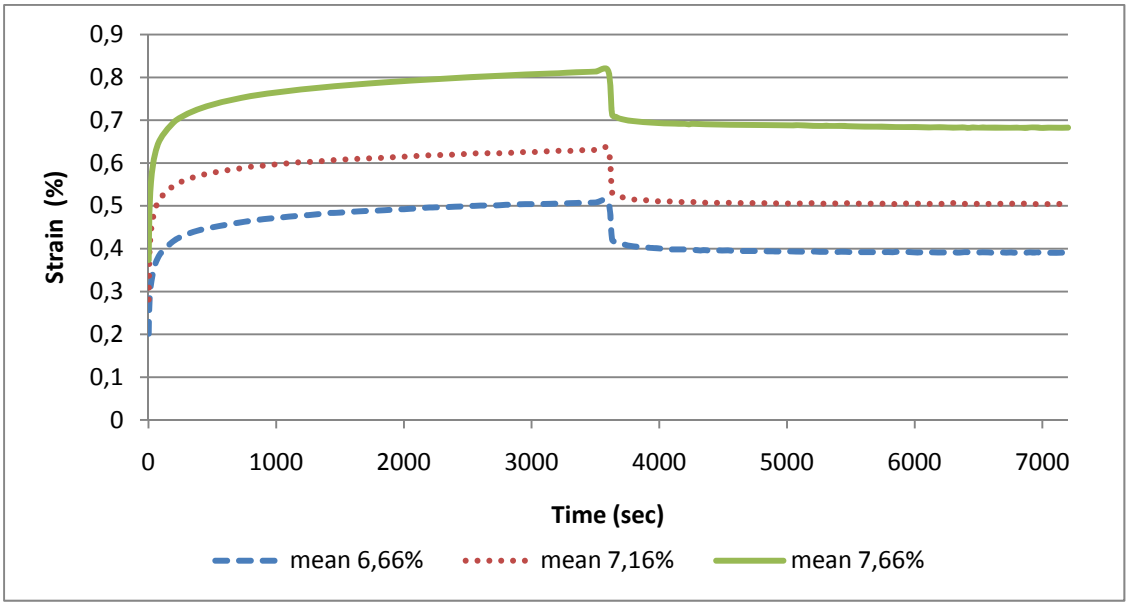

Diagram 4.1: Strain-time plot of the mean curves from the creep test for Mix 6,66%, 7,16% and 7,66%

From the static creep test the results obtained are shown in the following tables:

	Mix 4 6,66%			
	mean	**max**	**min**	**Units**
J_1	2,013E-03	2,229E-03	1,654E-03	[cm^2/daN]
J_{10}	2,838E-03	3,258E-03	2,311E-03	[cm^2/daN]
J_p	3,901E-03	6,176E-03	2,349E-03	[cm^2/(daN*s)]
ε_1	0,2013	0,2229	0,1654	[%]
ε_{10}	0,2838	0,3258	0,2311	[%]
$\varepsilon_{elastic}$	0,0869	0,0923	0,0812	[%]
$\varepsilon_{plastic}$	0,1143	0,1342	0,0781	[%]
$\varepsilon_{viscoelastic}$	-0,0319	-0,0444	-0,0245	[%]

Table 4.5: static creep test results for mix 4 at 6,66% of bitumen

	Mix 4 7,16%			
	mean	**max**	**min**	**Units**
J_1	2,890E-03	3,043E-03	2,697E-03	[cm^2/daN]
J_{10}	4,254E-03	4,778E-03	3,745E-03	[cm^2/daN]
J_p	6,051E-03	8,085E-03	4,587E-03	[cm^2/(daN*s)]
ε_1	0,2890	0,3043	0,2697	[%]
ε_{10}	0,4254	0,4778	0,3745	[%]
$\varepsilon_{elastic}$	0,1065	0,1195	0,0986	[%]
$\varepsilon_{plastic}$	0,1825	0,1943	0,1683	[%]
$\varepsilon_{viscoelastic}$	0,0300	-0,0345	-0,0212	[%]

Table 4.6: static creep test results for mix 4 at 7,16% of bitumen

	7,66%			
	mean	**max**	**min**	**Units**
J_1	3,737E-03	6,989E-03	2,064E-03	[cm^2/daN]
J_{10}	5,059E-03	8,206E-03	3,071E-03	[cm^2/daN]
J_p	6,827E-03	8,885E-03	4,033E-03	[cm^2/(daN*s)]
ε_1	0,3737	0,6989	0,2064	[%]
ε_{10}	0,5059	0,8206	0,3071	[%]
$\varepsilon_{elastic}$	0,1017	0,1245	0,0904	[%]
$\varepsilon_{plastic}$	0,2720	0,6066	0,1160	[%]
$\varepsilon_{viscoelastic}$	-0,0307	-0,0413	-0,0239	[%]

Table 4.7: static creep test results for mix 4 at 7,66% of bitumen

Where:

J_1 Deformability at 2 seconds

J_{10} Deformability at 10 seconds

J_p Plastic deformability

ε_1	Deformation at 2 seconds
ε_{10}	Deformation at 10 seconds
$\varepsilon_{elastic}$	Elastic deformation recovery
$\varepsilon_{plastic}$	Plastic deformation
$\varepsilon_{viscoelastic}$	Viscoelastic deformation recovery

J is calculated for the required instant (2sec, 10 sec) as:

$$J = \frac{strain_t}{Stress_t}$$

Jp is calculated as:

$$Jp = \frac{permanent\ deformation}{load\ stress}$$

ε_1 and ε_{10} are directly measured from the test, being ε_1,the deformation at 2 seconds and ε_{10} the deformation at 10 seconds.

$\varepsilon_{elastic}$ is calculated as the difference between the deformation at the of the load time and the first measured deformation when the unload time begins.

$\varepsilon_{viscoelastic}$ is calculated as the difference between the first measured deformation when the unload time begins and the deformation at the end of the test.

$\varepsilon_{plastic}$ is calculated as the difference between ε_1 and $\varepsilon_{elastic}$.

4.7 Semi-Circular Bend (SCB) Test

The gyratory compacted semi-circular specimens were used in Semi Circular Bend (SCB) test. The use of this type of specimens was first introduced by Mull et al. [2002] and later confirmed by the same author in another study [Mull et al., 2006]. Previously, Little and Mahboub [1985] and Dongre et al. [1989] used three point bending beam approach to evaluate the fracture resistance of asphalt mixtures. But they reported that the sagging of the beam

under its own weight, especially at elevated temperatures, might lead to a miscalculation of the critical value of J-integral. Gyratory compacted cylindrical specimens with desired notch depth were thought to be a possible solution to this problem. (kabir 2008).

The semi-circular shaped specimens were prepared by slicing a 150mm diameter by 65 mm high cylindrical specimens along their central axes into four semicircular samples, each sample was named according to the sample from which it came from using the same number, and according to its position, naming with H (High) the face compacted and with L (Low) the lower face, then with S or D depending on if it was the left side (S for (sinistra" in Italian) or right side (D for "Destra" in italian).

A vertical notch was then introduced along the symmetrical axis of each semicircular specimen in order to study the fracture properties of asphalt mixtures with regard to crack propagation. Two nominal notch depths of 33 mm and 15 mm were introduced using a special saw blade of 1,5 mm thickness, where each sample contained a single vertical notch along its symmetrical axis.

Mull et al. [2002] discussed that the linear elastic fracture mechanics theory is inadequate to evaluate the fracture resistance of asphalt pavements as they are considered as elasto-plastic material. Standard test methods that are used to evaluate the strength and stiffness of materials reveal only the behavior of homogeneous materials with no inherent defects. Being heterogeneous materials HMA mixtures do not fit into that category, which led researchers to characterize its fracture resistance using SCB test. This test is a traditional strength of materials approach that accounts for the flaws as represented by a notch of a certain depth which in turn reveals the resistance of the material to crack propagation, also known as the fracture toughness.

In this study, duplicate specimens were experimented for each notch depth and the test was performed at 20°C. To determine the critical value of J-integral (Jc), semi-circular specimens with at least two different notch depths

are needed to be tested. In this study, two notch depths of 15 mm and 33 mm were selected based on ongoing studies made by Cossale. Figure 4.18 shows the three-points bend load configuration used in the test and figure 4.19 shows the specimen dimensions.

Applying a constant cross-head deformation rate of 1 mm/min the specimens were loaded monotonically on an MTS machine till fracture failure occurred (Figure 4.18). The load and deformation were recorded continuously and the critical value of J-integral (Jc) was determined using the following equation presented by Rice [1968] that was later implemented by Wu et al. [2005]:

$$J_c = \left(\frac{1}{b}\right)\frac{dU}{da}$$

Where, b is sample thickness, "a" is the notch depth and U is the strain energy to failure.

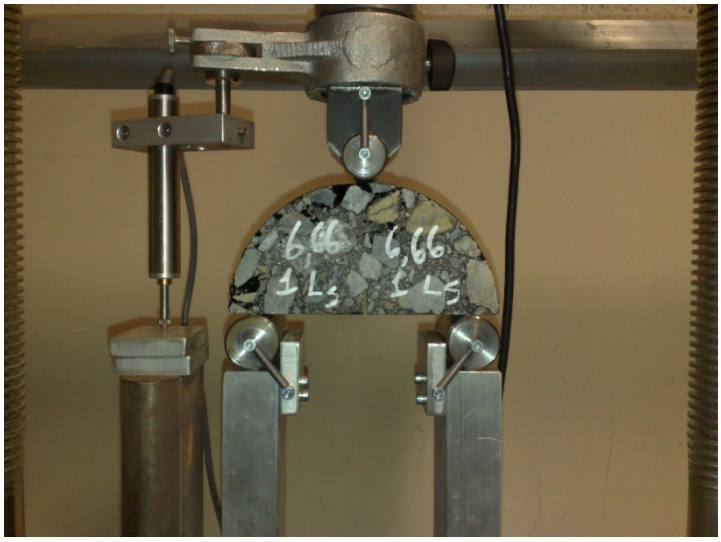

Figure 4.18: SCB Test Setup

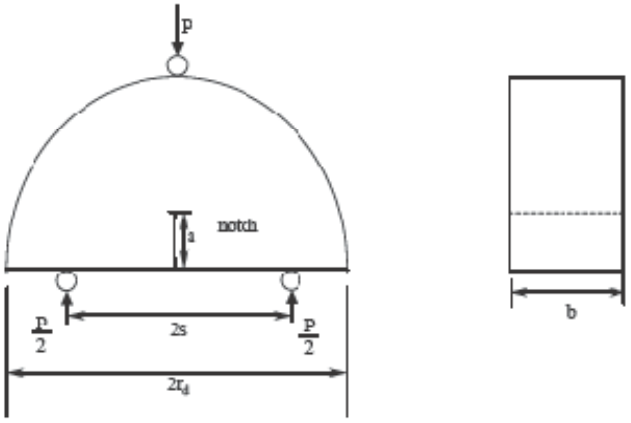

Figure 4.19: SCB sample dimensions. (Wu et al. 2005)

In Figure 4.21 a typical load-deformation plot obtained in a semi-circular fracture test is presented. In order to obtain the critical value of fracture resistance Jc, the area under the loading portion of the load deflection curves up to the peak load was measured for each notch depth per mixture. This area represents the strain energy to failure, U. The average values of U (calculated from duplicated specimens) were then plotted against the different notch depths to compute a slope of a regression line, which was the value of (dU/da). The critical value of facture resistance, Jc was then computed by dividing the dU/da value by the specimen width, b. (Kabir, 2008).

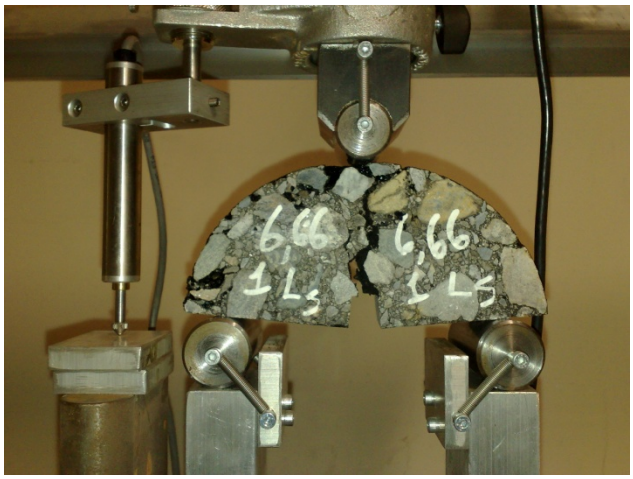

Figure 4.20: Failure of Specimen during SCB Test

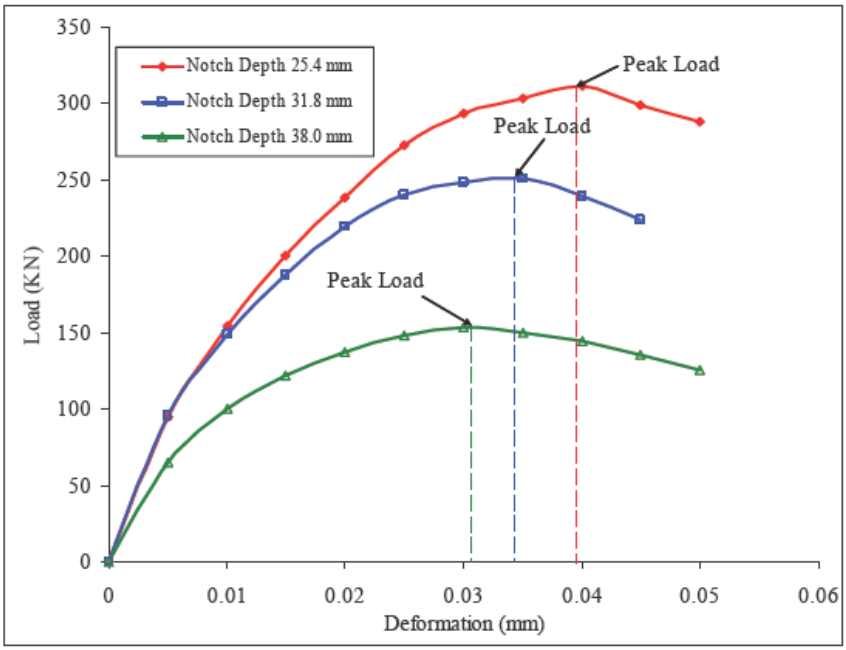

Figure 4.21: Typical Load Deflection Curves from a SCB Test (Kabir 2008)

The results obtained from the SCB test are resumed in the following table:

	notch (mm)	U (KJ)	Jc (KJ/m^2)
6,66%	15	0,00078	0,99472
	33	0,000183	
7,16%	15	0,000931	1,13452
	33	0,00022	
7,66%	15	0,000999	1,19309
	33	0,00025	

Table 4.8: Energy to failure (U) and fracture resistance (Jc).

Plotting these result it was obtain the following Diagram:

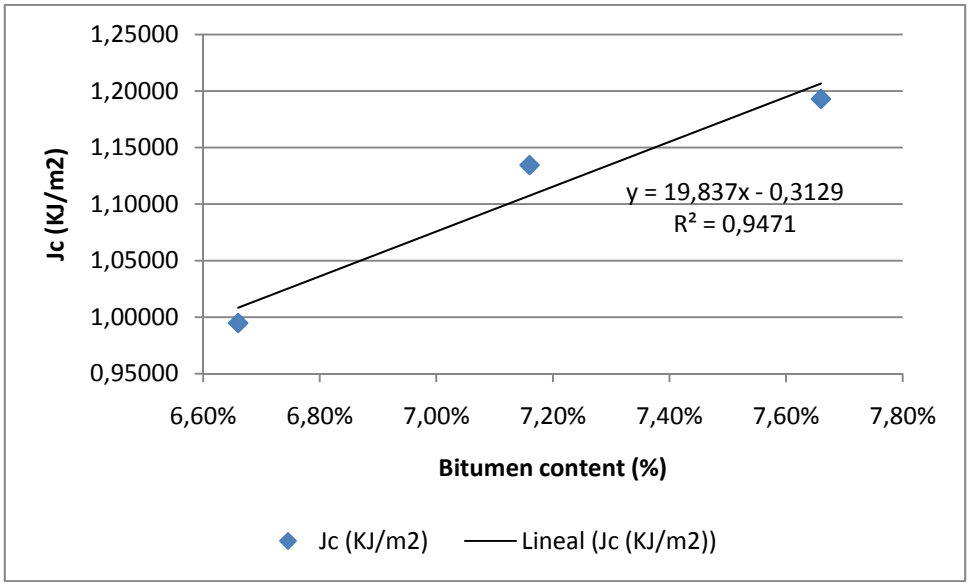

Diagram 4.2: Crack propagation resistance versus bitumen content.

4.8 Compaction of bituminous concrete slabs

For the compaction of the slabs, a BBPAC Roller Compactor from Vectra was used. This equipment allows to follow the specifications of the UNI EN 12697-33 legislation. The compactor consists of two parts, the compaction unit and the control boot (Figure 4.22).

Figure 4.22: Roller compactor

The control boot is where all the electro-mechanic elements that allow the input of the data to control the compaction are inserted. These parameters are: tire pressure, piston pressure, from which the force is applied to the material, the height of the plate from which the height of the slab is controlled and the passage position of the tire over the slab.

The compaction unit has three principal elements (Figure 4.23): a guide rail from which the tire moves horizontally (a), transversally and vertically, a steel level where the material is put and that can be moved to maintain the contact with the tire and allow the compaction (b), pneumatic pumps and electric systems of the machine (c).

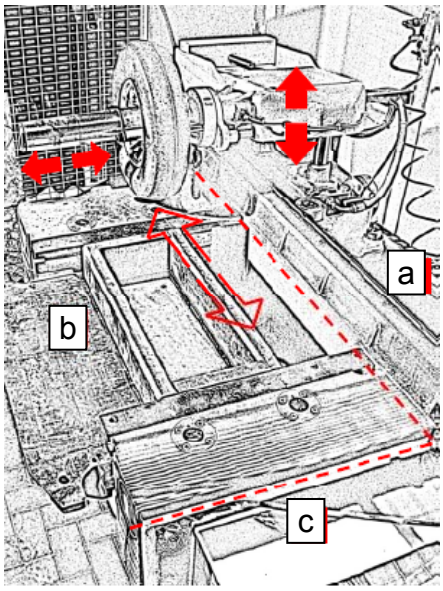

Figure 4.23: Principal elements of the compaction unit

Following the specifications of the European legislation, having the TMD value, the mould dimensions and the desired void percentage, the quantity of material to be compacted could be calculated as:

$$M = 10^{-6} * L * l * e * \rho_m * \left(\frac{100 - v}{100}\right)$$

Where:

L is the interior length of the mould.

l is the interior width of the mould.

e is the final thickness of the slab.

ρ_m is the value of the TMD test.

v is the desired void percentage.

The calculated mass needs to be augmented of 200g to take into consideration the material that is lost during the compacting process. The table presents the values used to calculate the quantity of bituminous material.

L (mm)	500
l (mm)	180
e (mm)	50
ρm (g/cm^3)	Variable depending on mix
v (%)	4
M (g)	Variable depending on mix

Table 4.9: Values used to determine the mass of binder to compact the slabs.

It is important to remember that the material before compaction needs to be heated at compaction temperature (160°C), with all the instruments that go in contact with the material (pans, moulds, plates and paddles).

Compaction process

The compacting process is divided in three stages, the first one is the homogenization stage, the second one the compacting stage and the third one is the finishing stage. The slab is divided into three stripes (front, rear and center) over which the tire passes (Figure 4.24).

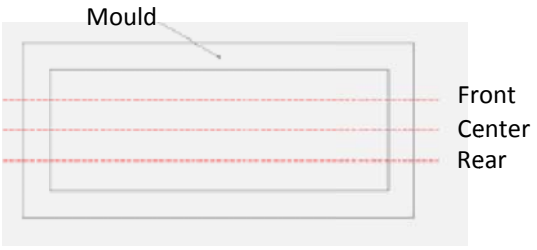

Figure 4.24: Divisions of the slab

The tire passages, as stipulated by the legislation, must be done following the different stripes in which the slab is divided. The tire pressure, the

load applied and the axle mode (blocked or freed) are also established by the legislation (Table 4.10).

	Number of passes					
	Position of the wheel					
	front	center	rear	Tire pressure (MPa)	Load (kN)	Axle mode
stage 1	1			0,1	1	Blocked
			1			
		1				
	1					
			1			
		1				
stage 2	2			0,6	5	Freed
			2			
		2				
	2					
			2			
		2				
	4					
			4			
		4				
	8					
			8			
		8				
	8					
			8			
		8				
	4					
			4			
		4				
	2					
			2			
		2				
	2					
			2			
		2				
stage 3	1			0,6	5	Blocked
			1			
		1				
	1					
			1			
		1				

Table 4.10: Sweep plan, heavy compaction for asphalt slabs

Geometrical void percentage

Once the nine slabs were compacted, the geometrical void percentage was calculated. Using the real measure of the slab, taken in 10 places along the length and 5 times along the width, and with the weight of the slab, the real void percentage was determined (Table 4.11).

MIX	TMD	weight (g)	Volume (mm^3)	density (Kg/cm^3)	%Voids
6,66% 1	2,558	11131,1	4619000	2,410	5,79%
6,66% 2	2,558	11127,8	4576400	2,432	4,94%
6,66% 3	2,558	11129,4	4637300	2,400	6,18%
7,16% 1	2,533	10661,5	4508100	2,365	6,63%
7,16% 2	2,533	10814	4753300	2,275	10,18%
7,16% 3	2,533	10981,5	4558000	2,409	4,88%
7,66% 1	2,51	10539,8	4424900	2,382	5,10%
7,66% 2	2,51	10701	4514400	2,370	5,56%
7,66% 3	2,51	10916,7	4459400	2,448	2,47%

Table 4.11: Geometrical real void percentage of the slabs

4.8.1 Asphalt beams

Once the slabs were done, it was needed to cut them in order to obtain the beams (Figure 4.25). The dimensions established for the beams were 381 ± 6.35 mm in length, 50.8 ± 6.35 mm in height and 63,5 ± 6.35 mm width. The slabs were cut at a marble cutting table. The samples were named according to the slab they came from with a number and the bitumen content and with a letter according to if it was the center of the slab (C), the right side (D for “Destra” in Italian) or the left side (S for “sinistra” in Italian).

Figure 4.25: Beams obtain from the asphalt slabs

4.9 Four-points bending fatigue test

The four-point bending fatigue test is an oscillatory one, which can be conducted with constant stress or strain over a prismatic beam of measures 500 mm in length, 50.8 ± 6.35 mm in height and 63,5 ± 6.35 mm width. On this type of testing, the beam is positioned on a frame blocked by four longitudinal and rotating cross-tilting supports (clamps) that can follow the deformation on the beam.

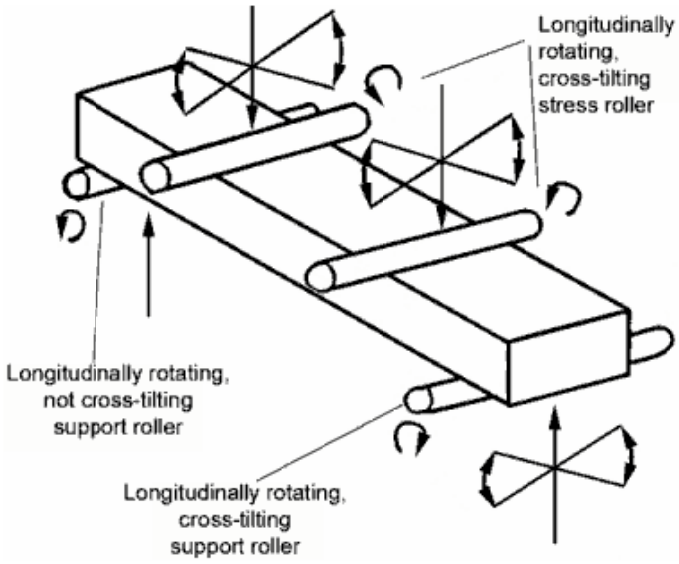

Figure 4.26: Schematic illustration of the four-point bending test

The two internal clamps are responsible for applying the vertical load over the beam; the two external ones remain fixed. It is usually followed the strain-control configuration; this creates a constant moment and deformation between the internal supports. During the test, the necessary applied forces to guaranty the strain are measure as a function of time, like the deflection and phase angle, allowing the calculation of the stiffness modulus and the fatigue behavior of the material.

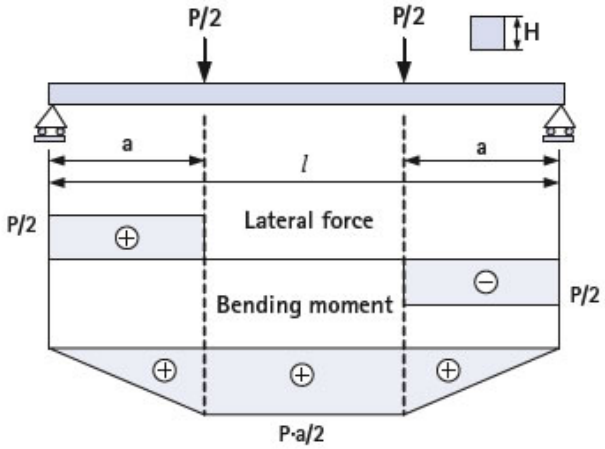

Figure 4.27: Schematic representation of the moments developed in a four-point bending fatigue test

According to the European regulations about Bituminous Mixtures UNI EN 12697-24: Test methods for hot mix asphalts, the frequency for the test should go between 0 and 60 Hz; the conditioning of the specimen should be of 1 hour for a test conducted at 20°C and of 2 hours if conducted at 0°C.

For a given temperature and frequency, the test shall be undertaken at not less than three levels in the chosen loading mode (three strain levels with the constant deflection mode). The levels for the chosen loading mode shall be chosen in such a way that the fatigue lives are within the range of 10^4 to $2*10^6$ cycles.

The initial value of the calculated stiffness modulus shall be calculated from the measured values of force, displacement and phase angle after the

hundredth cycle (n = 100). The test is terminated when the stiffness decreases to 50 percent of the initial stiffness or until the specimen breaks.. The output of the test is a curve of flexural stiffness as a function of load repetitions.

The calculated complex modulus of the specimen during one cycle, in MegaPascals (MPa) is obtained from the following equation:

$$|S^*| = \frac{12 * F_0 * L^3}{Z(X_s) * R(X_s) * B * H^3} *$$

$$* \sqrt{1 + 2\left[\cos\left(\varphi * (X_s)\right) * l(X_s) - \sin\left(\varphi * (X_s)\right) * J(X_s)\right] + [l^2(X_s) + J^2(X_s]}$$

Where:

F_0 represents the amplitude of the total force at the two inner clamps.

L is the distance between the two outer clamps.

$Z(X_s)$ is the amplitude of the deflection of the beam during inner cycle, measure on or between the two inner clamps at a distance X_s from the left outer clamp, in millimeters.

X_s is the co-ordinate where the deflection is measured, in millimeters.

B is the width of the prismatic specimen, in millimeters.

H is the height of the prismatic specimen, in millimeters.

φ is the phase angle during one cycle representing the system losses.

$R(X_s)$ is a weighing function, dimensionless, that depends on the distance x to the left outer clamp, the co-ordinate A of the left inner clamp and the effective length L between the two outer clamps. Is calculated with the expression:

$$R(x) = \frac{12 * L^3}{A * (3L * x - 3x^2 - A^2)}$$

$J(X_s)$ is the damping function, dimensionless, that depends on the distance x_s in order to account for damping (non viscous) effects in the system (system losses). It is calculated with the expression:

$$J(X_s) = T_{eq} * \frac{Z(X_s)}{F_0} * \omega_0 * 10^{-3}$$

ω_0 is the frequency of the applied sinusoidal load.

T_{eq} is the equivalent coefficient for damping, its value depends on the place where the deflection $Z(X_s)$ is measured. It's obtained using the following equation:

$$T_{eq} = \frac{R(X_s)}{R(A)} * T$$

The equipment used to perform this test (Figure 4.26 and 4.27) consists of a stainless steel load frame fitted with a pneumatic actuator and load transducer and capable of applying vertical loads. A LVDT deformation transducer allows to obtain the values of deformation at every cycle.

Figure 4.28: Load frame for the beam fatigue testing

Figure 4.29: NAT during a four-point bending fatigue test

The test needs to be conducted at a specific temperature of 20°C, so all the equipment is put into a temperature controlled cabinet (Figure 4.30). The samples were conditioned for at least one hour before testing.

Figure 4.30: Temperature controlled cabinet

The load frame is fixed inside the NAT with four bolts located on the lower plate; the upper part is fixed to the loading cell with a screw bolt (Figure

4.31). The beam is blocked inside the frame with four clamps, two outer and two inner ones. The deformation data of the beam is obtained with a transducer that comes in contact with the beam between the two inner clamps.

Figure 4.31: Screw bolt connection between load frame and loading cell

The “Four-points bending fatigue test” was performed following the SUPERPAVE protocol. The specimens were composed from same aggregate gradation and 3 different bitumen percentages, all subject to short-term oven aging. Beams specimens were tested using a 10-Hz loading frequency and It was chosen to use three different strain levels: 300, 450 and 600 microstrains.

4.9.1 Parameters for the four-point bending fatigue test

The test was conducted following the strain controlled procedure, inducing different deformations for the same material in order to obtain its fatigue curve. The temperature for the test was set at 20°C. Following what was indicated in the legislation, the initial complex modulus was obtained after 100 cycles, a frequency of 10Hz. The test was stopped when the fall of the initial complex modulus reaches 50% (Table 4.12).

Mode	Strain controlled
Frequency (Hz)	10
Temperature (°C)	20
test stop	50% of initial stiffness

Table 4.12: Parameters for the four point bending fatigue test

Chapter V

DATA ANALYSIS.

5.1 Statistic parameters

5.1.1 Mean

Where necessary a mean value ($\bar{X}$) was calculated as:

$$\bar{X} = \frac{\sum_{n=1}^{n} X}{n}$$

Where:

n is the number of measures

X the value for each measure

5.1.2 Standard Deviation

The standard deviation (SD) was calculated as:

$$SD = \sqrt{\frac{\sum(X - \bar{X})^2}{(n-1)}}$$

Where:

n is the number of measures

X the value for each measure

$\bar{X}$ is the mean value

5.1.3 Variation

The variation (V) was calculated as:

$$V = \frac{SD}{\bar{X}} * 100$$

Where:

SD is the value of the standard deviation

$\bar{X}$ is the mean value.

5.2 Mix design

As described in chapter III, for the mix design four different base mixtures were studied, choosing that which accomplished the SUPERPAVE gradation requirements. Then into the chosen mixture was varied the bitumen content in order to control the volumetric characteristics required by SUPERPAVE. In order to make an easier control of the volumetric characteristics, these are plotted in the following diagrams:

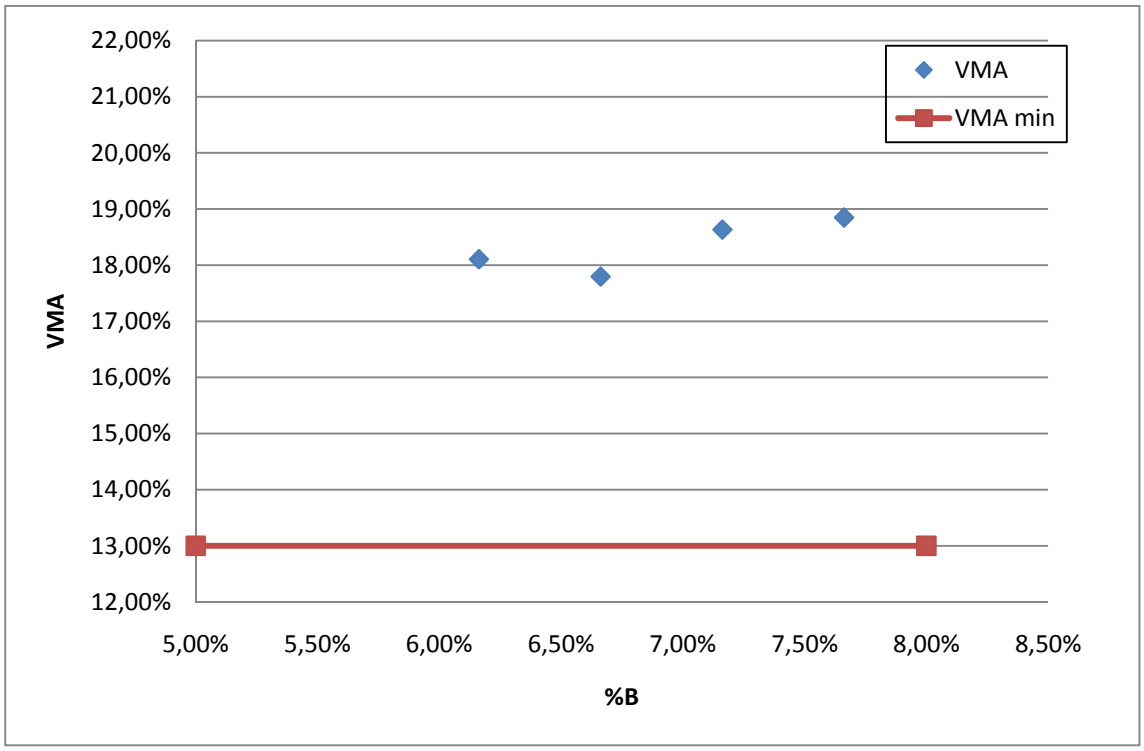

Diagram 5.1: Voids in Mineral Aggregate (VMA).

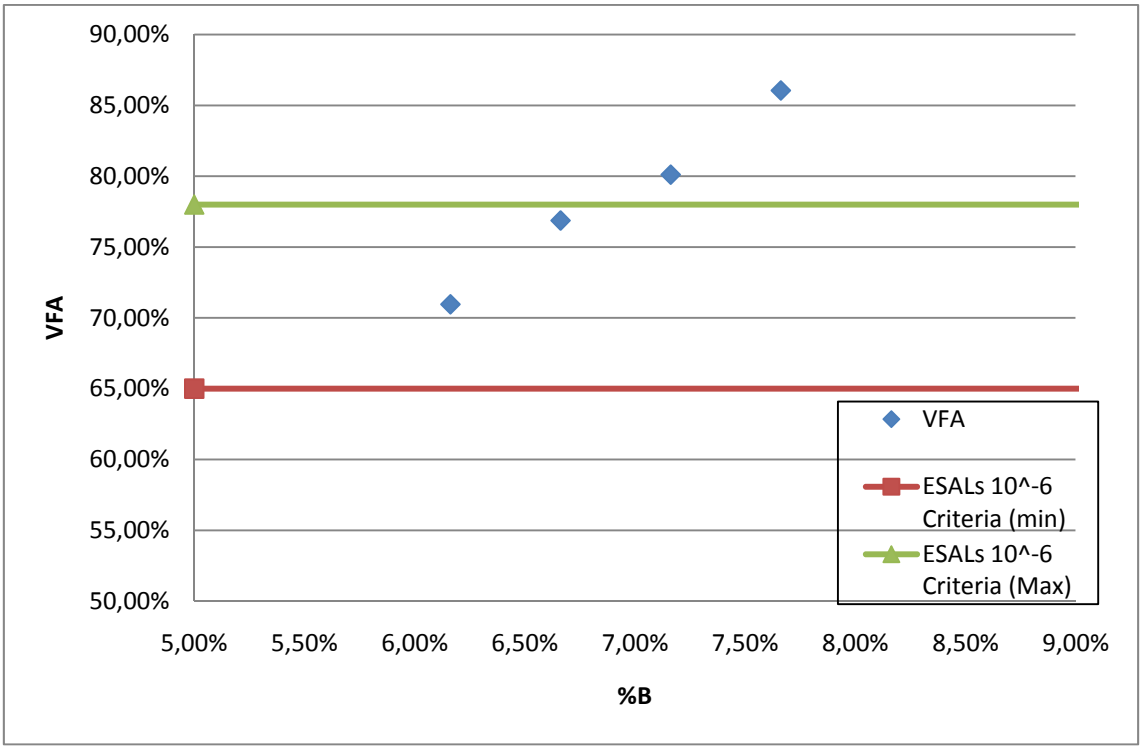

Diagram 5.2: Voids Filled with Asphalt (VFA).

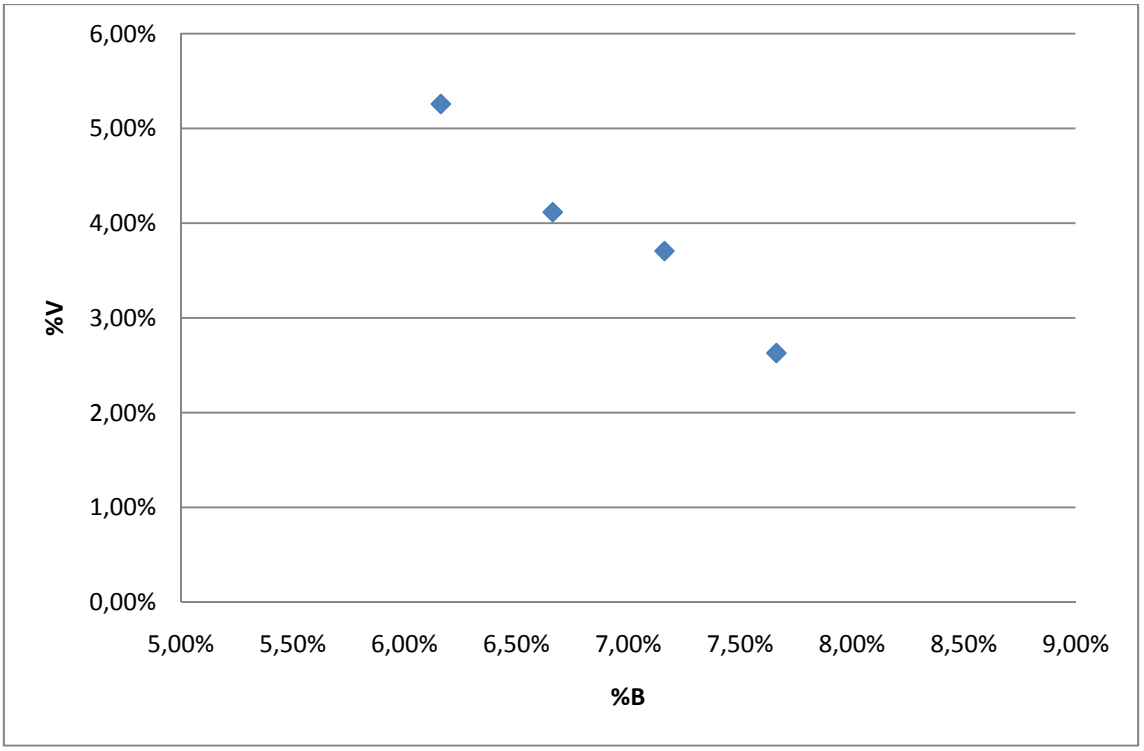

Diagram 5.3: Voids content (%).

From the plots above it is seen that every mixture accomplished the VMA SUPERPAVE requirement which requires for a mixture with a 19 mm nominal maximum size a VMA greater than or equal to 13% that is exceeded for every mixture; instead, regarding the VFA SUPERPAVE requires for a traffic level minor than $3x10^6$ ESALs a VFA between 65% and 78% In this case the mixtures with 6,16% and 6,66% bitumen content accomplished this. Regarding the voids content at Nd it is seen that the mixtures with 6,66% and 7,16% bitumen content accomplished this requirement of 4%±1% voids content.

Finally the only mixture that accomplished every requirement is the mixture with a 6,66% of bitumen content.

For extra data and for controlling the values which were used for plotting refer to the annexes.

5.3 Ring and ball test results

In the ring and ball test, two samples are tested in parallel thus two measures are taken, one for each samples. In this test was used the mean value as the final result because there were not a significant variation between each measure, the measures and the mean value are showed in the following table:

TOTAL 50/70			
Softening Point (°C):	**Measure 1**	**Measure 2**	**Mean value**
	48,5	48,3	48,4

Table 5.1: Results from Softening Point test on TOTAL 50/70.

5.4 TMD and apparent specific gravity (ASG) results

The apparent specific gravity was calculated for every granulometrical class and the theoretical maximum density for every asphalt concrete mixture; the results for the ASG are presented in the following table:

Class	A.S.G.[g/cm^3]
15-30	2,691
8-15	2,799
3-8	2,812
0-5	2,814
filler	3,050

Table 5.2: Results from A.S.G for aggregate classes.

While, the TMD for asphalt concrete are:

Mix 4	
%bitumen	TMD
6,16%	2,567
6,66%	2,558
7,16%	2,533
7,66%	2,510

Table 5.3: Results from TMD for asphalt concrete.

As expected for mixture 4, while the bitumen content increase its TMD decrease.

For extra data and for controlling the values which were used for calculations refer to the annexes.

5.5 Hydrostatic weight

The results for the hydrostatic weight are shown in the following tables:

				Weight (g)			
MIX Design 4	**diameter (mm)**	**height (mm)**	**volume (cm^3)**	**dry**	**immerged**	**Satured**	**bulk density**
+1%	150	49,6	876,5	2079,7	1234,5	2085,4	2,444
+0,5%	150	50,8	897,71	2087,4	1235,1	2090,9	2,439
-0,5%	150	50	883,57	2067,7	1228,9	2079,1	2,432
ottimo 6,66%	150	50,5	892,41	2072,3	1232,6	2077,5	2,453

Table 5.4: Bulk density For mix 4, mix design samples

					Weight (g)			
MIX Design 4	**diameter (mm)**	**height (mm)**	**volume (cm^3)**	**TMD**	**dry**	**immerged**	**Satured**	**bulk density**
+1% 1	150	60	1060,3	2,51	2868,5	1727,5	2870,4	2,510
+1% 2	150	60	1060,3	2,51	2650,1	1601,2	2654,3	2,516
+1% 3	150	60	1060,3	2,51	2570,5	1546,5	2573,7	2,502
+1% 4	150	60	1060,3	2,51	2489,5	1458,5	2494,5	2,403
+0,5% 1	150	60	1060,3	2,533	2804,7	1686,6	2807	2,503
+0,5% 2	150	60	1060,3	2,533	2823,3	1693	2826,2	2,491
+0,5% 4	150	60	1060,3	2,533	2448	1436,6	2455,5	2,403
ottimo 6,66% 1	150	60	1060,3	2,558	2716,9	1632,9	2726,5	2,484
ottimo 6,66% 2	150	60	1060,3	2,558	2557,1	1527,7	2560,9	2,475
ottimo 6,66% 3	150	60	1060,3	3,558	2583,4	1553,6	2586,3	2,502
ottimo 6,66% 4	150	60	1060,3	4,558	2581,2	1549,3	2585,2	2,492

Table 5.5: Bulk density For mix 4, Creep test samples

				Weight (g)			
MIX Design 4	**diameter (mm)**	**height (mm)**	**volume (cm^3)**	**dry**	**immerged**	**Satured**	**bulk density**
+1% 1	150	64,3	1136,3	2724,9	1615,6	2732,4	2,440
+1% 2	150	66,4	1173,4	2868,5	1727,5	2870,4	2,510
+0,5% 1	150	65	1148,6	2804,7	1686,6	2807	2,503
+0,5% 2	150	65,7	1161	2823,3	1693	2826,2	2,491
ottimo 6,66% 1	150	63,6	1123,9	2716,9	1632,9	2726,5	2,484
ottimo 6,66% 1	150	63,6	1123,9	2819,5	1699,5	2825,2	2,505

Table 5.6: Bulk density For mix 4, SCB test samples

						Weight (g)			
MIX Design 4	**Length (mm)**	**width (mm)**	**height (mm)**	**volume (cm^3)**	**TMD**	**dry**	**immerged**	**Satured**	**bulk density**
+1% 1	500	180	50	4500000	2,51	10539,8	6299,3	10562	2,473
+1% 2	500	180	50	4500000	2,51	10701	6395,6	10727	2,471
+1% 3	500	180	50	4500000	2,51	10916,7	6521,9	10954	2,463
+0,5% 1	500	180	50	4500000	2,533	10661,5	6377,8	10694	2,470
+0,5% 2	500	180	50	4500000	2,533	10814	6490,6	10828	2,493
+0,5% 3	500	180	50	4500000	2,533	10981,5	6596,8	10995	2,497
ottimo 6,66% 1	500	180	50	4500000	2,558	11131,1	6787,1	11157	2,547
ottimo 6,66% 2	500	180	50	4500000	2,558	11127,8	6698,4	11148	2,501
ottimo 6,66% 3	500	180	50	4500000	2,558	11129,4	6692,4	11152	2,496

Table 5.7: Bulk density For mix 4, slabs

Generally it is seen that for each mixture the bulk density is similar, in those cases where it is not the sample was studied the same. The difference could be due to the voids content is higher than the voids content in the others samples or also it could be possible that the voids distributions inside the sample affect directly the measures taken.

5.6 Indirect tensile test (Stiffness Modulus)

The results obtain from the indirect tensile test to determine the stiffness modulus are presented in the following tables:

Mix 6,66%		vertical force (KN)	horizontal stress (Kpa)	rise time (ms)	horizontal Deformation (microns)	pulse shape factor (%)	stiffness Modulus (Mpa)	
sample	Measure						measured	adjusted
2	1	1,52	107,7	126	6,9	0,684	2278	2373
2	2	1,54	108,9	123	7,0	0,683	2287	2381
2	3	1,42	100,6	126	7,0	0,681	2097	2179
SAMPLE MEAN		1,49	105,7	125	7,0	0,683	2221	2311
3	1	1,50	106,0	122	7,2	0,672	2164	2240
3	2	1,45	102,5	124	7,1	0,682	2109	2193
3	3	1,44	101,8	123	7,0	0,681	2129	2213
SAMPLE MEAN		1,46	103,4	123	7,1	0,678	2134	2215
4	1	1,65	116,4	121	7,0	0,668	2526	2613
4	2	1,58	111,7	123	7,1	0,681	2306	2399
4	3	1,67	118,1	123	7,1	0,668	2433	2516
SAMPLE MEAN		1,63	115,4	122	7,1	0,672	2422	2509
TEST MEAN		**1,53**	**108,19**	**123,44**	**7,04**	**0,68**	**2259**	**2345**
STANDARD DEVIATION		**0,09**	**6,35**	**1,39**	**0,07**	**0,01**	**148**	**150**
VARIATION		**5,93%**	**5,87%**	**1,12%**	**0,99%**	**0,77%**	**6,53%**	**6,39%**

Table 5.8: Mix 4, 6,66% %Bitumen, Indirect tensile test results.

Mix 7,16%		vertical force (KN)	horizontal stress (Kpa)	rise time (ms)	horizontal Deformation (microns)	pulse shape factor (%)	stiffness Modulus (Mpa)	
sample	Measure						measured	adjusted
1	1	1,46	103,3	124	7,0	0,679	2155	2237
1	2	1,45	102,8	123	7,0	0,682	2137	2222
1	3	1,33	94,1	126	7,1	0,692	1945	2029
SAMPLE MEAN		1,41	100,1	124	7,0	0,684	2079	2163
2	1	1,16	82,3	126	6,9	0,695	1739	1814
2	2	0,04	73,4	124	6,8	0,691	1571	1634
2	3	1,04	73,4	125	6,9	0,691	1568	1622
SAMPLE MEAN		0,75	76,4	125	6,9	0,692	1626	1690
4	1	1,21	85,6	124	7,0	0,682	1781	1848
4	2	1,18	83,2	122	7,1	0,683	1728	1785
4	3	1,18	83,4	121	7,1	0,686	1722	1790
SAMPLE MEAN		1,19	84,1	122	7,1	0,684	1744	1808
TEST MEAN		**1,12**	**86,8**	**124**	**7,0**	**0,687**	**1816**	**1887**
STANDARD DEVIATION		**0,34**	**12,09**	**1,39**	**0,11**	**0,00**	**235**	**246**
VARIATION		**30,30%**	**13,92%**	**1,12%**	**1,53%**	**0,70%**	**12,94%**	**13,04%**

Table 5.9: Mix 4, 7,16% %Bitumen, Indirect tensile test results.

Mix 7,66%		vertical force (KN)	horizontal stress (Kpa)	rise time (ms)	horizontal Deformation (microns)	pulse shape factor (%)	stiffness Modulus (Mpa)	
Sample	Measure						measured	adjusted
1	1	1,22	86,5	124	7,1	0,681	1789	1856
1	2	1,27	89,7	124	7,1	0,687	1844	1918
1	3	1,31	92,8	124	7,1	0,681	1902	1975
SAMPLE MEAN		1,27	89,7	124	7,1	0,683	1845	1916
2	1	0,94	66,6	122	7,2	0,691	1351	1402
2	2	0,94	66,3	121	7,1	0,692	1355	1408
2	3	0,86	60,6	126	7,3	0,692	1211	1256
SAMPLE MEAN		0,91	64,5	123	7,2	0,692	1306	1355
4	1	1,30	92,3	126	7,0	0,682	1930	2005
4	2	1,14	80,5	123	7,0	0,684	1680	1744
4	3	1,21	85,5	124	7,2	0,681	1725	1789
SAMPLE MEAN		1,22	86,1	124	7,1	0,682	1778	1846
TEST MEAN		**1,13**	**80,09**	**123,78**	**7,12**	**0,69**	**1643**	**1706**
STANDARD DEVIATION		**0,19**	**13,62**	**0,69**	**0,07**	**0,01**	**294**	**306**
VARIATION		**16,89%**	**17,00%**	**0,56%**	**0,97%**	**0,76%**	**17,90%**	**17,92%**

Table 5.10: Mix 4, 7,66% %Bitumen, Indirect tensile test results.

For each mixture three samples were tested and, as discussed on chapter IV, three measures were made on each sample; it was calculated the mean value for each specimen and then the mean, the standard deviation and the variation of the test, obtaining the result showed above.

Plotting the mean values of the stiffness modulus versus the bitumen content it is obtained:

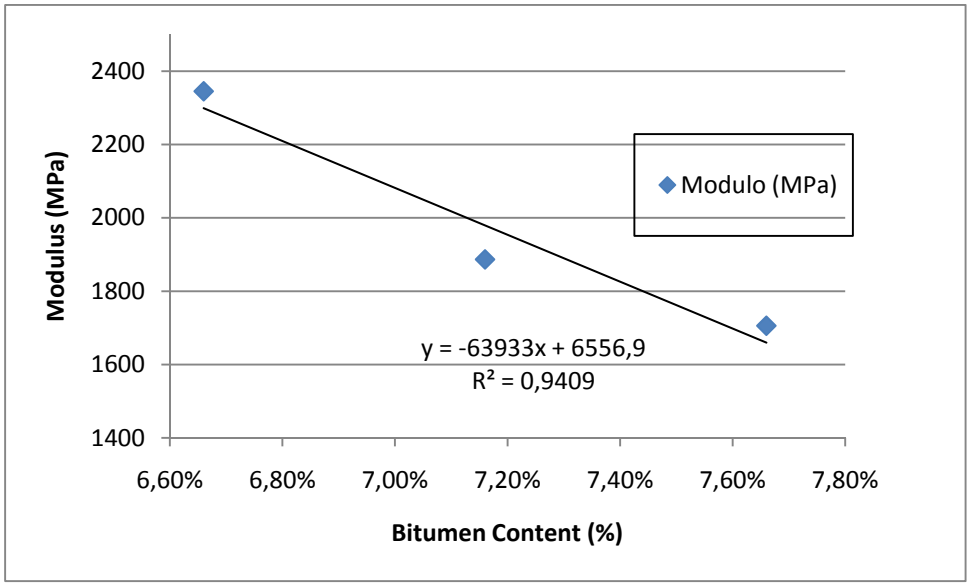

Diagram 5.4: Stiffness Modulus.

It could be seen that the mean values of the stiffness modulus decreases while the bitumen percentage increases, this was expected because is known that in a mixture when there is more bitumen its stiffness decrease and the viscoelastic respond increases. Regarding to the variation it was notice that it increases with the increment of the bitumen content.

5.7 Static Creep test

In the following plots are shown the results from the static creep test for each mix. It is shown one plot for each test, in the plot there is one curve for each sample, and the mean curve.

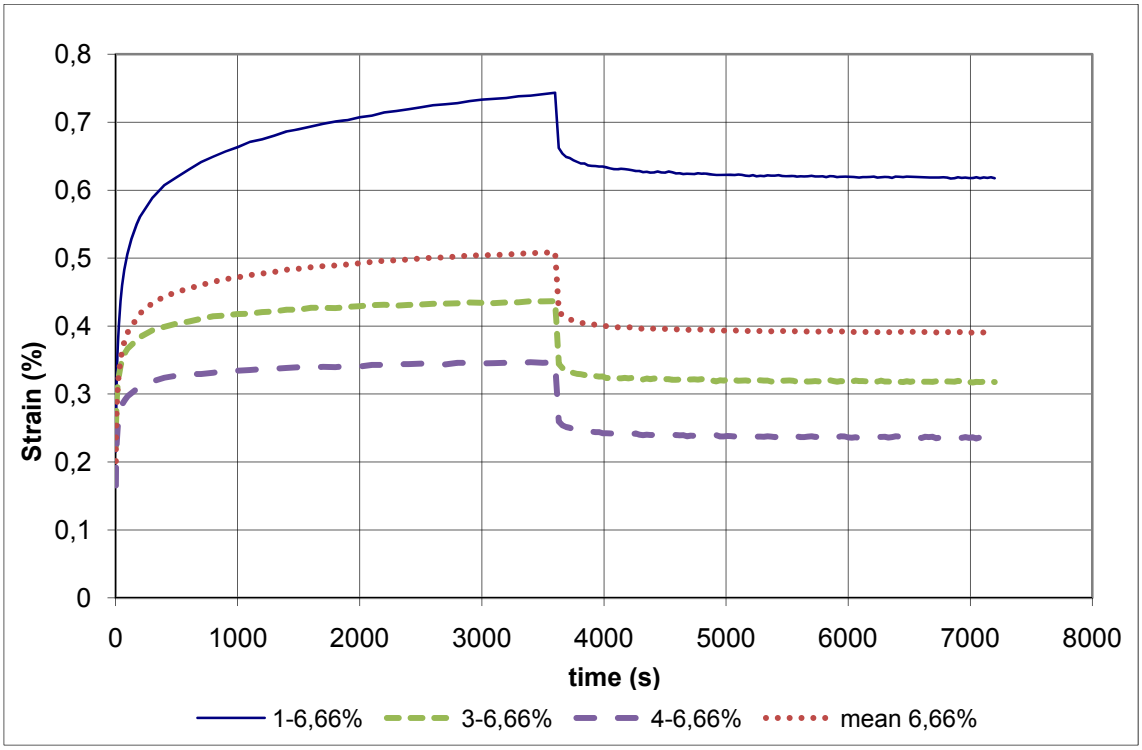

Diagram 5.5: Strain-time plot from creep test for Mix 6,66%

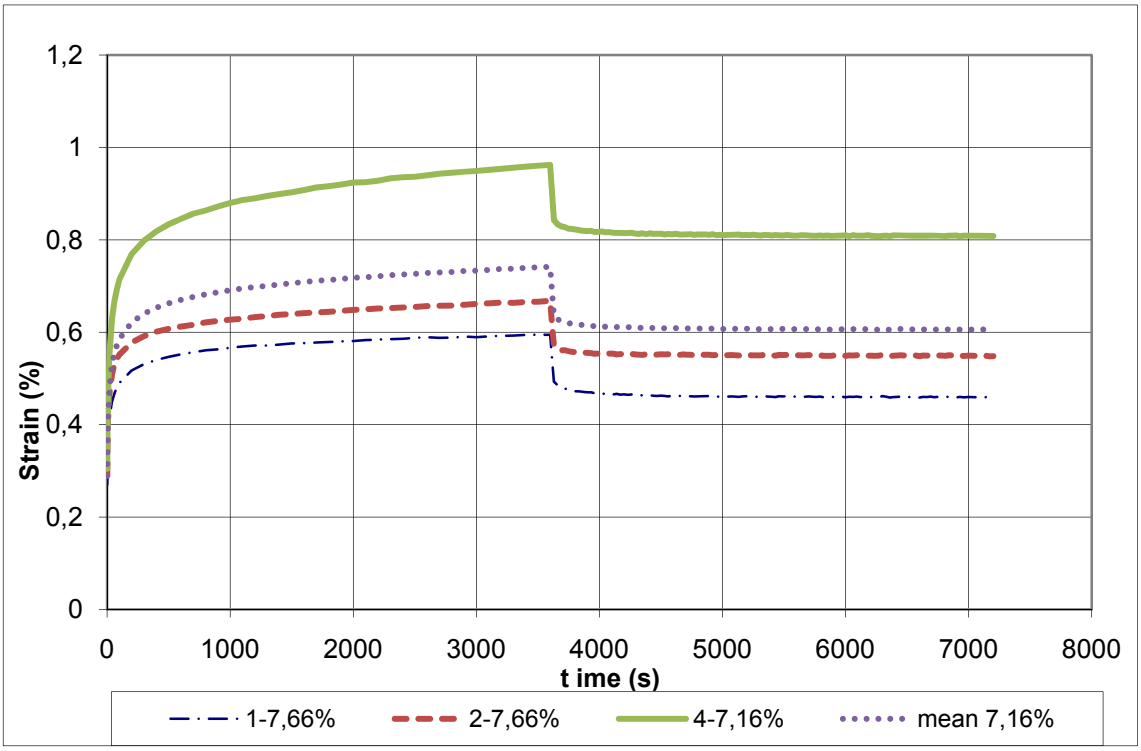

Diagram 5.6: Strain-time plot from creep test for Mix 7,16%

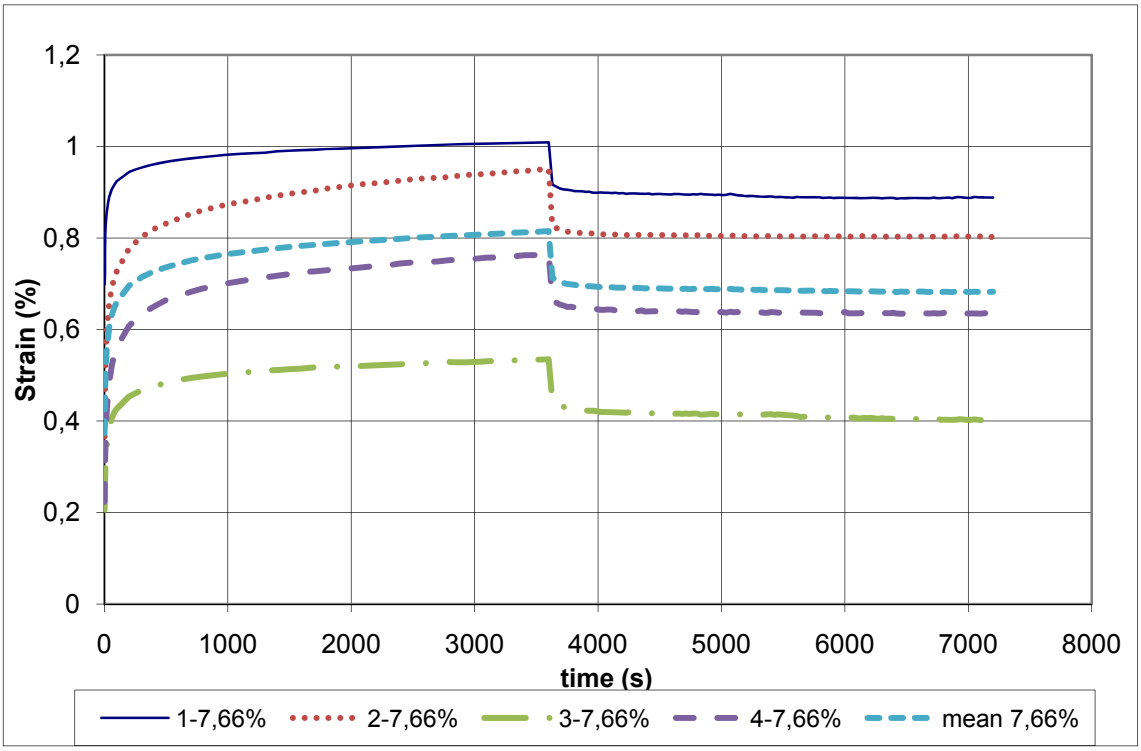

Diagram 5.7: Strain-time plot from creep test for Mix 7,66%

Plotting the mean curves of every mix in the same diagram is obtained:

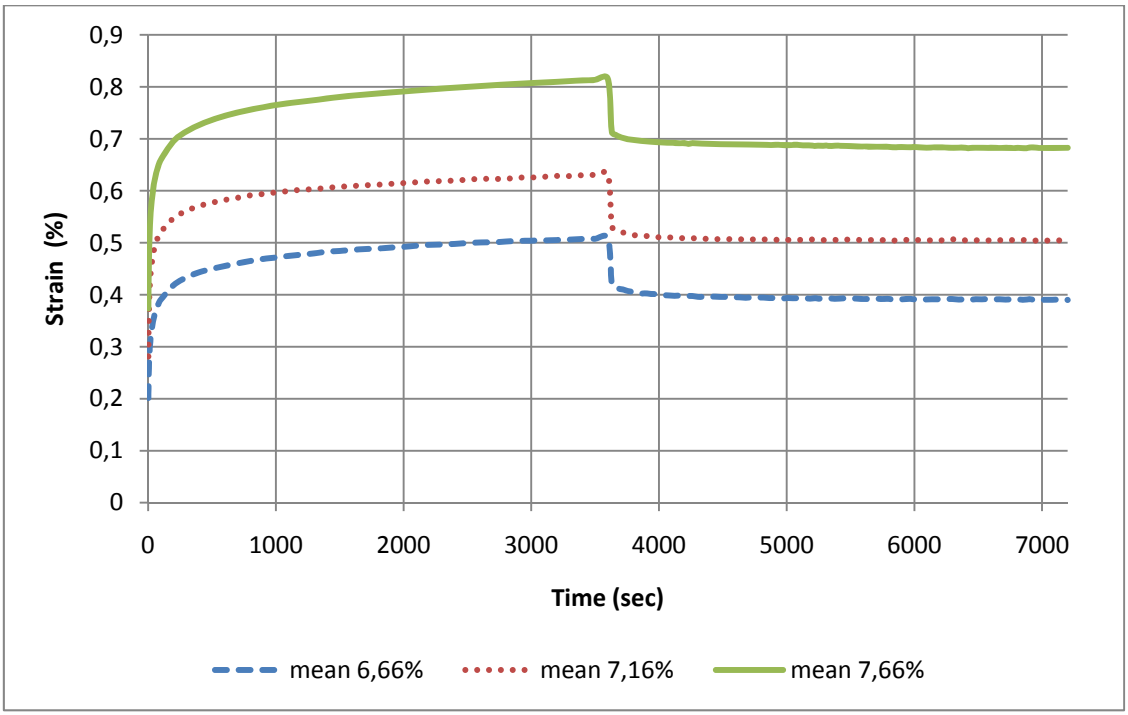

Diagram 5.8: Strain-time plot of the mean curves from creep test for Mixtures: 6,66%, 7,16% and 7,66%.

Resuming the most important values of the mean curves it is obtained the following tables:

	Mix 4 6,66%			
	mean	**max**	**min**	**Units**
J_1	2,013E-03	2,229E-03	1,654E-03	[cm^2/daN]
J_{10}	2,838E-03	3,258E-03	2,311E-03	[cm^2/daN]
J_p	3,901E-03	6,176E-03	2,349E-03	[cm^2/(daN*s)]
ε_1	0,2013	0,2229	0,1654	[%]
ε_{10}	0,2838	0,3258	0,2311	[%]
$\varepsilon_{elastic}$	0,0869	0,0923	0,0812	[%]
$\varepsilon_{plastic}$	0,1143	0,1342	0,0781	[%]
$\varepsilon_{viscoelastic}$	-0,0319	-0,0444	-0,0245	[%]

Table 5.11: static creep test results for mix 4 at 6,66% of bitumen

	Mix 4 7,16%			
	mean	**max**	**min**	**Units**
J_1	2,890E-03	3,043E-03	2,697E-03	[cm^2/daN]
J_{10}	4,254E-03	4,778E-03	3,745E-03	[cm^2/daN]
J_p	6,051E-03	8,085E-03	4,587E-03	[cm^2/(daN*s)]
ε_1	0,2890	0,3043	0,2697	[%]
ε_{10}	0,4254	0,4778	0,3745	[%]
$\varepsilon_{elastic}$	0,1065	0,1195	0,0986	[%]
$\varepsilon_{plastic}$	0,1825	0,1943	0,1683	[%]
$\varepsilon_{viscoelastic}$	0,0300	-0,0345	-0,0212	[%]

Table 5.12: static creep test results for mix 4 at 7,16% of bitumen

	7,66%			
	mean	max	min	Units
J_1	3,737E-03	6,989E-03	2,064E-03	[cm^2/daN]
J_{10}	5,059E-03	8,206E-03	3,071E-03	[cm^2/daN]
J_p	6,827E-03	8,885E-03	4,033E-03	[cm^2/(daN*s)]
ε_1	0,3737	0,6989	0,2064	[%]
ε_{10}	0,5059	0,8206	0,3071	[%]
$\varepsilon_{elastic}$	0,1017	0,1245	0,0904	[%]
$\varepsilon_{plastic}$	0,2720	0,6066	0,1160	[%]
$\varepsilon_{viscoelastic}$	-0,0307	-0,0413	-0,0239	[%]

Table 5.13: static creep test results for mix 4 at 7,66% of bitumen

Plotting the most important mean values for each mix respect the bitumen percentage it is obtained:

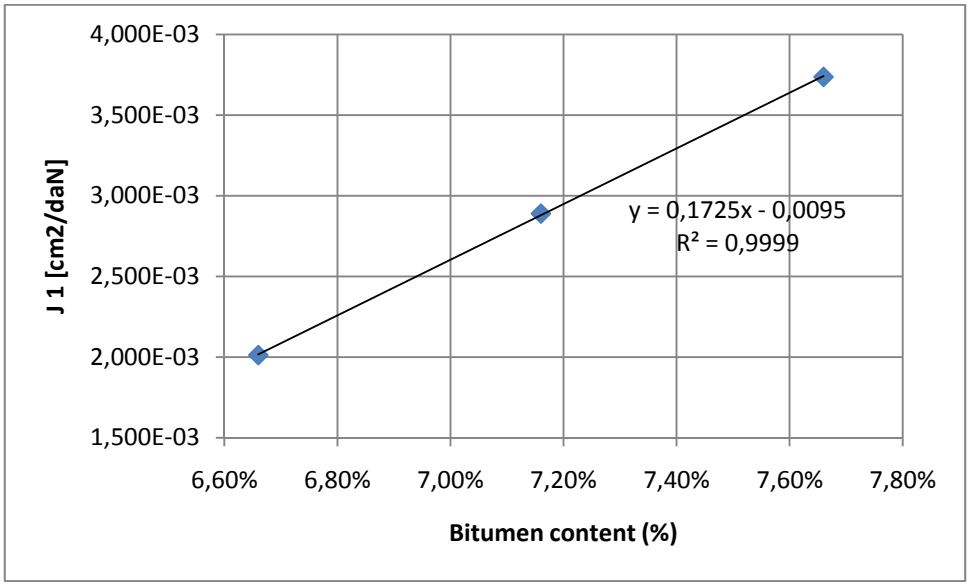

Diagram 5.9: Deformability at 2 seconds

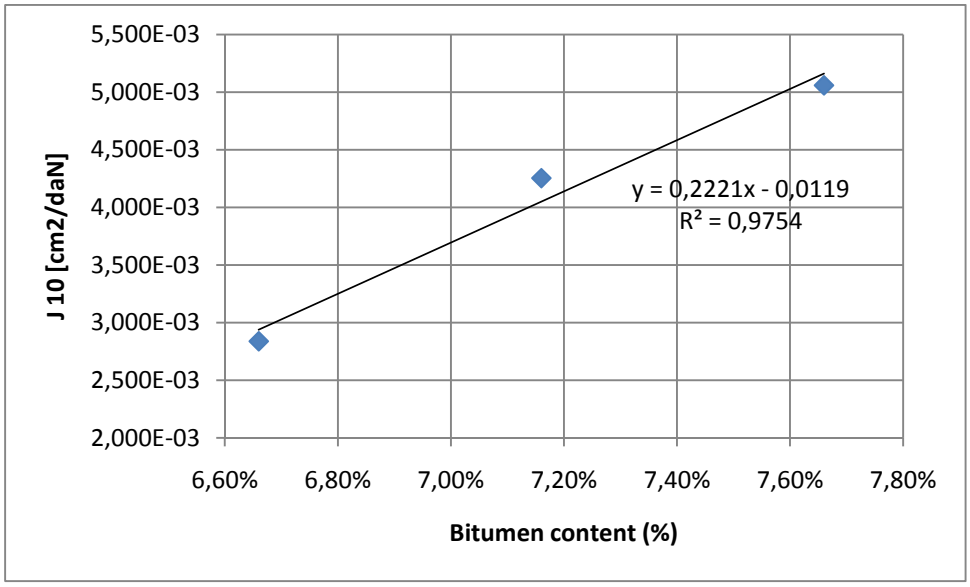

Diagram 5.10: Deformability at 10 seconds

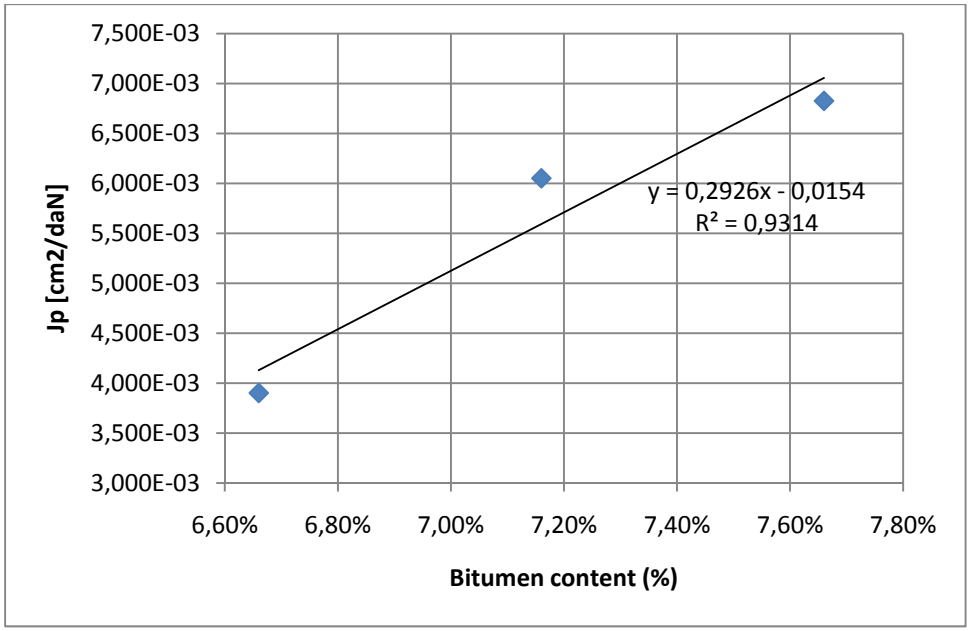

Diagram 5.11: Plastic Deformability

Analyzing these diagrams it is seen that at a greater bitumen content greater is the plastic deformability and the deformability at 2 and 10 seconds; it means that applying the same tension, a mix with more bitumen will deform more at the beginning and the permanent deformation respect load time will be

also greater. In every plot it is seen that the mean values present a linear increasing trend.

Plotting the mean deformations it is obtained:

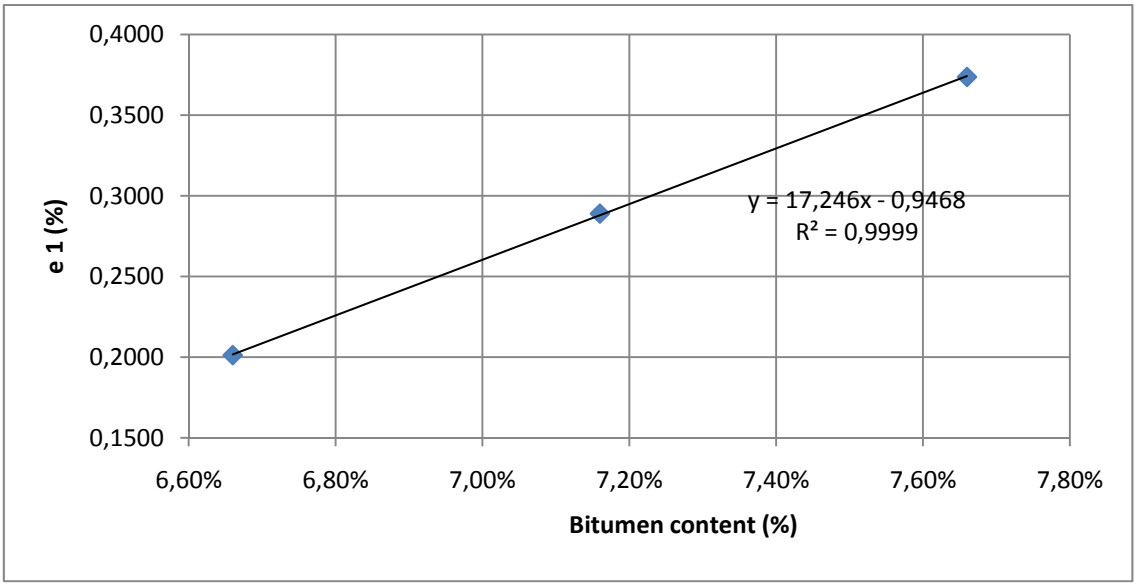

Diagram 5.12 : Deformation at 2 seconds

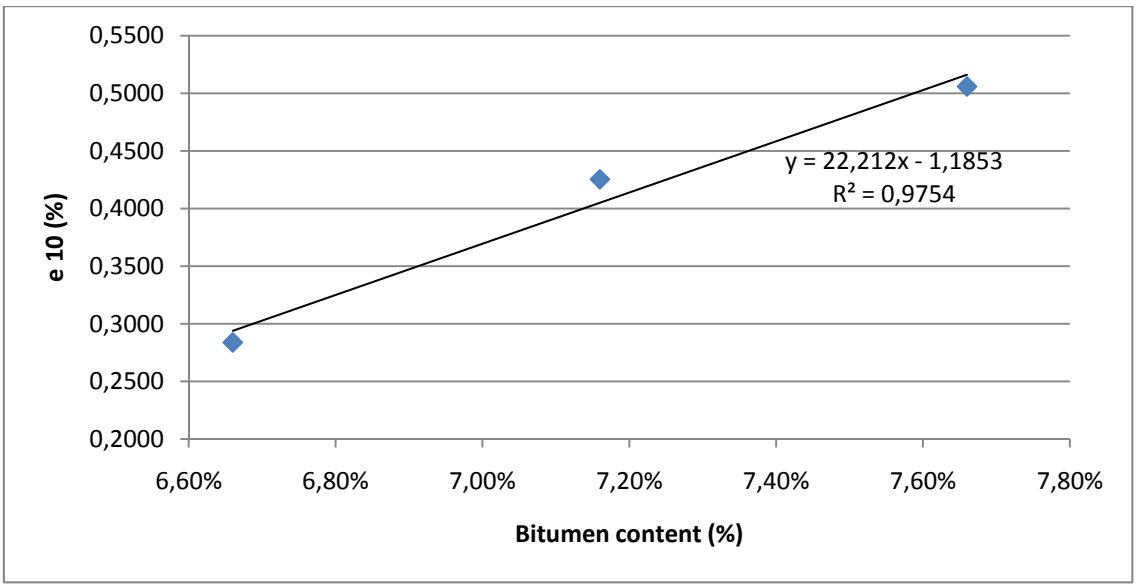

Diagram 5.13: Deformation at 10 seconds

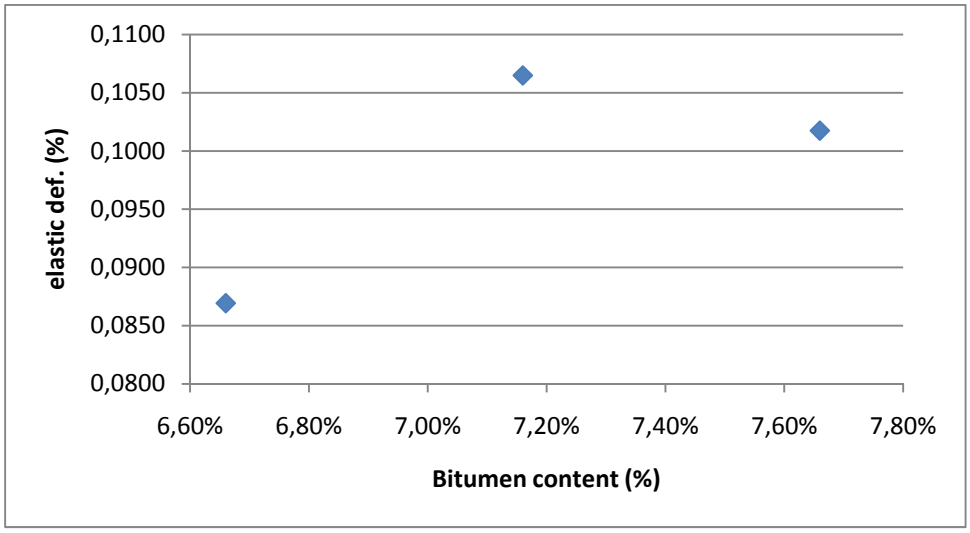

Diagram 5.14: Elastic Deformation Recovery

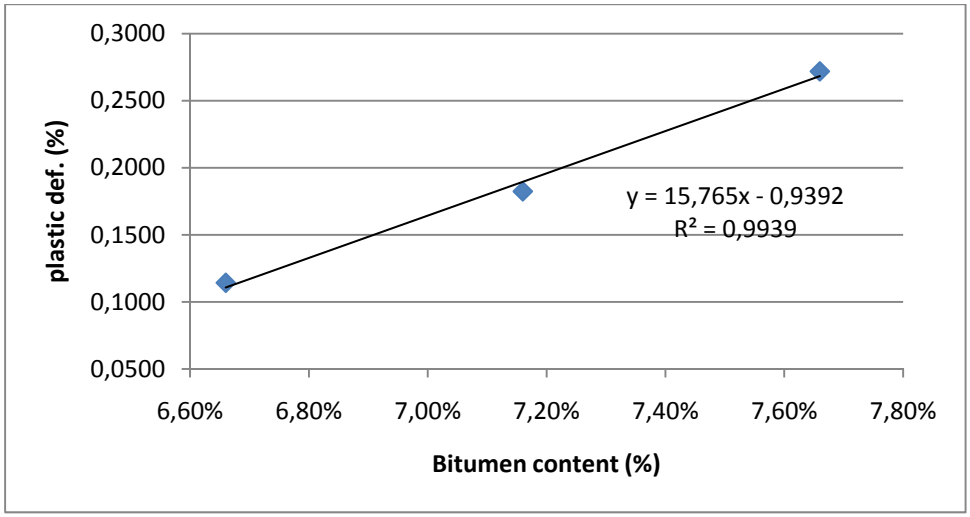

Diagram 5.15: Plastic deformation

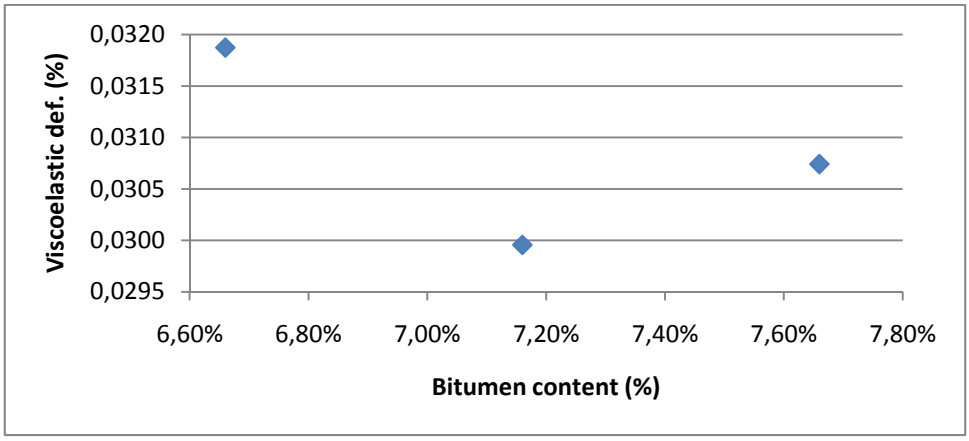

Diagram 5.16: Viscoelastic deformation recovery

Analyzing these plots it is seen that at a greater bitumen content greater the initial deformation at 2 and 10 seconds, also as the plastic deformation; it means that a mix with a greater bitumen content will deform more when a load is applied but also will have a greater residual deformation. Instead regarding the elastic deformation recovery it is seen first an increasing trend an after a decreasing trend, which could mean that after a certain bitumen content the elastic respond start decreasing. Regarding the viscoelastic deformation recovery it is seen a trend change, first it tends to decrease and after increase. Knowing that the viscoelastic effects are time-dependent and that the viscolelastic deformation (recovered deformation) was calculated based on the elastic deformation an explanation for this behavior could be that after a certain bitumen content the elastic response decreases (as seen on the previous plot where it was an asymptotic behavior) but its viscoelastic response increases. In the plots of the mean values for the deformation at 2 and 10 second also as the plastic deformation it is seen a linear increasing trend.

For extra data and for controlling the values which were used for plotting, refer to the annexes.

5.8 SCB test results

For the Semicircular bending test, the most important results and measures for each specimen tested are showed in the tables below:

MIX 6,66%	max load (KN)	max def (mm)	height (mm)	Real Inertia (mm4)	theorical Inertia (mm4)	rate Ir/It	U (KNmm)	U normalized (KNmm)	width (b) (mm)
Notch 15 mm									
6,66 1 HD	1,51	0,883	73,48	1E+06	1019004	0,94	0,8217	0,7727	29,0
6,66 1 LS	1,73	0,644	74,6	1E+06	1107422	0,984	0,6753	0,6646	31,5
6,66 2 HD	1,83	0,985	74,85	1E+06	1038867	0,994	1,0339	1,0277	29,6
6,66 2 LS	2,01	0,631	72,1	1E+06	1121484	0,888	0,7381	0,6557	31,9
mean	1,77	0,786	73,76	1E+06	1071694	0,952	0,8173	0,7802	30,5
Notch 33 mm									
6,66 1 HS	0,43	0,402	74,19	1E+06	1036758	0,968	0,1245	0,1205	29,5
6,66 1 LD	0,61	0,428	73,52	1E+06	1116738	0,942	0,1691	0,1593	31,8
6,66 2 HS	0,71	0,593	72,05	9E+05	1065762	0,887	0,2759	0,2446	30,3
6,66 2 LD	0,8	0,428	74,85	1E+06	1142578	0,994	0,2074	0,2062	32,5
mean	0,64	0,463	73,65	1E+06	1090459	0,948	0,1942	0,1827	31,0

Table 5.14.1: Results and measures from the SCB test for Mix 6,66%.

MIX 6,66%	U/b (KNmm/mm)	UC energy	weight (KN)	mass energy ME	total energy KNxmm (UC+ME)	(U)/ (TE)	Jc (J/mm^2)
Notch 15 mm							0,00099
6,66 1 HD	2,6660E-02	1,8249	6,73E-05	5,94E-05	1,8250	45,02%	
6,66 1 LS	2,1097E-02	1,5284	6,73E-05	4,33E-05	1,5284	44,18%	
6,66 2 HD	3,4779E-02	1,8445	6,73E-05	6,63E-05	1,8446	56,05%	
6,66 2 LS	2,0556E-02	1,6488	6,73E-05	4,25E-05	1,6489	44,76%	
mean	2,6978E-02	1,7117	6,73E-05	5,29E-05	1,7117	47,51%	
Notch 33 mm							
6,66 1 HS	4,0872E-03	0,3586	6,28E-05	2,52E-05	0,3586	34,72%	
6,66 1 LD	5,0137E-03	0,4971	6,28E-05	2,69E-05	0,4971	34,01%	
6,66 2 HS	8,0696E-03	0,7127	6,28E-05	3,72E-05	0,7127	38,71%	
6,66 2 LD	6,3440E-03	0,5216	6,28E-05	2,69E-05	0,5216	39,77%	
mean	6,2573E-03	0,5225	6,28E-05	2,91E-05	0,5225	36,80%	

Table 5.14.2: Results and measures from the SCB test for Mix 6,66%.

MIX 7,16%	max load (KN)	max def (mm)	height (mm)	Real Inertia (mm4)	theorical Inertia (mm4)	rate Ir/It	U (KNxmm)	U normalized (KNmm)	width (b) (mm)
Notch 15 mm									
7,16 1 HD	1,07	1,163	72,22	1E+06	1121133	0,893	0,8027	0,7166	31,9
7,16 1 LS	1,13	1,762	74,68	1E+06	1083867	0,987	1,3221	1,3052	30,8
7,16 2 HD	1,28	0,903	74,7	1E+06	1117969	0,988	0,8173	0,8075	31,8
7,16 2 LS	1,26	1,661	72,18	1E+06	1096875	0,891	1,0024	0,8933	31,2
mean	1,18	1,372	73,44	1E+06	1104961	0,94	0,9861	0,9307	31,4
Notch 33 mm									
7,16 1 HS	0,43	0,891	74,86	1E+06	1110938	0,994	0,2819	0,2803	31,6
7,16 1 LD	0,41	0,526	72,08	9E+05	1059961	0,888	0,1384	0,1228	30,2
7,16 2 HS	0,53	0,675	72,27	1E+06	1115156	0,895	0,2391	0,2140	31,7
7,16 2 LD	0,54	0,666	74,76	1E+06	1094238	0,99	0,2634	0,2609	31,1
mean	0,48	0,69	73,49	1E+06	1095073	0,942	0,2307	0,2195	31,1

Table 5.15.1: Results and measures from the SCB test for Mix 7,16%.

MIX 7,16%	U/b (KNxmm/mm)	UC energy	weight (KN)	mass energy ME	total energy KNxmm (UC+ME)	(U)/ (TE)	Jc (J/mm^2)
Notch 15 mm							0,00113
7,16 1 HD	2,2471E-02	1,9202	6,73E-05	7,82E-05	1,9203	41,80%	
7,16 1 LS	4,2337E-02	2,5739	6,73E-05	1,19E-04	2,5741	51,36%	
7,16 2 HD	2,5394E-02	1,6922	6,73E-05	6,08E-05	1,6923	48,30%	
7,16 2 LS	2,8633E-02	1,8072	6,73E-05	1,12E-04	1,8073	55,46%	
mean	3,1471E-02	1,9984	6,73E-05	9,23E-05	1,9985	49,23%	
Notch 33 mm							
7,16 1 HS	8,8713E-03	0,6828	6,28E-05	5,59E-05	0,6828	41,29%	
7,16 1 LD	4,0741E-03	0,3931	6,28E-05	3,30E-05	0,3931	35,20%	
7,16 2 HS	6,7453E-03	0,5743	6,28E-05	4,24E-05	0,5743	41,64%	
7,16 2 LD	8,3825E-03	0,6990	6,28E-05	4,18E-05	0,6990	37,68%	
mean	7,3783E-03	0,5873	6,28E-05	4,33E-05	0,5873	38,95%	

Table 5.15.2: Results and measures from the SCB test for Mix 7,16%.

MIX 7,66%	max load (KN)	max def (mm)	height (mm)	Real Inertia (mm4)	theorical Inertia (mm4)	rate Ir/It	U (KNxmm)	U normalized (KNmm)	width (b) (mm)
Notch 15 mm									
7,66 1 HD	0,98	1,55	72,35	9E+05	1044316	0,898	1,0030	0,9004	29,7
7,66 1 LS	1,25	1,138	74,35	1E+06	1123066	0,974	0,9166	0,8930	31,9
7,66 2 HD	1,16	1,304	75	1E+06	1102148	1	1,0766	1,0766	31,4
7,66 2 LS	1,08	1,676	72,81	1E+06	1120781	0,915	1,2327	1,1276	31,9
mean	1,12	1,417	73,63	1E+06	1097578	0,947	1,0572	0,9994	31,2
Notch 33 mm									
7,66 1 HS	0,47	1,104	73,84	1E+06	1056797	0,954	0,3696	0,3526	30,1
7,66 1 LD	0,24	0,991	72,9	1E+06	1139063	0,918	0,1787	0,1641	32,4
7,66 2 HS	0,29	1,316	72,8	1E+06	1102148	0,915	0,2605	0,2383	31,4
7,66 2 LD	0,38	0,992	74,07	1E+06	1122363	0,963	0,2561	0,2467	31,9
mean	0,34	1,101	73,4	1E+06	1105093	0,938	0,2662	0,2504	31,4

Table 5.16.1: Results and measures from the SCB test for Mix 7,66%.

MIX 7,66%	U/b (KNxmm/mm)	UC energy	weight (KN)	mass energy ME	total energy KNxmm (UC+ME)	(U)/ (TE)	Jc (J/mm^2)
Notch 15 mm							
7,66 1 HD	3,0310E-02	2,2134	6,73E-05	1,04E-04	2,2135	45,31%	
7,66 1 LS	2,7954E-02	2,0476	6,73E-05	7,66E-05	2,0476	44,76%	
7,66 2 HD	3,4342E-02	2,2311	6,73E-05	8,77E-05	2,2312	48,25%	
7,66 2 LS	3,5369E-02	2,5288	6,73E-05	1,13E-04	2,5289	48,74%	
mean	3,3866E-02	2,2552	6,73E-05	9,53E-05	2,2553	46,77%	0,00119
Notch 33 mm							
7,66 1 HS	1,1731E-02	0,7923	6,28E-05	6,93E-05	0,7924	46,64%	
7,66 1 LD	5,0645E-03	0,4192	6,28E-05	6,22E-05	0,4192	42,62%	
7,66 2 HS	7,6008E-03	0,6956	6,28E-05	8,26E-05	0,6957	37,45%	
7,66 2 LD	7,7284E-03	0,7213	6,28E-05	6,23E-05	0,7214	35,51%	
mean	8,5360E-03	0,6571	6,28E-05	6,91E-05	0,6572	40,56%	

Table 5.16.2: Results and measures from the SCB test for Mix 7,66%.

Calculating the mean values for the energy results of each mix and plotting these versus the notch depth the following plot is obtained:

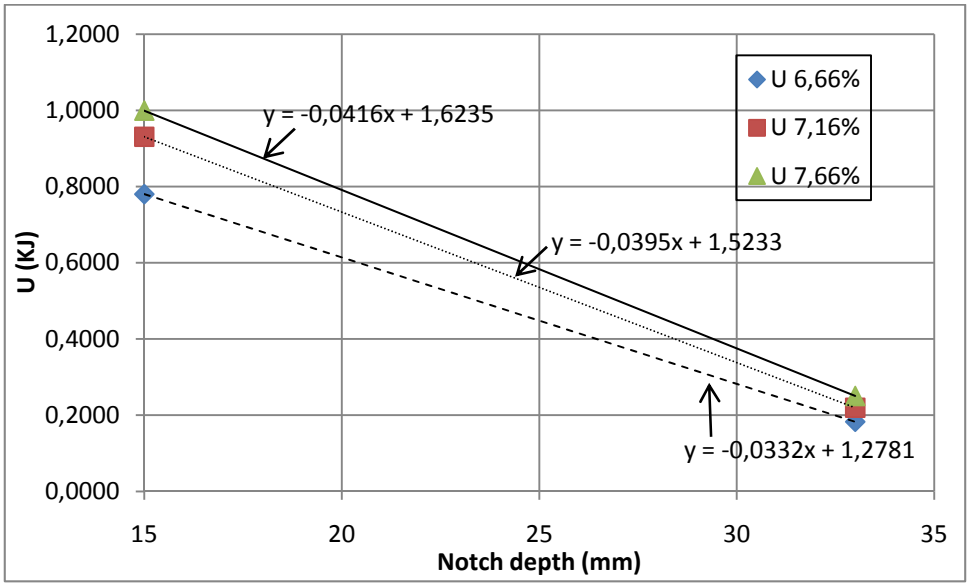

Diagram 5.17: Energy to failure vs notch depth

Knowing that the crack propagation resistance is the slope of the linear regression of the plot above divided by the specimen thickness, it could be plotted the crack propagation resistance versus the bitumen content; doing this it is obtained:

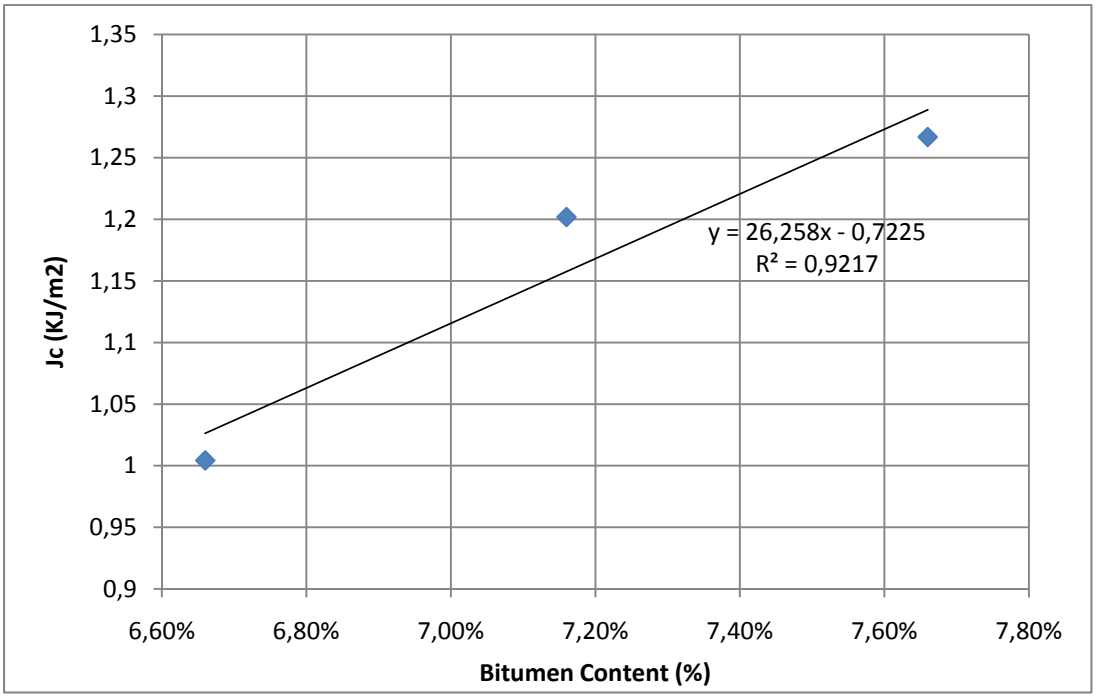

Diagram 5.18: Crack propagation resistance

Analyzing the previous plot it is seen that the crack propagation resistance tends to increase while the bitumen content increases, but it is also seen that a linear regression is not perfectly adjusted, noticing that the gap between the mix with a bitumen content of 6,66% and the mix with 7,16% is bigger than the gap between the mix 7,16% and the mix 7,66%.

It is to notice that every mixture have a high crack propagation resistance comparing with what is presented in other studies (Kabir 2008 and Mull et al., 2002) where was considered that any mixture achieving a crack propagation resistance greater than 0,65 KJ/m^2 is expected to exhibit good fracture resistance, making the same consideration it is seen that every mixture is above

the value of 0,65 KJ/m^2 and those with the higher percentage of bitumen content achieved almost 2 times that value.

For extra data and for controlling the test results refer to the annexes.

5.9 Four-points bending

The results from the fatigue test and the criteria of a 50% reduction of the stiffness modulus are plots in the following diagrams:

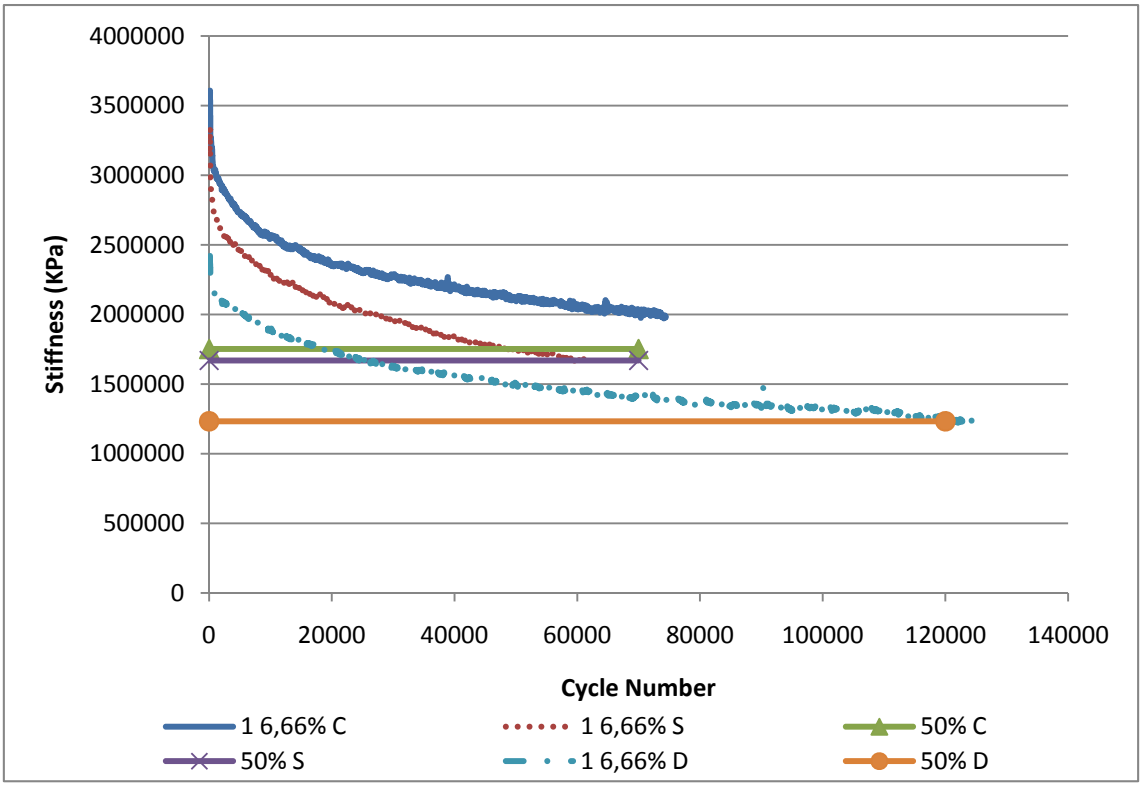

Diagram 5.19: fatigue test at 300 microstrains for mix 6,66%

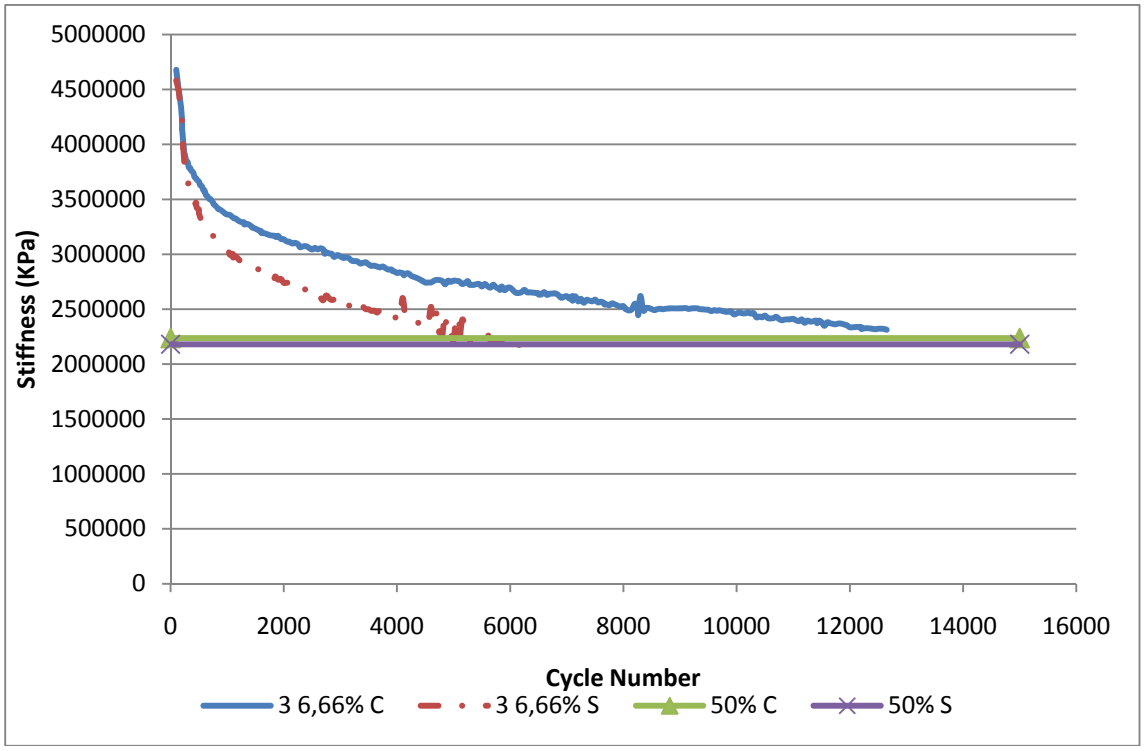

Diagram 5.20: fatigue test at 450 microstrains for mix 6,66%

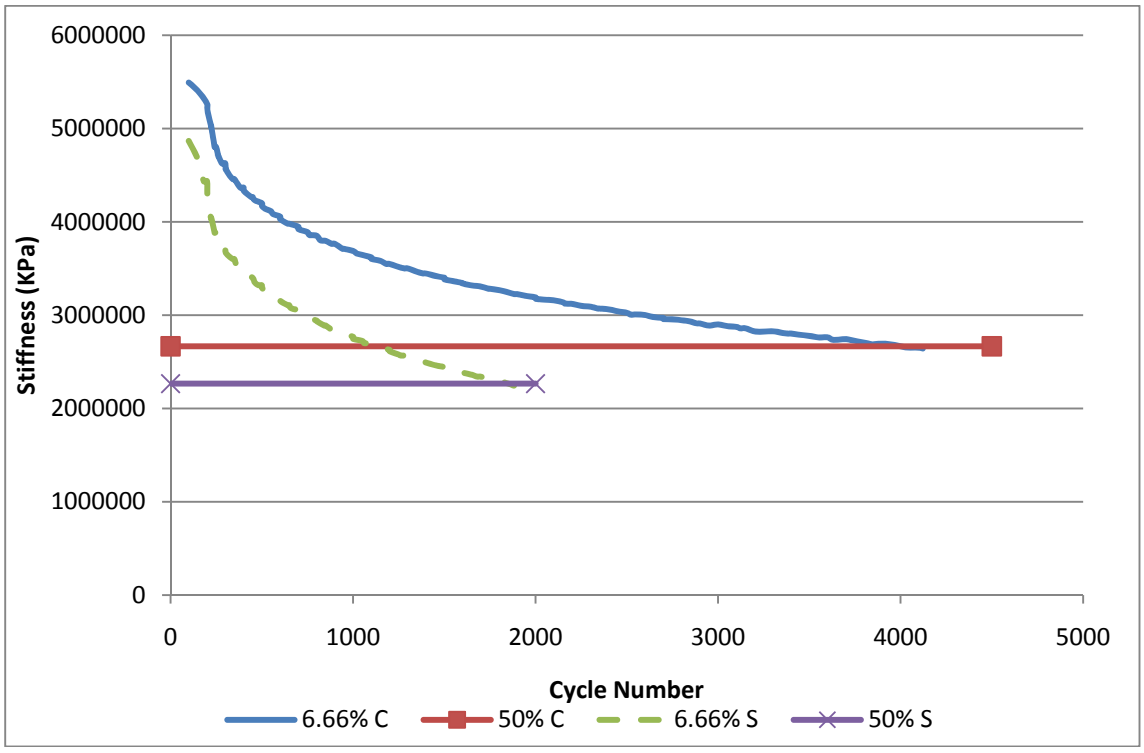

Diagram 5.21: fatigue test at 600 microstrains for mix 6,66%

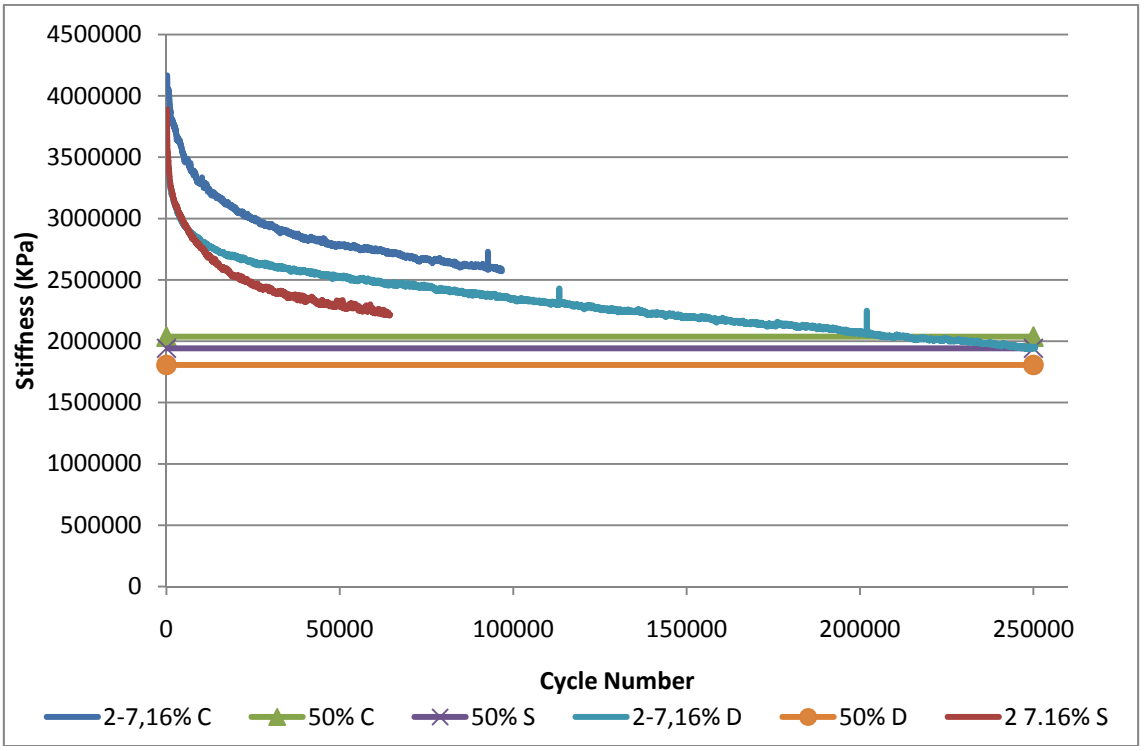

Diagram 5.22: fatigue test at 300 microstrains for mix 7,16%

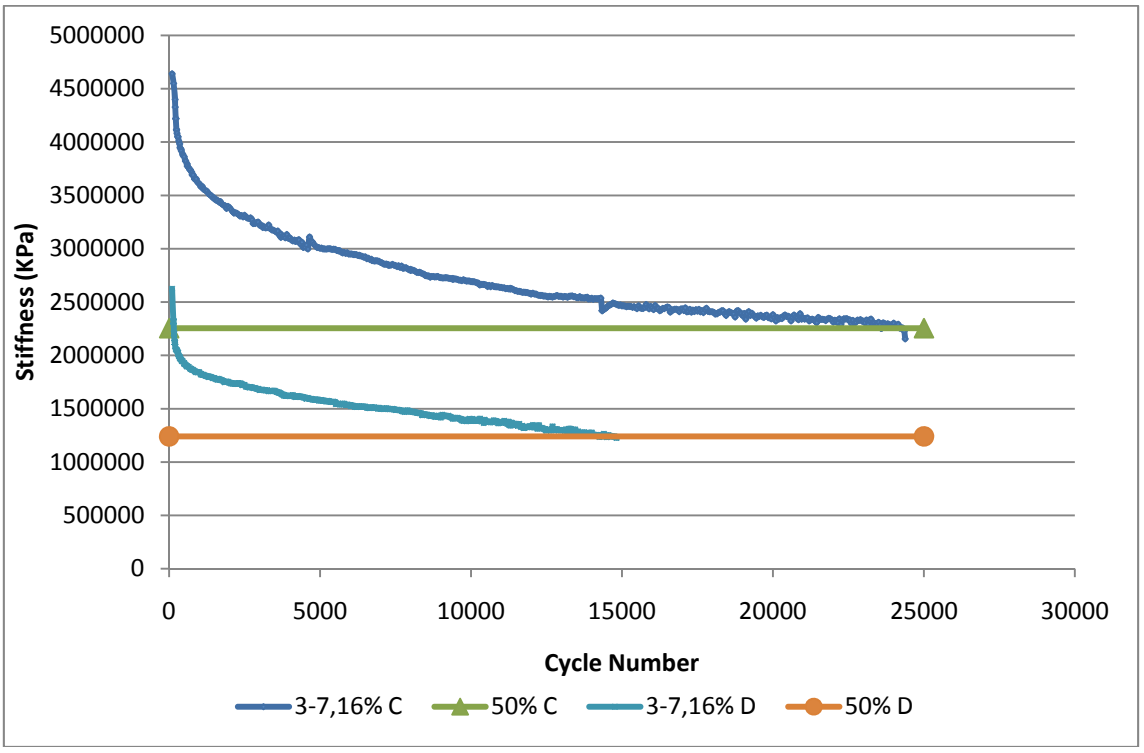

Diagram 5.23: fatigue test at 450 microstrains for mix 7,16%

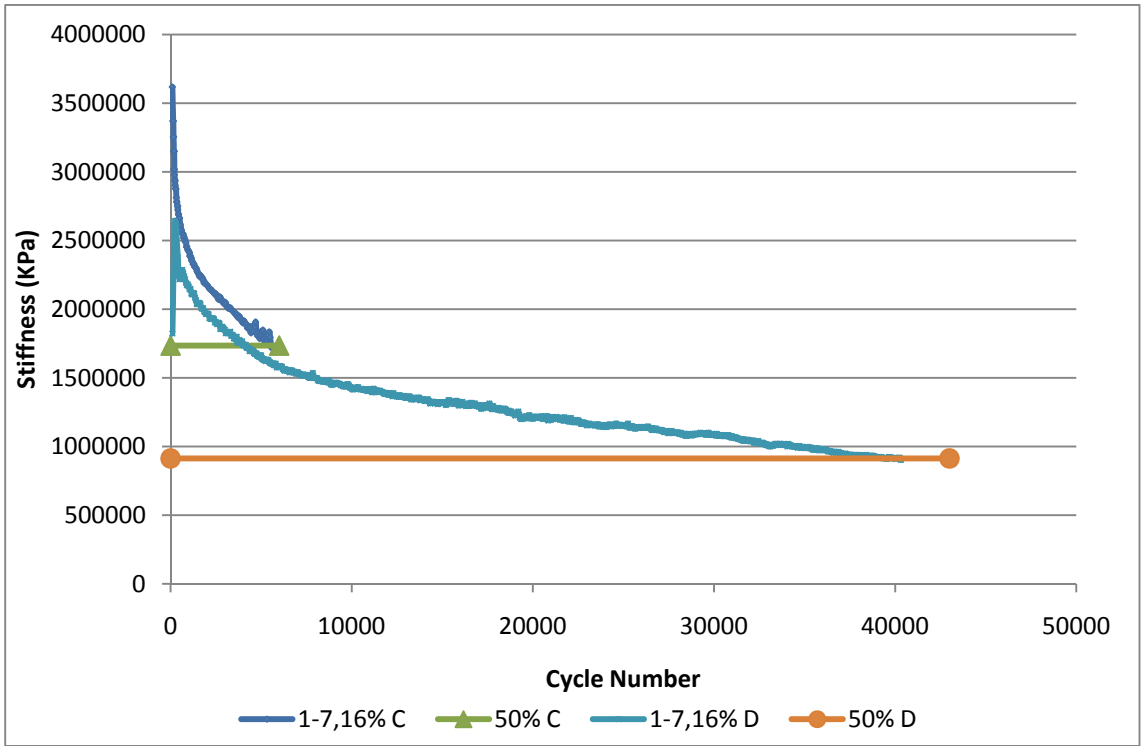

Diagram 5.24: fatigue test at 600 microstrains for mix 7,16%

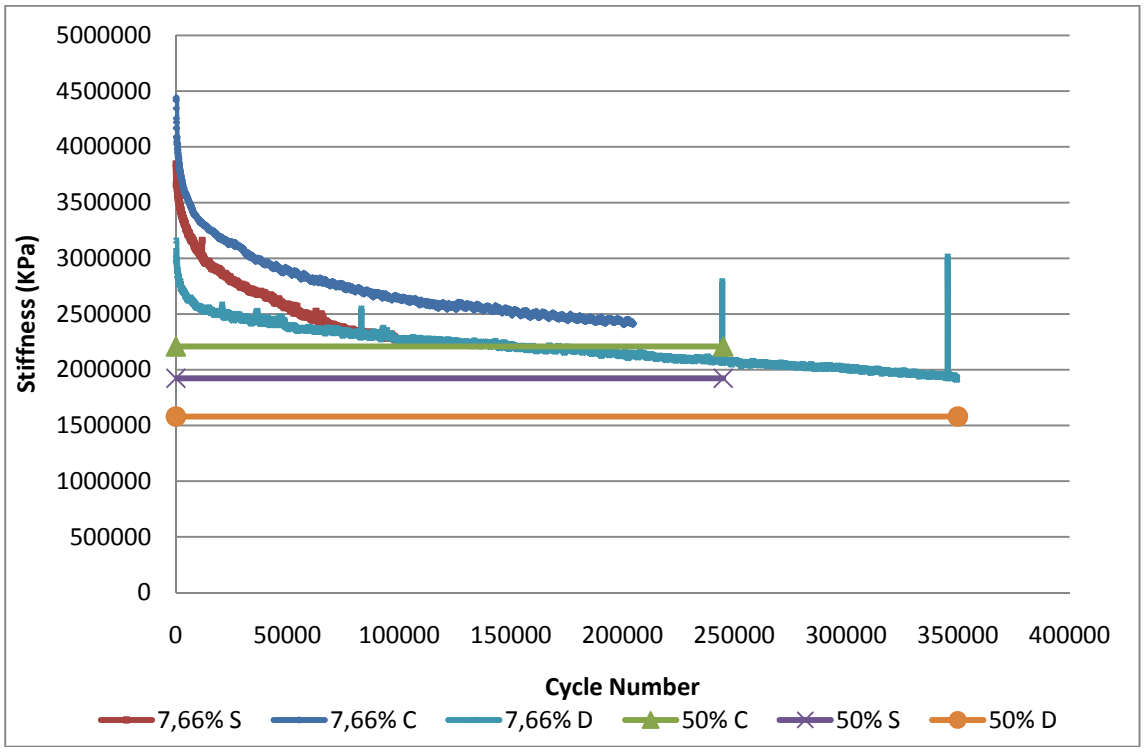

Diagram 5.25: fatigue test at 300 microstrains for mix 7,66%

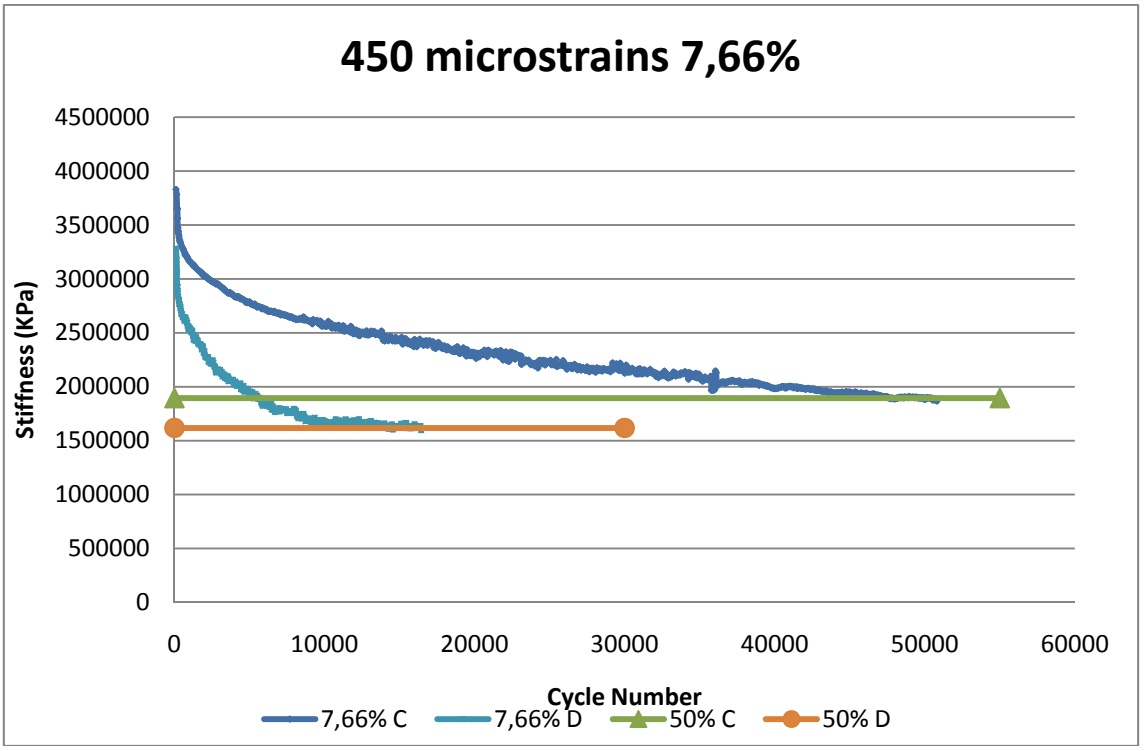

Diagram 5.26: fatigue test at 450 microstrains for mix 7,66%

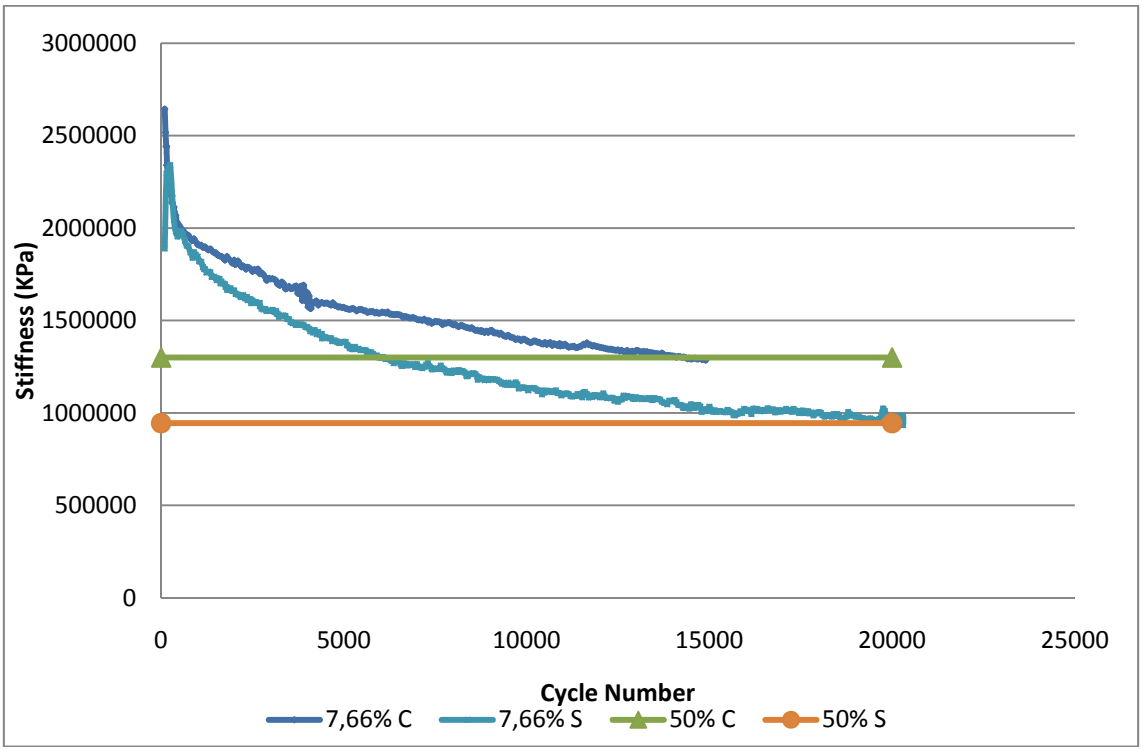

Diagram 5.27: fatigue test at 600 microstrains for mix 7,66%

In this test, considering the material heterogeneity, the operator inexperience and the difficulties for preparing the samples (slabs), the data dispersion was expected. However, analyzing the results it is seen that generally for each test the fatigue behavior was similar.

Analyzing the results for mix 6,66% it has to be clarified that for the tests at 450 microstrains and 600 microstrains the specimen fracture is considered fragile, because three of four samples, one at 450 microstrains and both samples at 600 microstrains, did not achieve a 10.000 load cycles, thus it could not be said that the fatigue phenomenon was developed. However, these tests at 450 and 600 microstrains were taken for comparison versus the others mixtures because the others mixtures did achieve more than 10.000 load cycles.

Analyzing the results for mix 7,16% it is seen that for 300, 450 and for one sample at 600 microstrains the fatigue phenomenon was developed, lasting more than 10.000 load cycles, but it has to be notice that there is an important data dispersion at 450 and 600 microstrains; at 450 microstrains the initial stiffness varied significantly from one sample to another and for the 600 microstrains test it is also seen that the cycles number to fracture also varied significantly from one sample to another been one sample fragile and the other not.

Analyzing the results for mix 7,66% it is seen that for every test all the samples achieve more than 10.000 load cycles so the fatigue phenomenon was developed. This mixture is the one that shows the better fatigue resistance, during longer than the others mixtures.

Calculating the mean load cycles for each mixtures at each strain level and plotting them versus the bitumen content it was obtained the following diagrams:

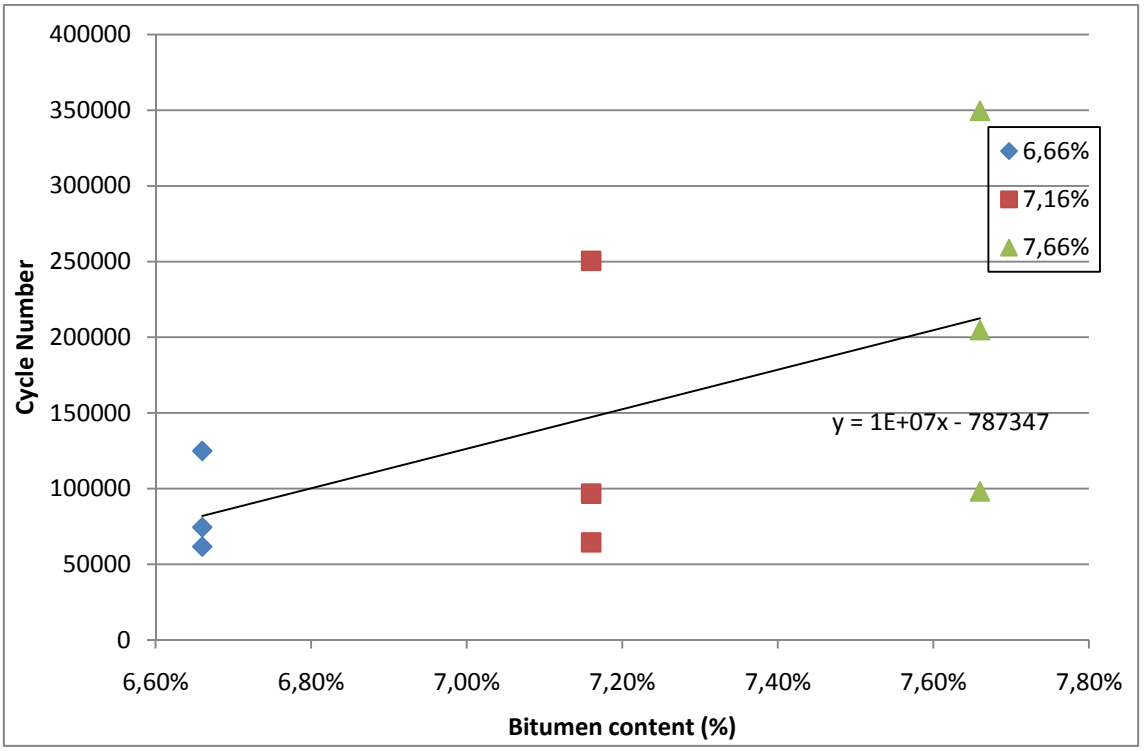

Diagram 5.28: Mean cycle numbers to failure at 300 microstrains vs bitumen content (%)

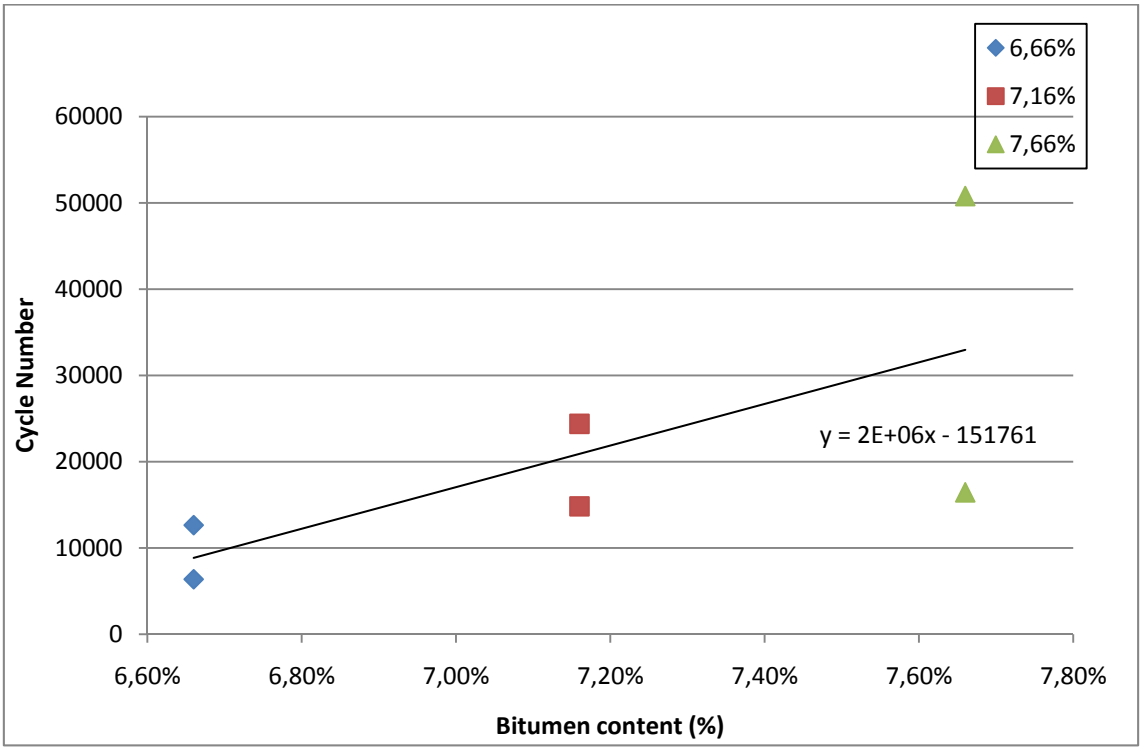

Diagram 5.29: Mean cycle numbers to failure at 450 microstrains vs bitumen content (%)

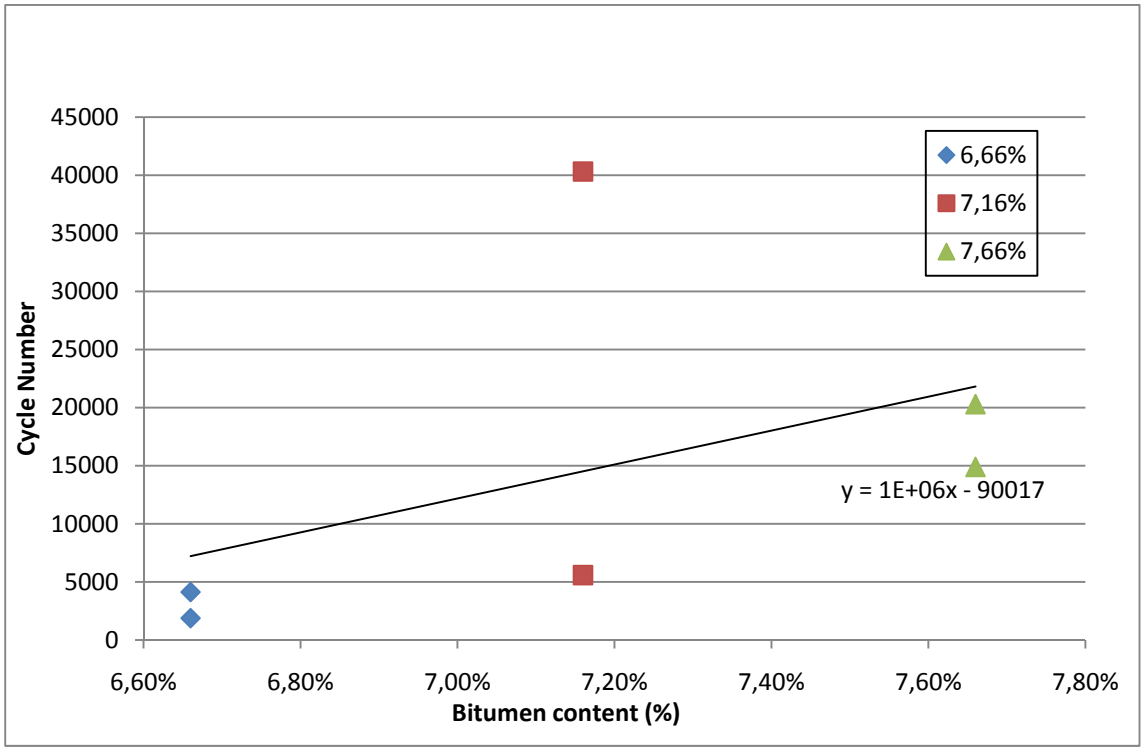

Diagram 5.30: Mean cycle numbers to failure at 600 microstrains vs bitumen content (%)

Analyzing the previous plots, even considering the data dispersion, it is seen that there is a trend to increase the fatigue resistance (load cycles to fracture) with the increment of the bitumen content for every strain level studied.

For extra data and for controlling the values which were used for plotting refer to the annexes.

Conclusion

In this thesis four different base mixtures were designed and analyzed according to the SUPERPAVE protocol; determining every granulometrical gradation, bitumen content and controlling that the mixtures accomplished the SUPERPAVE requirement. For doing this control it was necessary to characterize volumetrically all the mixtures, testing them to know their Theoretical Maximum Density (TMD), weighting them hydrostatically and analyzing their compaction curves obtained from the gyratory shear compactor.

Only one of these base mixtures was considered appropriated for testing (Mix 4), because it achieved the voids percentage at the specified cycle number and respect every other SUPERPAVE restriction as VFA and VMA. This mixture was then enriched with an extra 0,5% and 1% of bitumen to design two Rich Bitumen Base mixtures also to be tested.

These three mixtures (base (6,66%), base+0,5% and base+1% of bitumen content) were characterized related to their performance, determining their deformability with the static creep test, their crack propagation resistance with the Semicircular Bending test and their fatigue behavior with the four-points bending test.

It is to notice that being bituminous concrete a heterogeneous material, high data dispersion was expected in the tests results. Especially in the four-points bending test was seen this data dispersion, but even so, generally an increasing trend could be identified.

Regardless on the data dispersion, comparing the mean results obtained in each test it was seen that generally the Rich Bitumen Base with more bitumen (1%) performs better, having a higher crack propagation resistance and longer fatigue life. However it was also seen that the Rich Bitumen Base with +0,5% of bitumen content performs better than the base mixture in every test

and only slightly less than the more enriched mixture regarding the crack propagation resistance. Even regarding the fatigue resistance, it could be said that the difference between the two enriched mixtures was small considering that the greater different obtained at 300 microstrains could be due to the different in voids content in each mixture, being greater the voids content in the sample of the mixture with +0,5% of bitumen content than the voids content in the sample of the mixture with +1% of bitumen content.

Recommendations

Considering the recommendation strong heterogeneity of the material further studies should be made with a larger sample population and controlling carefully the sample preparation and the parameters related to compaction, seeking to obtain more homogeneous samples either geometrically and volumetrically.

It is also suggested to analyze the behavior in regard to the crack propagation resistance in the case of enriched bitumen bases with more than 1% of the optimal bitumen content determined using the SUPERPAVE protocol to see if there is threshold where the crack resistance stop increasing.

Also the economic factor should be taken into account to understand if over a certain level of bitumen enrichment the characteristics obtained are worthy or not, because as it was seen on the results from the SCB test and the four-points bending test the gain from one enriched mixture (+0,5%) to the other (+1%) is smaller than the gain respect the optimum base mixture.

References

Asphalt Institute. (1962). *The Asphalt Handbook*. Manual Series No. 4 (MS-4). Asphalt Institute. Lexington, KY

Asphalt Institute. (1997). *Superpave Performance Graded Asphalt Binder Specification and Testing*. Superpave Series No. 1 (SP-01)

Asphalt Institute. (2002). *2001 Asphalt Usage Survey*.

Asphalt Pavement Alliance (2002). *Perpetual Pavements: A Synthesis*. Asphalt Pavement Alliance. Lanham, MD.

Asphalt Pavement Alliance (APA). (2001). Recycling Asphalt Pavement Background. Paper posted on the APA website. http://www.asphaltalliance.com/focusareas/focusareas_pdfs/recycled/focus_recycling-BG.pdf.

Dongre, R., Sharma, M.G., and Anderson, D.A. 1989. "Development of Fracture Criterion for Asphalt Mixes at Low Temperatures." *Transportation Research Record: Journal of the Transportation Research Board,* No. 1228, Transportation Research Board of the National Academies, Washington, D.C., pp.94-405.

EN 12697-26: Bituminous mixtures. Test methods for hot mix asphalt: stiffness. 2004

Federal Highway Administration (FHWA). (1998). *Assessing the Results of the Strategic Highway Research Program*. Publication No. FHWA-SA-98-008. Federal Highway Administration. Washington D.C.

Federal Highway Administration (FHWA). (1998). *Assessing the Results of the Strategic Highway Research Program*. Publication No. FHWA-SA-98-008. Federal Highway Administration. Washington D.C.

Federal Highway Administration. (2001). *Reclaimed Asphalt Pavement User Guideline: Asphalt Concrete (Hot Recycling)*. Web page on the Turner-Fairbanks Highway Research Center web site. http://www.tfhrc.gov/hnr20/recycle/waste/rap132.htm.

Kabir S. “effect of hydrated lime on the laboratory performance of superpave mixtures”, Bangladesh. May 2008.

Little, N., and Mahboub, K. 1985. “Engineering Properties of First Generation Plasticized Sulfur Binders and Low Temperature Fracture Evaluation of Plasticized Sulfur Paving Mixtures.” *Transportation Research Record: Journal of the Transportation Research Board*, No. 1034, Transportation Research Board of the National Academies, Washington, D.C., pp.103-111.

Mull, M.A., Othman, A., Mohammad, L. 2006. “Fatigue Crack Growth Analysis of Hot-Mix Asphalt Employing the Semi-Circular Notched Bend Specimen.” *Transportation Research Board 85th Annual Meeting CD-ROM*, Washington, D.C.

Mull, M.A., Stuart, K. and Yehia, A. 2002. “Fracture Resistance Characterization of Chemically Modified Crumb Rubber Asphalt Pavement” *Journal of Materials Science*, Vol. 37, pp.557-566.

National Asphalt Pavement Association (NAPA). (2001). *HMA Pavement Mix Type Selection Guide,* Information Series 128. National Asphalt Pavement Association. Landham, MD.

National Stone, Sand and Gravel Association (NSSGA). (1991). *The Aggregate Handbook*. National Stone, Sand & Gravel Association. Arlington, VA. http://www.nssga.org.

National Stone, Sand and Gravel Association (NSSGA). (2002). What is NSSGA? From the NSSGA Web site. http://www.nssga.org/whoweare.

Northeast Center for Excellence for Pavement Technology (NECEPT). (2001). *Superpave System*. Web page on the NECEPT web site. The Pennsylvania Transportation Institute, Pennsylvania State University. University Park, PA. http://www.superpave.psu.edu/superpave/system.html.

Northeast Center for Excellence for Pavement Technology (NECEPT). (2001). *Superpave System*. Web page on the NECEPT web site. The Pennsylvania Transportation Institute, Pennsylvania State University. University Park, PA. http://www.superpave.psu.edu/superpave/system.html.

Rice, J.R. 1968. “A Path Independent Integral and the Approximate Analysis of Strain Concentration by Notches and Crack” *Journal of Applied Mechanics*, Vol. 35, pp.379-386.

Roberts, F.L.; Kandhal, P.S.; Brown, E.R.; Lee, D.Y. and Kennedy, T.W. (1996). *Hot Mix Asphalt Materials, Mixture Design, and Construction*. National Asphalt Pavement Association Education Foundation. Lanham, MD

Transportation Research Board (TRB). (2001). *Perpetual Bituminous Pavements*. Transportation Research Circular No. 503. Transportation Research Board, National Research Council. Washington, D.C.

WSDOT. (January 2001). *Key Facts: A Summary of Transportation Information*. WSDOT Finance and Administration Service Center. Olympia, WA. http://www.wsdot.wa.gov/KeyFacts/default.htm.

WSDOT. (May 1999). *Washington State Highway Pavements: Trends, Conditions and Strategic Plan*. WSDOT Field Operations Support Service Center, Materials Laboratory. Olympia, WA. http://www.wsdot.wa.gov/fossc/mats/pavement/Pavement%20Plan.pdf.

Wu, Z., Mohammad, L.N., Wang, L.B. and Mull, M.A. 2005. "Fracture Resistance Characterization of Superpave mixtures Using the Semi-Circular Bending Test", *Journal of ASTM International*, Vol. 2, Issue 3.

Websites:

http://www.asphaltwa.com/wapa_web/modules/03_materials/03_aggregate.htm

http://www.asphaltwa.com/wapa_web/modules/03_materials/03_asphalt.htm

http://www.asphaltwa.com/wapa_web/modules/02_pavement_types/02_pavement_types.htm

http://www.asphaltwa.com/wapa_web/modules/02_pavement_types/02_what_is_superpave.htm

Annexes

Compaction curves from the gyratory shear compactor

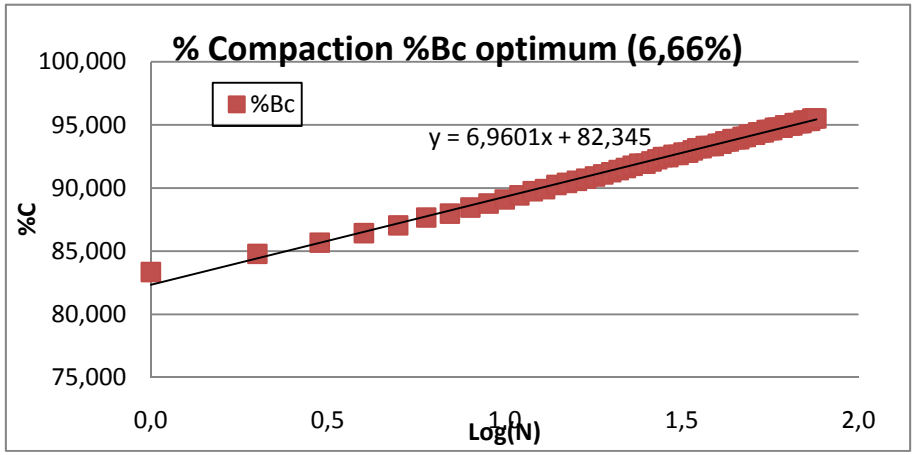

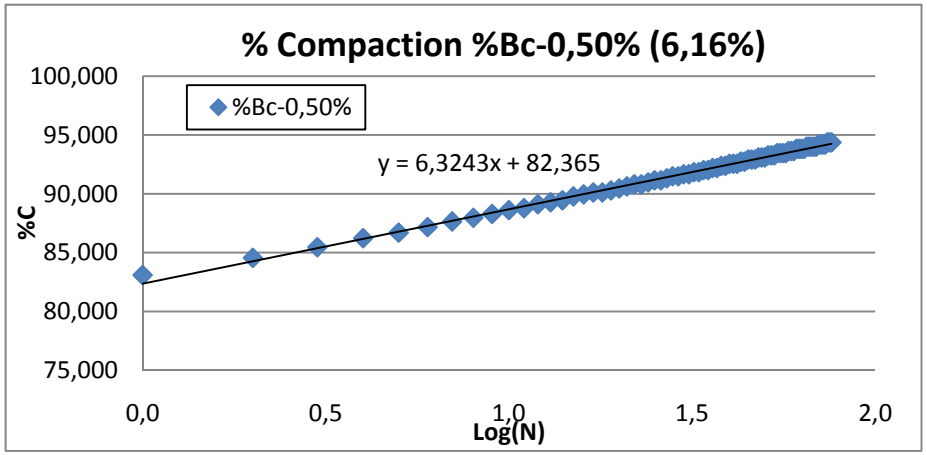

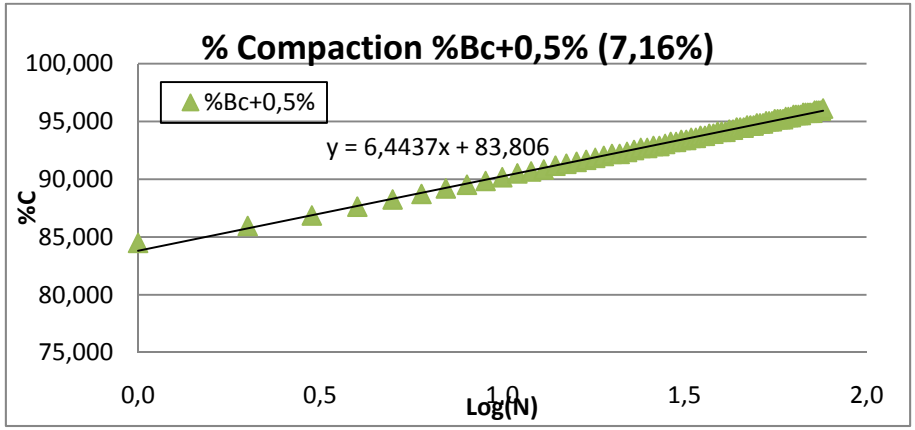

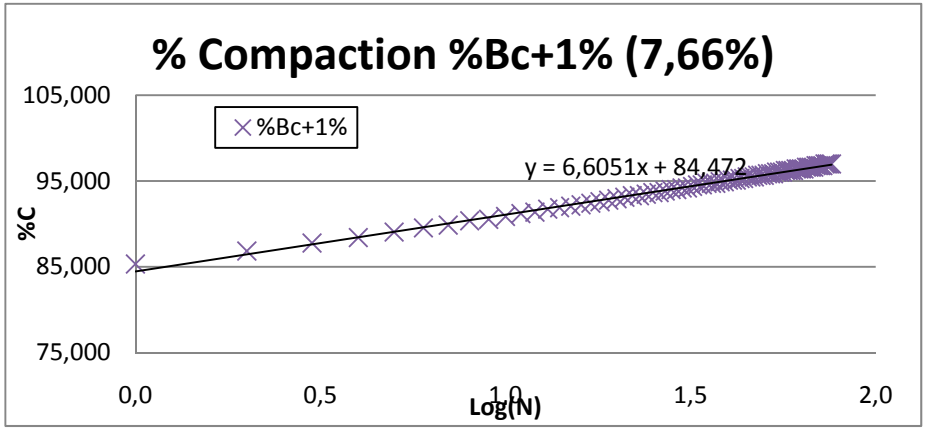

Individuated curves for the mean curve from the creep test for mix 6,66%

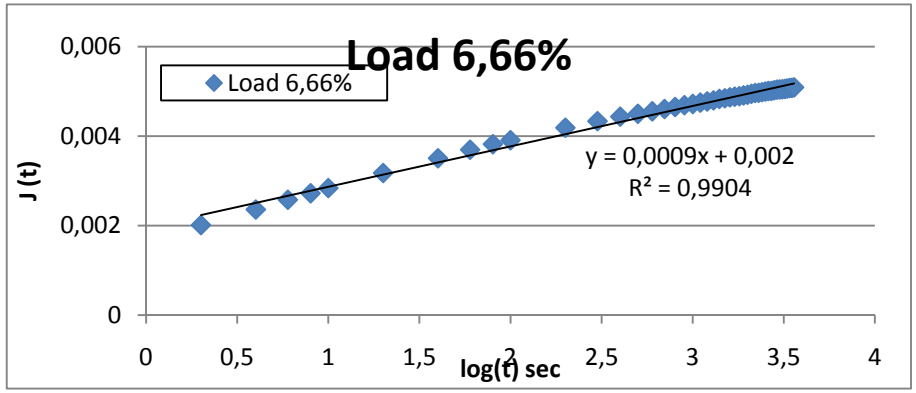

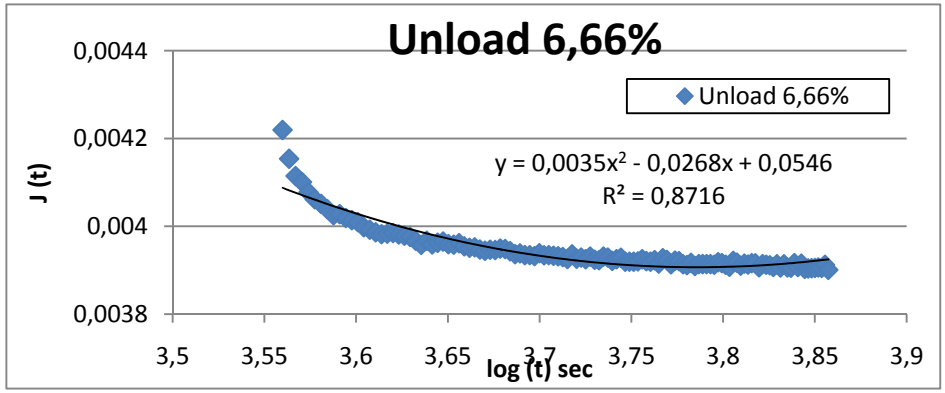

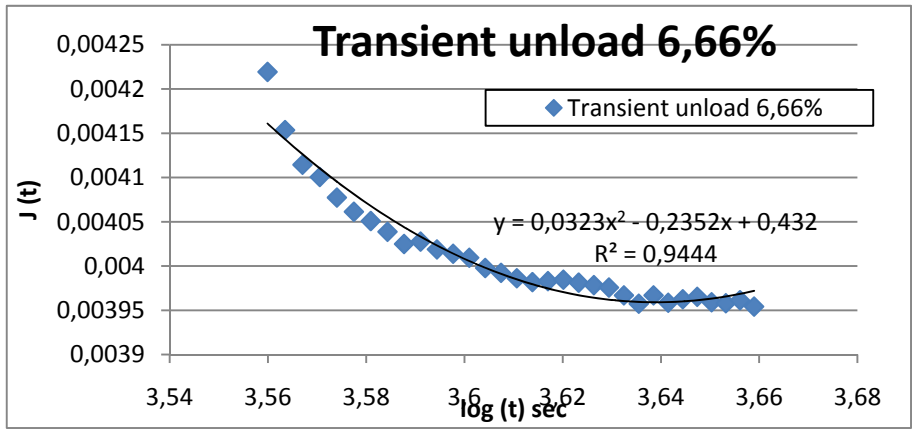

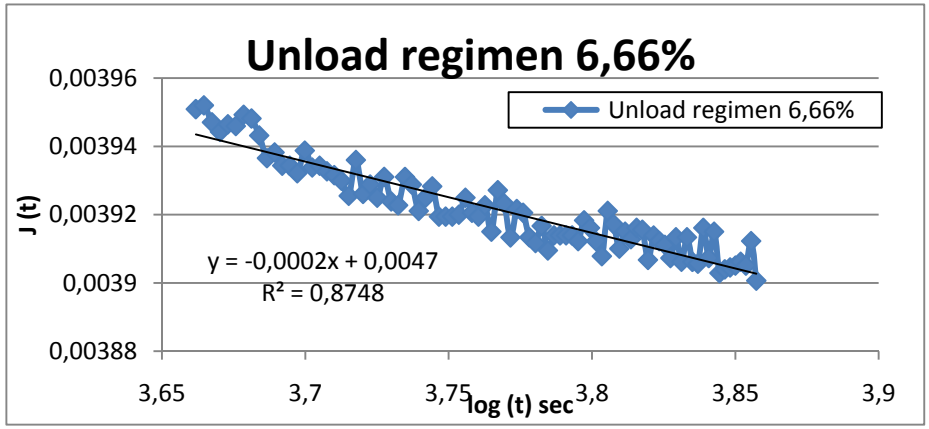

Individuated curves for the mean curve from the creep test for mix 7,16%

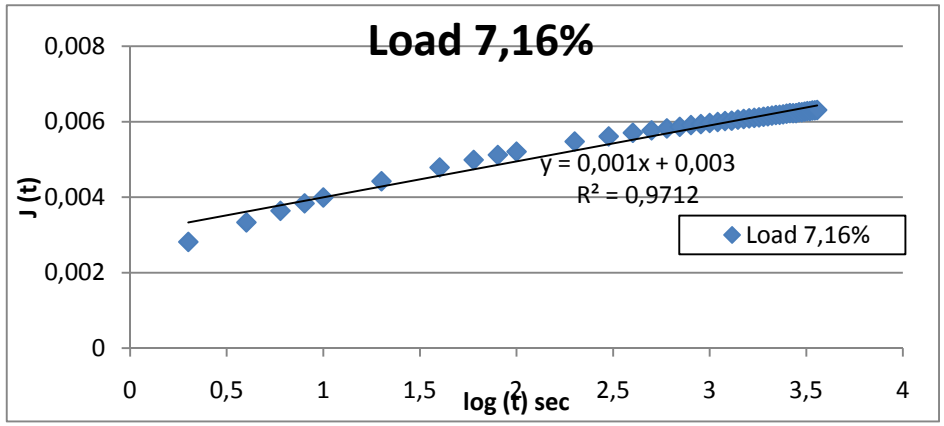

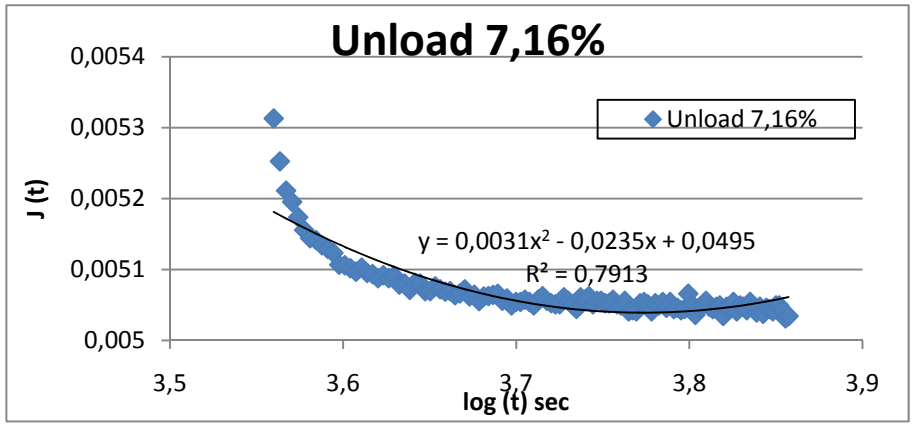

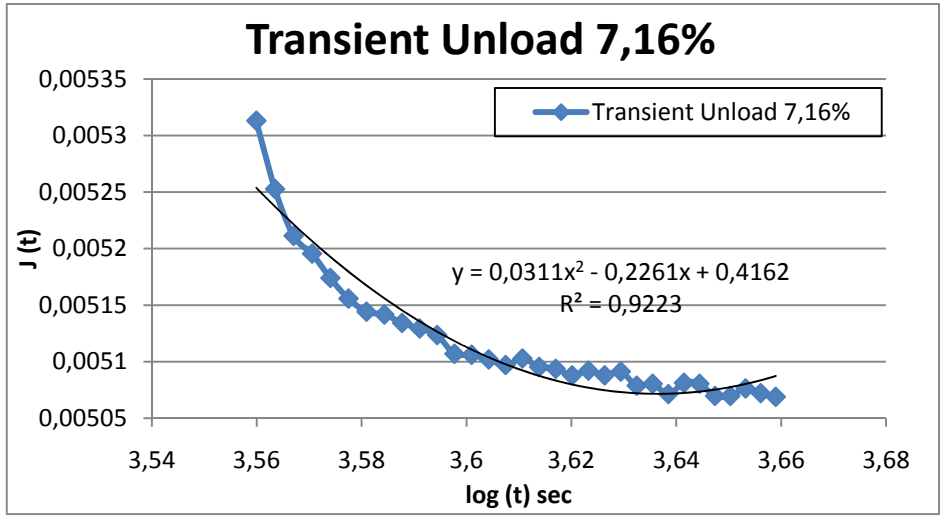

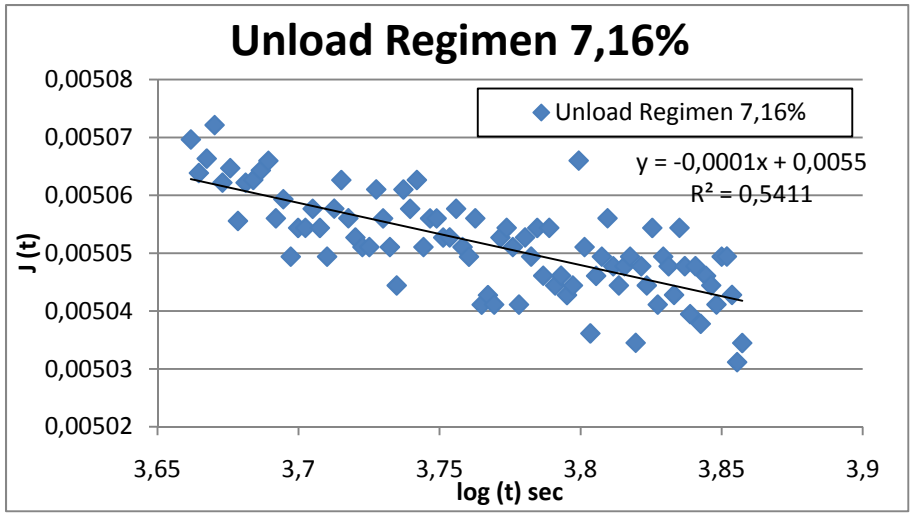

Individuated curves for the mean curve from the creep test for mix 7,66%

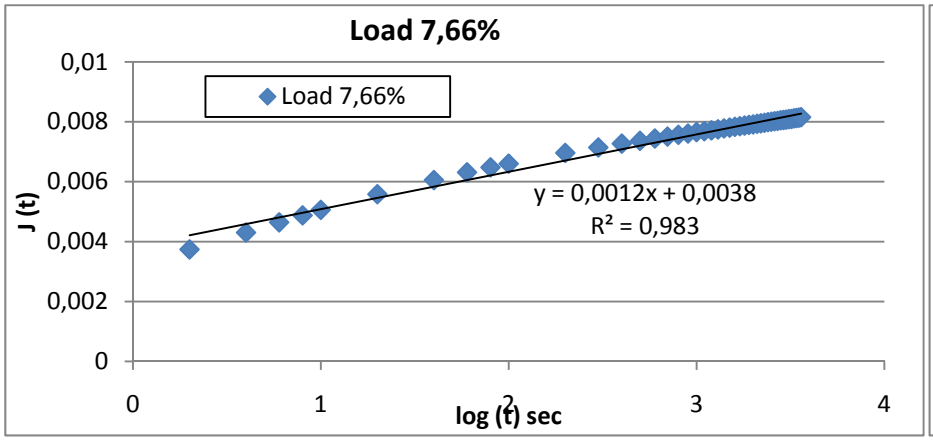
Load 7,66%
Load 7,66%
y = 0,0012x + 0,0038
R² = 0,983
J (t)
log (t) sec
0,01
0,008
0,006
0,004
0,002
0
0
1
2
3
4

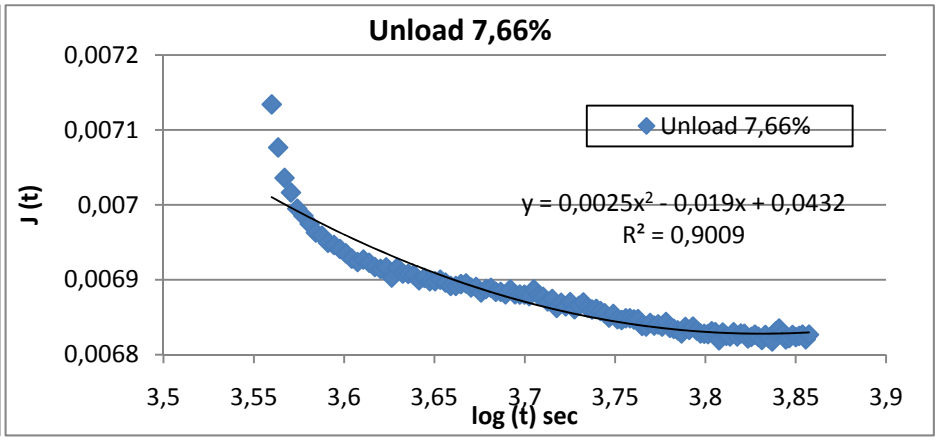
Unload 7,66%
Unload 7,66%
y = 0,0025x² - 0,019x + 0,0432
R² = 0,9009
J (t)
log (t) sec
0,0072
0,0071
0,007
0,0069
0,0068
3,5
3,55
3,6
3,65
3,7
3,75
3,8
3,85
3,9

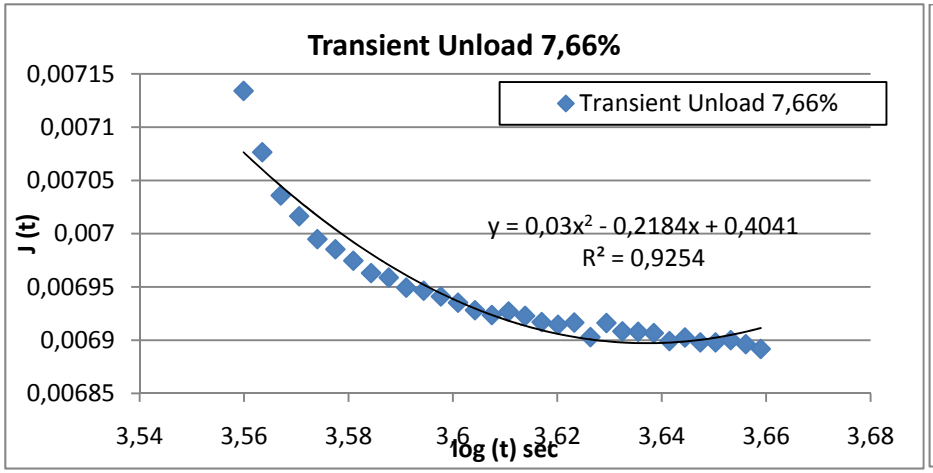
Transient Unload 7,66%
Transient Unload 7,66%
y = 0,03x² - 0,2184x + 0,4041
R² = 0,9254
J (t)
log (t) sec
0,00715
0,0071
0,00705
0,007
0,00695
0,0069
0,00685
3,54
3,56
3,58
3,6
3,62
3,64
3,66
3,68

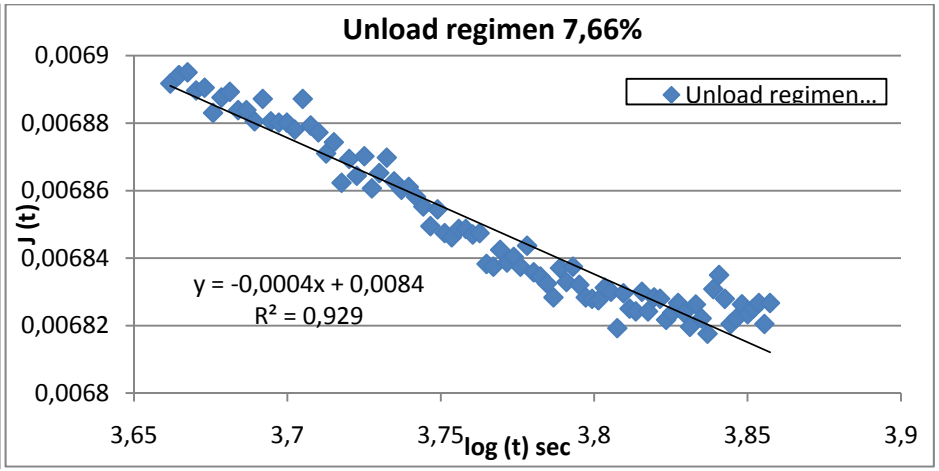
Unload regimen 7,66%
Unload regimen...
y = -0,0004x + 0,0084
R² = 0,929
J (t)
log (t) sec
0,0069
0,00688
0,00686
0,00684
0,00682
0,0068
3,65
3,7
3,75
3,8
3,85
3,9